Title

Mechanisms of cold tolerance in tardigrades (Hypsibius exemplaris)

Author

Lyons, Ana Marie

Publication Date

2022

Peer reviewed|Thesis/dissertation

Mechanisms of cold tolerance in tardigrades (*Hypsibius exemplaris*)

by

Ana Marie Lyons

A dissertation submitted in partial satisfaction of the

requirements for the degree of

Doctor of Philosophy

in

Integrative Biology

and the Designated Emphasis

in

Computational Biology and Genomics

in the

Graduate Division

of the

University of California, Berkeley

Committee in charge:

Professor Caroline Williams, Chair
Professor Nicholas Ingolia
Professor Peter Sudmant
Professor Noah Whiteman

Summer 2022

Abstract

Mechanisms of cold tolerance in tardigrades (*Hypsibius exemplaris*)

by

Ana Marie Lyons

Doctor of Philosophy in Integrative Biology

and the Designated Emphasis in Computational Biology and Genomics

University of California, Berkeley

Professor Caroline Williams, Chair

Tardigrades are microscopic, aquatic animals that are an emerging model system for studying physiological responses to a wide range of environmental stressors. Past research has explored tardigrades' extreme tolerance to desiccation and radiation, but little is known about the phylum's tolerance to subzero temperatures, especially under more ecologically relevant conditions. Here, I use *Hypsibius exemplaris*—a lab-friendly cosmopolitan species, with a publicly available genome—as a model species to characterize the physiological response of active, hydrated tardigrades to low temperatures ranging from 1°C to -20°C. I develop methods to characterize numerous cold tolerance phenotypes in tardigrades, through multiple lenses: high-accuracy measurement of survival, plasticity of chill coma, and comparative proteomics and ice-affinity purification of cold-treated tardigrades (aimed at identifying underlying molecular mechanisms of cold tolerance and putative tardigrade-specific ice-binding proteins).

In Chapter 1, I develop new methods to score mortality of cold-exposed tardigrades using the live/dead cell-marker SYTOX Green, to improve the accuracy of survival-based assays. I determined that visualization of SYTOX Green uptake was a more accurate and more specific method of determining mortality in tardigrades, compared to the traditional methods of scoring survival based on locomotion. This new method for determining survival allows for higher throughput of scoring tardigrade phenotypes and provides differentiation of live, dead, and injured tardigrades (showing localized regions of damage in the tardigrade body-plan, as they first experience cellular death). Using this new assay, I monitored survival of hydrated mixed-staged adult *H. exemplaris* over a range of acute exposure times (2-120 hours) and subzero temperatures (-10°C, -15°C, and -20°C), in order to dissect the impacts of time, temperature, and their interaction on cold tolerance. Tardigrades exposed to -10°C showed little SYTOX Green uptake and high survival across all timepoints, and samples supercooled rather than froze. Survival of tardigrades exposed to -15°C was highly variable, and depended on the water-state of the cold exposed samples (liquid or frozen). When exposed to -20°C, tardigrade survival declined exponentially with increasing exposure time and nearly all samples froze. Although I predicted that freezing may drive tardigrade mortality based on these results, I

surprisingly found that tardigrades incubated with the ice-nucleating bacteria *Pseudomonas syringae* had significantly improved survival after cold exposure, illustrating the importance of ice-formation dynamics and environmental microbes. Lastly, a 3-week thermal acclimation of tardigrades to mild cold (1°C & 4°C) did not significantly improve survival to low temperature, while acclimation to 15°C (vs the standard culture condition of 20°C) did. This work suggests that *H. exemplaris* is sensitive to ecologically relevant cold and assays developed here will be useful for exploring the thermal physiology of additional tardigrade species. More so, evidence collected here suggests that this tardigrade species is capable of surviving environmental freezing, under certain ecologically relevant conditions.

The goal of Chapter 2 was to explore cold tolerance phenotypes of tardigrades at low but non-freezing temperatures. Although no such phenotype was documented in past tardigrade literature, I predicted that tardigrades would experience a state of reversible paralysis known as chill coma, with exposure to sufficiently low temperatures and exposure times. Chill coma is often a non-lethal phenotype commonly seen in insects, but it nonetheless can impact the ecology and overall fitness of an organism living in winter conditions, as it prevents individuals from feeding, reproducing, and evading predators. Chill coma has been demonstrated to be a plastic phenotype in response to a variety of environmental conditions, as seen in insects. I predicted that the amount of time required for tardigrades to recover from chill coma (known as chill coma recovery time or CCRT) would vary with low temperature and exposure time. By analyzing video recordings of tardigrades recovering from cold-exposure, I observed that tardigrades experience a cold-induced state of reversible paralysis indicative of chill coma after 12h at 1°C. The impact of longer mild cold exposures depended on temperature: above -1°C, recovery times decreased with increasing duration of exposure, indicating that beneficial acclimation may have occurred. Below -1°C to -4°C, recovery times increased with increasing exposure duration, suggesting that sublethal damage may have accumulated. I also observed that chill coma recovery time was plastic depending on photoperiod acclimation. Tardigrades that were acclimated to shorter-day photoperiods (winter-like) for 2 weeks had significantly faster CCRTs than tardigrades acclimated to longer-day photoperiods (summer-like). In summary, this chapter characterizes a new cold tolerance phenotype in tardigrades, as well as its plasticity. Determining the underlying mechanisms that control the chill coma plasticity in tardigrades will further illustrate similarities or differences between the insect and tardigrade nervous system, in future work.

The goal of Chapter 3 was to characterize how the tardigrade proteome responds to cold exposure, as well as to discover and functionally verify candidate proteins that help tardigrades perturb freeze damage—especially novel candidate ice-binding proteins. Here, I used comparative proteomics to broadly determine how the protein repertoire shifts in *H. exemplaris* due to ecologically relevant cold conditions. Cohorts of 1000+ adult tardigrades were exposed to a cold treatment down to -10°C (or a control treatment of 20°C), and proteins were extracted from whole-animals via optimized sample preparation methods for data-independent acquisition mass spectrometry (DIA-MS). In a parallel set of samples, I performed a specialized ice-affinity purification method (IAP) and DIA-MS to enrich for and identify proteins that bind to ice. I predicted that tardigrades utilize a wide

range of biochemical mechanisms related to cold tolerance, as seen in insects, as well as IBPs or other cold tolerance proteins that are unique to the phylum, with novel structures or functions. Gene ontology (GO) enrichment analysis of proteins are significantly more abundant after cold illustrated changes in neuron and neuromuscular function, calcium ion balance, cell division processes (such as apoptosis), and glucose metabolism. GO enrichment of proteins less abundant after cold treatment suggested changes in lipid metabolism, cuticle production, development, and redox. Ice-affinity purification and a bioinformatics pipeline identified a ranked list of novel candidate ice-binding proteins that tardigrades may utilize to survive freezing. This study is the first comparative proteomics study exploring the impacts of cold stress, in any eukaryotic animal, and results provide a framework for what molecular mechanisms tardigrades may use to survive cold.

This dissertation fills a gap in knowledge about the fundamental physiology and molecular mechanisms that an especially cold-hardy microscopic organism (tardigrades, specifically *Hypsibius exemplaris*) uses to survive subzero temperatures. Development of new phenotypic assays allowed for the rigorous characterization of the plasticity of tardigrade survival and chill coma, in response to time, temperature, and their interaction. Despite tardigrades' reputation for being virtually indestructible, I determined numerous time and temperature-dependent conditions that result in increased mortality and reduced performance (CCRT), that may impact tardigrade ecology and winter-time behavior. Interestingly, I also determined that tardigrade's survival to environmental freezing improves drastically when animals are exposed to ice-nucleating microbes, which may be found in their natural environments. Finally, I determined a number of molecular mechanisms that may underlie cold tolerance in tardigrades, as illustrated by the first-ever comparative proteomics study of any animal in response to cold, along with generating a ranked list of novel, tardigrade-specific candidate ice-binding proteins. Overall, I hope that the tools and findings of this work will help establish tardigrades as an increasingly important and tractable model system, in the field of comparative physiology and beyond.

Dedication

For my parents, James and Valerie, who gave me everything and always encouraged my various childhood passions, no matter how quirky.

For Diane and Jack, for your endless encouragement, generosity, and for welcoming me into the world of science like family—along with sharing all things tardigrades.

Epigraph

"*It is not a question of if you will survive this, but what beautiful things await you when you do*."
— Chanel Miller, Know My Name

"*In the days of the frost, seek a minor sun.*"
— Loren Eiseley

Contents

List of Figures

List of Supplemental Tables

Acknowledgements

I am deeply thankful to my family, friends, mentors, colleagues, students, and community for supporting my Ph.D. journey—and everything that has led up to it. My journey has been long and winding, so there are many people to offer sincere thanks.

Thank you to my parents James and Valerie. Your endless examples of love, resilience, and integrity have guided me, in every aspect of my life. Words cannot thank you enough. Thank you to my sister, Renae, who devised the raddest tardigrade-themed birthday party at the tender age of 7 (complete with a 'pin the claw on the tardigrade' party game), before tardigrades were "cool." And more importantly, whose humor, talent, compassion, and care inspires me every day. Thank you to my brother John, who irradiates unparalleled warmth, generosity, and kindness—and who never ceases to make me laugh so hard I cry, reminding me to not take myself or life *too* seriously. Thank you to my grandmother Lonna for encouraging my creativity throughout the years, and for all of her warmth, love, and strength. Thank you to my Aunt Sueann, for always being one of my biggest supporters, and for helping me have the confidence to venture into entirely new areas, geographically and intellectually (often leading by example). Thank you to my grandparents, Gordon and Audrey, who always encouraged me to "go all the way" with my education—despite not having the opportunities to attend university themselves. And of course, thank you to all other members of my family, who are deeply appreciated but not specifically named here.

Thank you to my Ph.D. advisor: To Prof. Caroline Williams, thank you for providing me with an incredible opportunity to develop tardigrades as an emerging system, guided by your rich expertise of comparative physiology and entomology, in such an interdisciplinary and diverse research group. Your mentorship and rigor offered what was truly a once-in-a lifetime opportunity, and I am sincerely thankful to have joined such an amazing community of researchers under your leadership. Your feedback has allowed me to grow as a scientist and person, and I am sincerely thankful for your generosity of time and spirit. Thank you for the invaluable opportunities to mentor undergraduate students and collaborate in K12 outreach. I have learned so much from you as both a mentor and educator, and it has been profoundly impactful to work with you over the years.

To my committee members: Thank you to Profs. Nicholas Ingolia, Peter Sudmant, and Noah Whiteman for all of your invaluable guidance, support, and suggestions throughout the years. Thank you to Nicholas Ingolia for your incredible support throughout my entire graduate school journey: starting early-on as my first-year graduate advisor, guiding me towards an eye-opening body of molecular cold tolerance literature for my qualifying exam, suggesting that I attend an ice-binding protein seminar (thus catalyzing an international collaboration and inspiring my final dissertation chapter), supporting as my faculty mentor for Berkeley Connect Computational Biology throughout the various COVID-19 lockdowns, and for always providing helpful and quick feedback on my scientific writing. It was a rare and much appreciated opportunity to work with someone with expertise in both translational regulation and temperature-sensitive proteins

(someday I hope to finally explore tardigrade TRP channels!). Thank you to Noah Whiteman, for instilling a deep appreciation for the art and science of both molecular evolution and natural history. Thank you for your thoughtful guidance throughout my qualifying exam, all the way to providing insightful comments on my thesis, which helped me to better see things “in the light of evolution” and the broader context. Your courses in Evolution and Population Genetics were unforgettable, and they made a strong impression on the lens I use as a scientist. Thank you Noah for your dedication to DEI initiatives; you have a special gift for helping junior scientists feel valued and seen. Thank you to Peter Sudmant, for also serving as an excellent mentor and source of guidance, on my thesis committee. The skills you shared through your Quantitative Methods in Biology course proved immensely helpful in my thesis work, and only time will tell if my *Hypsibius* tardigrades can outlive your deep-sea rockfish! Thanks also must be given to Jonathon Stillman, who served on my qualifying exam committee and provided me with an excellent foundation on the insect and animal cold tolerance literature. Thanks to Jonathon for introducing me to the amazing world of “Biochemical adaptations” and antifreeze proteins, and thank you for suggesting that I apply to the NSF Antarctica Research Training program. This encouragement to apply, despite my very junior status and lack of prior experience in polar research, catalyzed such a formative experience in my life, for which I am immensely grateful.

Likewise, thank you to my mentors and colleagues, who joined me on this Antarctic adventure, and who profoundly motivated my curiosity of exploring life at low temperatures, especially: Prof. Donal Manahan, Prof. Deneb Karentz, Drs. Francis Pan, Leigh Boardman, Joshua Lonthair, Til Harter, Brandon Hassett, Luana Lins, Emily Matys, Pacifica Sommers, and many others. It was an honor to work with you, as a team on the ice.

A heartfelt thanks must be given to my dear mentor and friends, Drs. Diane and Jack Nelson, who graciously introduced me into the incredible world of scientific research, tardigrades, and the community of tardigrade researchers. Thank you for welcoming me into your lab as a shy 15 year-old high school student, supporting me through so many seasons of my career, and sharing with me the vibrancy of your lives. Your generosity genuinely changed the course of my life and career, and it has been such a privilege to have you in my life.

Extensive thanks must be given to the many additional collaborators and colleagues that have supported or inspired this work, in many unique ways: Profs. Ralph Schill, Nadja Møbjerg, Kazuharu Arakawa, Megumu Tsujimoto, Steven Lindow, Hugo Tapia, Lars Tomanek, Vladimir Gross, Bob Goldstein, Thomas Boothby, Peter Davies, Laurie Graham, Michael Shapira, as well as Michelle Salemi and Brett Phinney at the UC Davis Proteomics Core. A special thanks must be given to Prof. Ralph Schill, for sharing his passion for tardigrade cold tolerance, sharing tardigrade specimens, and for welcoming me into his research group in 2012-2013, where I learned everything I know about tardigrade culture and care. Thank you to Nadja for providing an exemplary body of tardigrade physiology literature to aspire to, and for giving an influential virtual guest seminar to our research group during the pandemic. Thank you to Kazuharu for his

generosity of time and resources, and his support of key genomic tools for tardigrades, as well as sharing tardigrades specimens. Thank you to Megumu, for her collaborative spirit and also her generosity of sharing tardigrade specimens. Thank you to Prof. Lindow for sharing with me his expertise in ice-nucleating proteins and the ingenious idea to seed tardigrade samples with *P. syringae* to induce controlled ice formation, which he generously provided. Thank you to Michael Shapira for sharing his laboratory facilities and allowing me to spend hundreds of hours on his fluorescent microscope. Thank you to Hugo for sharing an abundance of tardigrade comradery and support; especially during my first year of graduate school and as I prepared my postdoctoral fellowship application. Thank you to Lars for your helpful comments towards optimizing proteomics sample preparation. Thank you to Bob and Thomas for sharing the first cultures of *Hypsibius exemplaris*, that seeded my entire UC Berkeley tardigrade culture. Thank you to Peter and Laurie for providing AFP3 plasmids, helping with initial TH measurements, and for all of your encouragement and support for all things antifreeze proteins. Thank you to Michelle and Brett for teaching me everything I know about proteomics and for all of your time and patience, in implementing what was a multi-year comparative proteomics study; you were truly amazing to work with.

A huge thank you to the incredible high school and undergraduate researchers, that I have had the honor to work with throughout the years: Hannah Ritchie, Walter Wu, Daisy Stock, Kylie Cheng, Lily Shang, Nicole Kang, Dejénaé See, Kyla Woyshner, Iris Chow, Catherine Lu, Veronica Ellis, Stavi Tennenbaum, Hannah Grossman, Ananya Krishnapura and Emma Isella. Working with you all was the absolute highlight of my Ph.D. training, and I continue to be amazed by what incredible individuals and scientists you all are. Your tireless work, dedication, and curiosity made this Ph.D. dissertation possible. Many of my best memories of my graduate work were from collaborating and learning with you. I am lucky to have you as colleagues, hopefully for many years to come.

Thank you to all of the additional friends, teachers, scientists, people, and places, who welcomed me and held space for me—throughout the last decade of my life. Thank you to my amazing labmates at UC Berkeley: Lisa, Kevin, Andre, Emily, Rebecca, Baojun, Serena, Jackie, Lourenço, and Elliott. You all helped me beyond measure with my Ph.D. work and in terms of encouragement and support. A special thanks to Kevin for all of his tireless work, driving key data analysis in Chapter 1, and for being such an amazing scientist and person. A special thanks to Lisa for organizing writing groups, being the social glue that held the lab together, and providing much needed support and feedback. Thank you to Andre, for your infectious enthusiasm for all things insects, as well as your incredible support. Thank you to Jackie, for all of your helpful suggestions for GO analysis and comparative -omics. Thank you to Emily, for sharing your many talents with the lab, as well as rocking another non-insect ectotherm in the group. Thank you to Serena, for all of your support and helpful feedback on my NSF PRFB application. Thank you to Lourenço for your much appreciated contributions to the lab group, and being an amazing ‘cat dad’ to Biggie. Thank you to my incredible friends from UC Berkeley who have also offered community and support, especially in the Integrative Biology and Molecular and Cell Biology Departments, the Center for Computational Biology, the S&S&S team, as well as Project Fe and the Building a Better Fieldwork Future Program: Dennis, Nicolas,

Kirsten, Jessica, Dat, Allison, Debora, Nina, Chenling, Isabel, Yun, Stacy, Arturo, Ryan, Sam, Ashley, Helen, Emily, Jenna, Ixchel, Carrie, Melissa, Dylan, Eric, Jaemin, Kwasi, Camilla, Eric, Alex, Tannis, Patrick, Aaron, Tim, Emlen, Winston, and Nikki. A special thanks to Dennis and Nicolas, for being amazing colleagues, study-group members, and extraordinary friends. A huge thank you to Lydia Smith, Monica Albe, Dr. Lisa White, Yvonne, Abrar, Elizabeth, Betsabe, Kaitlin, and many others, for their community and tireless efforts for the COVID-19 hand sanitizer initiative. An additional special thanks must be given to Lydia Smith, for her superhero levels of leadership in this initiative, as well as her extraordinary help with many aspects of this Ph.D. conducted and the Evolutionary Genetics Lab. Thank you to my friends and colleagues at the COVID-19 testing clinic, especially Clara Williams and Matt Mcelroy.

Thank you to the many colleagues and professors that I have had the pleasure of co-teaching with during my time at Berkeley, who played important roles in shaping my scientific perspectives: Dr. Jules Winters, Joshua Povich, Tami Mau, Profs. Andy Martin, Isabelle LeBlanc, David Builder, Craig Miller, Xavier Darzacq, Kevin Paudian, James Bishop, Liana Lareau, Saul Perlmutter, Alison Gopnik, John Campell, Catherine Flynn, and Xuan Quach.

Thank you to prior educators and professors, who made especially impactful contributions to my intellectual development and curiosity: Laurie Lindstrom, Matthew Williams, Nancy Williams, Paul Bigford, everyone at the Center for Excellence in Education (especially Maite Ballestero, John Rickert, and Jenny Sendova), Profs. Quayshawn Spencer, B.D. Colen, Gaston Sanchez, Brent Mischler (and the entire bryophyte community), Rasmus Nielsen, Lisa Barcelos, Paul Bartels, Nigel Marley, Sandra McInnes, Brent Sinclair, and Heath MacMillan. Thank you to principal investigators and mentors who have welcomed me into their research labs and offered additional training, prior to the onset of my Ph.D. work: Profs. Uri Alon, Mansoor Amiji, Penny Chisholm, Dr. Daniel Sher, Profs. Dan Hartl, Rebekah Rogers, Aviv Regev, and Dr. Jay Konieczka, Dr. Sushmita Roy, and Dr. Jason Funt. Thanks must also be given to my first-year rotation mentors, who helped expand my experimental toolbox and perspectives: Profs. Doug Koshland, Hugo Tapia, Susan Marqusee, Dr. Charlotte Nixon, Prof. Jennifer Doudna, Dr. Janice Chen, Dr. Alex Seletsky, Prof. Kathy Collins, and Dr. Heather Upton.

Thank you to my friends at the Hebrew University of Jerusalem in Rehovot, who opened their lab to me in the final stages of my Ph.D., despite the global pandemic, from where I revised the final versions of my dissertation chapters. A massive and sincere thanks must be given to Prof. Ido Braslavsky, where words cannot begin to thank you enough. Not only did you support my high-risk tardigrade ice-binding protein project, but you provided an amazing research group and professional support system that I will remember for the rest of my life—not to mention your world-class saxophone skills. Sincere thanks to: Shay, Daniel, other Daniel, Tal, Naomi, Nitsan, Gil, Einat, and Tally. You were incredible friends and colleagues, at such a critical time of synthesis and reflection in my life.

Thank you to the members of the Kato lab, who have already welcomed me into their group with open arms (despite *C. elegans'* lack of those): Saul, Muneki, Grace, Ray,

Jackson, Yifan, Hannah and Greg. You provided much needed motivation and encouragement, and I am so grateful and excited to soon begin this next chapter of my scientific career.

Thank you to all of the amazing students I've had the privilege to work with here at UC Berkeley, via RSI, EduExplora, Jeju Global, SPLASH, and otherwise. Thank you to my former 7th grade science classes at X371 Urban Institute of Mathematics, in the Bronx NY, who encouraged me to "go back to school" and study tardigrades full-time, because I was "too much of a nerd," even as their science teacher. You taught me so much that I cherish about humility, community, and the power of joy in education.

Thank you to an incredible group of friends and loved ones, who have supported me throughout the years. Thank you to Rebecca, Jingyun, Nora, Shamarah, Vinay, Ann, Rita, Sofia, Kristen, Dijana, Steffi, Jeff, Nathan, Russell, Galina, Kim, Travis, Erica, Steve, Kristina, Sam, and Carolyn. Thank you to Jeonghwan and his family, for providing years of encouragement and support throughout my PhD years, and especially 한상천 and 정 안엽 for their keen interest in my scientific discoveries and career. Special thanks to Jeonghwan for years of transportation (to and from lab, no matter what hour), help with tardigrade care, and years of sincere friendship. Thank you to Pyay Aung for your unparalleled kindness and support, towards both me and Alfie, and for introducing me to the meditation community and being the incredible person that you are. Also, thanks are due to Pyay Aung for helping me debug the beast that was coding regular expressions and implementing Pannzer2 on a non-model organism. Thank you to Yuya for your friendship and for creating a remarkable digital rendering of *Hypsibius exemplaris* that has proved immensely useful for a variety of my scientific illustrations.

And of course, thank you to all of the amazing animals who shared friendship with me throughout the years. To the various cats throughout my scientific career: Thi, George, Bella, Minnie, Pinto, LaJean, Alfie, and the many street cats of Rehovot that I have befriended (and fed) while editing this dissertation. To Buddy the dog.

And last but not least, thank you to the tardigrades. I am grateful for the sacrifices of thousands of brave tardigrades that enabled the discoveries described here, although I admit that you did not have much of a say in the matter, for which I apologize and appreciate. Thank you for exemplifying that "strength lies in softness," and thank you for all the mysteries you hold—with your tiny, adorable claws.

Preface

Eighteen years ago, I stumbled across a thick, cobalt blue copy of the book "Ecology and Classification of North American Freshwater Invertebrates" in my local library—with an SEM image of an alien-like animal with eight legs, a piercing stare, and "whiskers," that was also strangely charming. Having grown up in the farmlands of rural Michigan, I thought I had seen my fair share of wildlife, but here was an animal that I had never seen before. Investigating further, I read that this strange creature was a microscopic animal called a "tardigrade," and that these tardigrades could apparently be found anywhere there was a thin film of water. Interesting, "*Michigan does have quite a lot of water, maybe we have tardigrades too?"* I wondered. "*Also how strange, that no one has ever said anything about tardigrades before*," I thought. Reading onwards, this book's chapter on tardigrades introduced me to many new concepts I had never considered before, as a then 14-year old:

> Tardigrades belonged to their own phylum. ("*What is a phylum?*" I wondered, "*it sounds important to have your own.*")
>
> There were many species of tardigrades, thousands actually, with new species being described every year. ("*Wow, there are still 'new' species? And what does it even mean to be a new 'species,' in such a weird organism?*")
>
> Tardigrades lived in a parallel microscopic world. ("*How is this world different? Is there really a whole zoo of living, microscopic things with complexity beyond bacteria, viruses, and Paramecium? And we all just…coexist, in our own little worlds?*")
>
> Scientists didn't know about tardigrades until relatively recently (1773) because most early scientists didn't have the tools to observe animals of their size, i.e. microscopes. ("*We can be limited by our technical ability to observe things? And this can prevent us from not knowing 'what we don't know'?*")
>
> Tardigrades were given a name in Latin that means "slow walkers" because early scientists observed them struggling to walk on glass slides, even though in reality, tardigrades can walk quite fast on their natural substrates of moss, lichen, soil, sand, etc. ("*If we study organisms too far removed from their natural habitats, we can be comically misguided?*")
>
> Tardigrades could survive many environmental stresses that would kill most other organisms. ("*But how?*")
>
> Tardigrades could sometimes 'pause time' to survive stresses. (*"Again, how?"*)
>
> Tardigrades had long been ignored in the modern scientific community, because they had no clear economic or ecological impact from the human perspective. ("*Human centric-utility is what drives most scientific discovery? And do we really have 'nothing' useful to learn from things like tardigrades?*")
>
> And there were still very many things about tardigrades that were unknown, waiting to be uncovered. (*"There are still many discoveries left to be made?"*)

This last point—of discoveries still waiting to be made—was an especially revolutionary idea in my young mind. Up until this point, I took nearly everything I read in my state-issued K12 science textbooks quite literally, implicitly believing that all important scientific knowledge could be neatly organized into chapters, diagrams, and glossaries. In all the years prior, I had just assumed that all the “major discoveries” of the natural world had already been made, because no one in my sphere of educational instruction had said otherwise. I thought that “science” could only be found in textbooks, not living on a clump of moss in my own backyard. Now, here in this Ph.D. dissertation, I am happy to report that there are indeed more questions than answers, especially regarding such strange animals as tardigrades.

For the next several years, the impact of reading this chapter on tardigrades extended far and wide. I corresponded with the author of that textbook tardigrade chapter, Dr. Diane Nelson, who graciously offered to mentor me in all things tardigrades. From the moment I first saw a live tardigrade that I collected from an ash tree in my childhood home's yard, I was entirely captivated. Our mentorship began remotely, with my father—a skilled outdoorsman—generously driving me all over Michigan, so I could sample tardigrades from a wide diversity of mosses and lichens across the state. Shortly afterwards, Diane invited me to visit her research lab, where she trained me on handling and identifying a wide range of tardigrade species. As a first generation (pre)college-student, I had no idea what it meant to “be” a scientist, let alone a female scientist who was a major leader of an entire scientific field. The time and care that she (and her husband Jack) took, to share her stories had a profound impact on my life and future career. As the first tardigrade researcher in the United States starting in the 1960s-70s, Diane had an amazing collection of photographs, notebooks, and preserved tardigrade specimens that completely challenged the way I viewed science as a deeply personal and lifelong pursuit. She introduced me to the incredible Paul Bartels during fieldwork, as well as many other remarkable researchers at future tardigrade conferences. This truly brought science alive for me and made me feel welcomed. More so, I was profoundly impacted by the collaborative aspect of the highly international tardigrade community, which inspired me to seek a wide range of perspectives across the world, in future work.

Fast forwarding to the Ph.D. research presented here, I am elated to have integrated many of my original interests of tardigrades with techniques that I have been privileged to learn in more conventional model systems. I am also happy to have integrated many biological questions, across the molecular level, on the scale of organismal phenotypes, and behavior—all under more ecologically relevant conditions than tardigrades are typically exposed to in the laboratory. This way, we can aspire towards a more holistic understanding of how tardigrades evolve, survive, and behave. Likewise, we can better appreciate under what circumstances tardigrades are merely mortal, perhaps constrained by principles in physics, biochemistry, or foundational biological processes, like any other living organism. Additionally, this work has been largely interdisciplinary, requiring perspectives of comparative physiology, molecular biology, molecular evolution, as well as the collaboration of biophysicists, on the global scale (taking me to several continents, including Antarctica).

Ralph Schill, Nadja Møbjerg, Roberto Guidetti and many other scientists had long convinced me that cold tolerance in tardigrades was an exciting and understudied frontier in tardigrade research, and biology at large. This emphasis on cold tolerance also offered

a satisfying layer of coherence in my own life's timeline, given the freezing cold winters of my childhood. Unlike in the case of other environmental stressors where tardigrades fell into almost inert dormancy (curling into small ball-like shapes called "tuns" and ceasing all movement and nearly all metabolism), it was less clear what tardigrades did in winter months without the formation of these tuns. More so, there stands much to be developed, in terms of translational applications of tardigrades' molecular mechanisms to survive cold, especially in the biomedical and biotechnology spheres. The work of collaborators Ido Braslavsky and Peter Davies has also deeply inspired me, to investigate the fascinating world of biomolecules that interact with ice. And of course, I was immensely inspired by the rich cold literature of insects and methodology to study cold tolerance in ectotherms, especially by my Ph.D. advisor Caroline Williams, and Profs. Brent Sinclair, Heath MacMillan, and many others. Together, this left me with many unanswered questions: Under what ecologically-relevant conditions can otherwise active tardigrades survive low temperatures? How can a microscopic animal (like tardigrades) survive freezing conditions, while living in water? What parts of their bodies are damaged, if any, in response to cold? How can we best determine death, in an organism that often ceases movement in response to stress? In what ways do tardigrades experience sublethal damage in response to cold? Does cold impact their behavior? Does cold impact their biochemical processes, potentially in ways that help confer survival? Are there any novel proteins that tardigrades may employ, to survive cold? And more broadly, can studying organisms at low temperatures challenge anything we know about the basic "rules of life"? Although I could not address all of these questions in full detail, I hope to have provided a framework for exploring more, and to have opened the conversation.

It is my ultimate scientific goal to help establish tardigrades as a model system for many cross-disciplinary questions in biology, with a similar scale of tools and resources that we see in *C. elegans*. Tardigrades share many of the practical advantages of *C. elegans*, with several distinct benefits. Tardigrades rapidly reproduce, are easy to culture in laboratory conditions, have transparent bodies (which are easily stained, labeled, and visualized under the microscope), and likely can be manipulated by many of the tools already developed for nematodes. However, tardigrades have an arguably more complex body-system, with legs, eyespots, and enhanced abilities for perception, locomotion, and behavior, thus opening up their utility to a much wider range of questions in basic science. With a well-annotated genome in at least two model species (*Hypsibius exemplaris*, studied here, as well as *Ramazzottius varieornatus*), the field of comparative -omics in tardigrades is ripe with numerous questions waiting to be explored. The study of cold tolerance in tardigrades is especially exciting, but the challenges of studying microscopic animals at low temperatures have emphasized many of tardigrades' strengths as a model system, while providing an opportunity to overcome prior technical limitations.

Although my Ph.D. dissertation cannot possibly rival the clarity and excitement of Diane's classic textbook introduction to tardigrades, I hope that it can be received as an equally enthusiastic invitation to any reader, especially for those who can be convinced to share my enthusiasm for understanding life at low temperatures. While this work emphasized that tardigrades (at least the species *Hypsibius exemplaris*) cannot actually "survive anything" as the "toughest animal in the world," we did discover in Chapter 1 that there are a number of conditions were they can survive freezing conditions, especially with the help of environmental microbes, which is a truly remarkable feat for any hydrated,

microscopic organism. Whether the tardigrades themselves actually freeze (intracellularly or extracellularly), or just the water freezes around them, remains to be described. In Chapter 2, we found that tardigrades share a similar form of cold-induced paralysis ("chill coma") that is also found in cold-exposed insects. Although tardigrades can recover from this cold-induced paralysis much quicker than most insects, this general phenomena suggests potential overlap in the architecture of insect and tardigrade nervous systems, which will be interesting to explore in future work. Lastly, by studying how abundances in proteins change in tardigrades in response to low temperatures, we identified dozens of biological processes and novel proteins that may underlie tardigrade cold tolerance. Many of these findings come full circle to the initial curiosities that first motivated me as a young scientist, both relating to natural history, experimental biology, and the philosophy of science. I hope at least some of the findings presented here will help initiate additional avenues for future research among high-schoolers, undergraduates, graduate students, citizen-scientists and more senior researchers alike, from all corners of the macroscopic and microscopic world.

Chapter 1

Survival *of Hypsibius exemplaris* to subzero temperatures depends on the intensity and duration of cold exposure as well as the presence of ice-nucleating bacteria, as shown by large-scale SYTOX Green-based assays

1.1 Key Findings

- Active, hydrated tardigrades—with no prior acclimation to cold—have high survival of temperatures above -15°C, even in response to prolonged exposures.
- Below -15°C, tardigrade survival declines exponentially with increasing exposure time
- Incubating tardigrades with ice-nucleating bacteria significantly improves survival after cold exposure, illustrating the importance of ice-formation dynamics and environmental microbes.
- A 3-week acclimation of tardigrades to mild cold (1°C & 4°C) does not significantly improve survival to low temperature, while acclimation to 15°C (vs the standard culture condition of 20°C) does.
- Uptake of the dye SYTOX Green is a more accurate metric of tardigrade mortality in response to cold exposure, compared to the traditional method of scoring lack of locomotion during recovery.

1.2 Abstract

Tardigrades are an emerging model system for understanding a diversity of environmental stress responses, yet few studies describe the physiology of cold tolerance in hydrated, active tardigrades. Here, we develop methods to screen tardigrades for survival in a high-throughput manner, to investigate the impacts of several key environmental conditions on survival: extent of low temperature, duration of cold exposure, thermal acclimation, and the presence of bacterial ice nucleators. Here, the visualization of SYTOX Green uptake in hydrated, cold-exposed *Hypsibius exemplaris* allows us to quickly and accurately quantify the survival of thousands of animals, under a range of ecologically-relevant low temperatures, exposure times, conditions, and thermal acclimations. As a proof-of-concept, we show that SYTOX Green uptake more accurately predicts 2-week survival outcomes of tardigrades post-cold exposure, compared to previous methods of scoring survival (locomotion). We show that hydrated, active tardigrades survive mild cold exposures of -10°C at high rates of ~98%. Survival of tardigrades to exposures of -15°C depends on environmental freezing in pure mineral water, and survival decreased exponentially with exposure time at -20°C (to 45% after 24 hours; with freezing occurring at nearly all -20°C timepoints). To investigate the role of environmental ice-formation on tardigrade survival vs. temperature, we incubated unacclimated tardigrades with ice-nucleating bacteria—which initiate environmental freezing at higher temperatures (-1.8 to 3.8°C). Surprisingly, we found a significant increase in survival of tardigrades frozen at -20°C (p-value = 0.0152) with the addition of *Pseudomonas syringae* compared to non-inoculated controls, as well as observing high-survival tardigrades in ice-nucleated samples exposed to -10°C and -15°C. This indicates the species' tolerance to environmental ice formation and exposure to our lowest

temperature (-20°C), under certain conditions of controlled environmental ice formation. A 3-week acclimation of tardigrades to mild cold (1°C and 4°C) in constant darkness did not significantly improve survival after acute exposure to low temperature, but acclimating animals to 15°C did. Overall, we find that *H. exemplaris*—an emerging tardigrade model species—has a range of cold tolerance capabilities, dependent on time, temperature, environmental ice-formation, and culturing conditions. This work offers a framework with new tools for performing large-scale physiological assays in numerous species, establishing tardigrades as a tractable and uniquely informative model system in comparative physiology and the study of environmental stress.

1.3 Introduction

Tardigrades are a group of microscopic animals that have captured the curiosity of scientists, both for their abilities to survive environmental extremes, and for their high potential to be developed as a model system for a wide range of biological questions (Goldstein 2018) and translational applications (Giovannini et al. 2022; Piszkiewicz et al. 2019; Kirke et al. 2020; Hashimoto et al. 2016; Schill et al. 2009). Under certain environmental stresses, tardigrades evade harm by entering various forms of protective dormancy known as cryptobiosis or encystment, as seen in desiccation, osmotic stress, or radiation (Møbjerg and Neves 2021). As one especially striking example of survival, researchers found that a species of Antarctic tardigrades *Acutuncus antarcticus* could be successfully revived from storage in the tun state (desiccated) at -30°C for over 30 years, with no addition of cryoprotectants or special storage protocols. These forms of protective dormancy involving tun or cyst formation, however, are not often seen in cases of cold-exposed tardigrades originating from less-extreme habitats (Guidetti and Møbjerg 2018; Guidetti et al. 2011).

Instead, many species of cold-exposed tardigrades are believed to go into a physiological state known as cryobiosis, where active animals can survive low temperatures and their overall morphology remains largely unchanged, compared to tun or cyst formation (Hengherr and Schill 2018). Supporting this claim, a recent ecological survey of microfauna in snow algae blooms in northern Japan indicated that physiologically active tardigrades were among the most abundant organisms, thus suggesting that tardigrades do not rely on deep dormancy in snowy environments (Ono et al. 2021). Likewise, a microbiome diversity survey conducted in British Columbia detected a high abundance of snow algae genetic material in tardigrade gut contents, indicating snow algae consumption by tardigrades during winter months (Yakimovich et al. 2020). Despite these observations indicating tardigrades' abilities to tolerate winter conditions, few studies have rigorously characterized the impact of cold on hydrated, active tardigrades, especially under ecologically relevant conditions where exposure time, temperature, and environmental ice-inoculators may vary (Schill 2018). Methodological challenges in handling and scoring these unique microscopic animals—especially with the high accuracy and throughput needed to interrogate interactions between these crucial factors—have historically contributed to this gap in knowledge.

Low temperatures and freezing are undoubtedly a major selective pressure that tardigrades experience, given their global distribution in cold climates with seasonal or frequent subzero temperatures (McInnes and Pugh 2018). All tardigrade species require

a film of liquid water in order to locomote, feed, and reproduce, and ice-formation threatens this requirement, presumably impacting essential elements of tardigrades' metabolic function, cellular integrity, and other temperature-dependent physiological processes (Bertolani et al. 2004). As microscopic water-dwelling organisms, tardigrades are especially vulnerable to rapid shifts in ice-formation, yet environmental factors impacting their survival to subzero temperatures and ice-formation are not well understood. In order to survive subzero temperatures while hydrated, tardigrades are believed to deploy one of two major cold tolerance strategies: freeze avoidance or freeze tolerance (Hengherr and Schill 2018). Organisms using freeze-avoidant strategies cannot survive internal ice formation, and use colligative solutes such as glycerol or trehalose to suppress the freezing point of their body fluids or employ cryoprotective dehydration to avoid ice formation (Denlinger and Lee 2010). Freeze tolerant organisms can survive extracellular or even intracellular ice formation, and often do so by inoculating ice formation at relatively warm subzero temperatures using ice-nucleating proteins, resulting in ice formation occurring more slowly (Denlinger and Lee 2010). It remains unknown if tardigrades produce their own antifreeze or ice-nucleating proteins, or if they are influenced by the ice-nucleating proteins or agents from any neighboring microorganisms, such as bacteria or fungi that share their winter-time habitat.

Although several studies have attempted to describe the cold tolerance strategies of tardigrades using calorimetry, with the goal to detect liquid to ice phase transitions in tardigrade samples, conclusions of the exact mode, plasticity, and robustness of cold tolerance remain ambiguous (Westh et al. 1991; Westh and Kristensen 1992). Early calorimetric studies conducted on limno-terrestrial species *Richtersius* (*Adorybiotus*) *coronifer* and *Amphibolus nebulosus* detected relatively high ice-crystallization temperatures (-6 to -7°C) for tardigrades, suggesting freeze tolerance as the primary strategy to survive cold (Westh and Kristensen 1992). Likewise, these authors predicted that ice nucleators likely played an important role in modulating the higher-than-expected freezing temperatures for these tardigrade species (Westh et al. 1991). More recent studies on nine tardigrade species indicated that phase transitions occurred at much lower temperatures, with tardigrades experiencing supercooling points ranging from roughly -10°C to -24°C, although most species survived ice formation well (Hengherr et al. 2009). However, most prior laboratory conditions lack ecological relevance, being carried out in minimal water volumes, on starved animals, and without the presence of any environmental microbes. We thus aimed to assess the impact of more environmentally relevant conditions on the cold tolerance strategy.

Here, we develop a series of phenotypic assays in the cosmopolitan eutardigrade species *Hypsibius exemplaris*, to explore foundational questions in tardigrade cold tolerance. *H. exemplaris* is an emerging model system due to its ease of propagation in laboratory settings, genomic resources, and the growing collection of knowledge surrounding the species' development, physiology, and stress tolerance (Goldstein 2018). Although several recent studies have focused on the desiccation tolerance of *H. exemplaris* and the evolution of its genome (Yoshida et al. 2017), documentation is absent on this species' cold tolerance strategy, as well as how cold stress impacts the physiology and viability of this experimentally important species. The type specimen of *H. exemplaris* was collected from a benthic sample from a pond in Darcy Lever, Bolton, Lancashire, England (latitude 53.566166, longitude -2.3925272; British National Grid Ref.

SD741078) (McNuff 2018) where animals likely experience fluctuating subzero temperatures throughout winter months, although members of this genus are believed to be globally widespread across temperate climates (GĄsiorek et al. 2018). A closely related species, *Hypsibius dujardini,* was found to have only "moderate" tolerance to cold compared to a set of six other tardigrade species studied (Guidetti et al. 2011), but whether *H. exemplaris* is more robustly cold-tolerant remains unknown. It is unclear whether *Hypsibius* genus tardigrades (and other tardigrade species) have a fixed level of cold tolerance, or if their sensitivity to subzero temperatures is dependent on fluctuations in environmental conditions such as the intensity and duration of low temperature, or the presence of external ice-nucleators. Filling this gap in knowledge would not only propel our understanding of a key aspect of this *H. exemplaris'* ecophysiology, but it would provide a more holistic context for understanding other forms of stress tolerance than this emerging model. More so, methodology developed in the more tractable *H. exemplaris* species could serve as a future framework to characterize cold tolerance phenotypes in a wide range of tardigrade species.

One limitation of previous studies assessing tardigrade cold tolerance (or any physiological assay that requires scoring tardigrade mortality) is the difficulty in determining whether animals are dead or alive, based on locomotion alone. For example, the largest cold tolerance study of tardigrades to date indicated that fully hydrated *Ramazzottius varieornatus* exhibit high levels of cold tolerance after exposures to -20°C, -80°C and -196 °C, but the scoring of animals relied on manual visualizing of locomotion alone, which is a laborious and time-sensitive process, limiting throughput (Møbjerg et al. 2022). Additionally, lack of locomotor activity can indicate mortality but can also indicate dormancy or temporary lack of motivation or ability to move (e.g. due to molting cycles), introducing considerable noise into survival measurements. Futhermore, tardigrades' microscopic size and transparent color can make such behavioral observations difficult and irreproducible. Thus, we optimized protocols to stain tardigrades with the live/dead cell marker dye SYTOX Green. SYTOX Green is a commonly used dye in flow cytometry to indicate mortality in high-throughput cellular screens, and it has been repeatedly demonstrated to bind to DNA only in nuclei that are highly permeabilized due to cell death (Thakur et al. 2015; Lebaron et al. 1998; Roth et al. 1997). This molecular dye was first demonstrated for use in tardigrades with a series of proof-of-concept experiments using sodium azide to induce mortality (Richaud and Galas 2018). Using this new methodological tool, we utilized tardigrades' microscopic size and transparent color to ultimately score mortality with greater accuracy and efficiency.

Here, we use *H. exemplaris* as a model system to experimentally assess the plasticity of tardigrade cold tolerance in response to different ecologically relevant temperatures, exposure times, and key environmental conditions (the presence of external ice-inoculators and the process of thermal acclimation). In our first experiment, we validate our new method to phenotypically screen the mortality of tardigrades after cold exposure in a more accurate and high-throughput manner, using SYTOX Green dye vs. locomotion as metrics of mortality. We then dissect the combined impacts of temperature and duration of cold exposure on survival, in thousands of tardigrades, using SYTOX Green to indicate mortality. Third, we explored the impact of natural (bacterial) ice-inoculators and the role of ice-formation on tardigrade survival. Lastly, we investigated the role of thermal acclimation prior to cold exposure on survival. Overall, this work

presents the first experimental evidence that tardigrade survival is significantly impacted by both the degree of low temperature and duration of cold exposure, as well as other environmental factors such as the presence of ice-inoculating bacteria and the process of acute thermal acclimation. Furthermore, methodological advancements of using SYTOX Green to score the survival of thousands of tardigrades allowed us to determine a range of scenarios where tardigrade cold tolerance varied between high (surviving freezing conditions) and low survival.

1.4 Methods

1.4.1 Tardigrade culture

Experiments were conducted on the eutardigrade species *Hypsibius exemplaris* Z151 (reclassified from *Hypsibius dujardini* in 2017), purchased from Sciento (Manchester, United Kingdom). Tardigrades were cultured in 100 x 25 mm deep-well petri dishes (USA Scientific, 8609-0625) in constant lowlight at 20°C, and animals were suspended in roughly 200mL of commercially sourced mineral water (Crystal Geyser). Tardigrades were fed with 15mL of dense *Chlorococcum sp.* (cultured from Sciento, Manchester, United Kingdom), and added bi-monthly directly to deep well petri dishes. The top 100mL of water and culture debris was skimmed from each petri dish bimonthly, via a 50mL serological pipette and pipette controller, and 100mL of fresh mineral water was added along with algae food source. Dishes were manually inspected for fungal infection (20X magnification) after each feeding, and each tardigrade culture plate was split into 2-5 new culture plates every 4 months.
To generate the tardigrade food source, *Chlorococcum sp.* algae starter cultures were added to 800mL of commercially sourced mineral water and Bold Modified Basal Freshwater Nutrient Solution (Sigma Aldrich B5282-500ML). These cultures were grown to high density (typically ~2-3 weeks at 20°C) in parafilm-sealed, autoclaved 1000mL Corning Pyrex Erlenmeyer Flasks, under white LED light and constant aeration. Algae aeration was achieved by inserting a sterile serological pipette into the flask, which was connected to an aquarium pump (Tetra Whisper, 20-40 gallon) with plastic tubing and a 0.2µm pore syringe filter.

1.4.2 Validation of SYTOX Green uptake as an improved survival assay

To determine the most accurate survival scoring metric (lack of locomotion or SYTOX Green uptake) to describe mortality in tardigrades after cold exposure, groups of tardigrades were exposed to low temperatures, initially scored with both metrics, and tracked for activity over a 14-day period (as a proxy for long-term survival outcomes). To achieve this experimental goal, groups of mixed staged adult *Hypsibius exemplaris* (n≈20 animals) were collected from culture dishes (at 20°C) via manual microaspiration (a Sigma-Aldrich A517 aspirator tube assembly with hand-pulled 150mm Glass Pasteur Pipette tip, connected with ~3cm of 1/4-Inch PVC tubing), washed in mineral water thrice to remove algae sediments in secondary petri dishes, and collected into a 1.5mL Eppendorf tubes with 100µl of mineral water (Crystal Geyser) to constitute one experimental sample. Samples (N = 10 in total, N = 2 per cold exposure time) were then exposed to cold treatments of -15°C for up to 48 hours (in increments of 4, 8, 12, or 48 hours) in a cooling circulator (VWR Scientific 1167P Heating/Cooling Recirculating Water

Bath, filled with 1 part Ethylene Glycol: 1 part Water, via placement into a secondary metal container submerged into glycerol antifreeze). After the desired length of cold exposure time, cooled tardigrade samples were then removed from the cooling circulator onto the benchtop at 20°C and allowed to warm for 20 minutes. A parallel set of tardigrade samples (N = 4, with N = 1 exposed to 4, 8, 12 or 48 hours of -15°C) where not cooled and acted as a room temperature control.

Tardigrade samples were then stained with an optimized concentration (1µM) of SYTOX Green for 1 hour (according to Richaud and Galas 2018), spun at low speed on a desktop centrifuge, washed with distilled water, placed onto wet mounts without coverslips, and immediately viewed under a fluorescent dissecting microscope at 120X magnification, using a Leica DMRXA2 upright fluorescent microscope equipped with a Leica I3 long-pass GFP filter and a Leica DC500 camera (Leica Microsystems, Wetzlar, Germany). Each image was captured by using identical settings. All animals were manually scored as 1) having the presence or absence of SYTOX Green uptake and 2) having the presence or absence of locomotor activity, by visual inspection. Select animals were photographed, to illustrate representative staining patterns of SYTOX Green uptake throughout the tardigrades' bodies. Individual animals were then transferred into wells of 48-well plates, containing 300µl of distilled water and 100µl of *Chlorococcum sp* food source. Locomotion was assessed daily for 14 days, via manual observation under 30X on a dissecting microscope, in order to determine long-term survival. Animals were scored as being "true positives" for mortality if they were observed to have coordinated locomotion for 1 day or less, during the 14-day observation period. Animals were scored as being "true negatives" for mortality if they were observed to have coordinated locomotion for at least 2 days during the 14-day observation period.

To determine which method of mortality scoring was more accurate for downstream use, we analyzed data using an Exact McNemar test (with central confidence intervals) using the exact2x2 package (Version 1.6.6) in Rstudio. We conducted this analysis for all cold-exposed tardigrades in aggregate (Figure 1.1G), as well as when partitioned according to water-state (Supplementary Figure 1.1A & 1.1B, as well as exposure time Supplementary Figure 1.2). For each mortality scoring metric, specificity was defined as TN / (TN+FP), sensitivity was defined as TP / (TP+FN), and accuracy was defined as (TP + TN) / (TP + TN + FP + FN). TP = # of tardigrades that were predicted dead and were confirmed dead (among the 14 day observation period). TN = # of tardigrades that were predicted alive and were confirmed alive. FP = # of tardigrades that were predicted dead and were confirmed alive. FN = # of tardigrades that were predicted alive and were confirmed dead.

1.4.3 Cold tolerance assays interrogating duration and temperature

To establish the survival of *H. exemplaris* in response to variation in the intensity and duration of cold exposure, we exposed groups of hydrated, active adult tardigrades (n = ~20 individuals/replicate, N = 6 replicates per treatment) to one of three ecologically-inspired cold temperatures (-10°C, -15°C -20°C) for 9 exposure times (0, 2, 4, 8, 12, 24, 48, 72 or 120h). Immediately prior to cold exposure, tardigrades were removed from standard culture conditions described above via manual microaspiration and placed into 1.5mL Eppendorf tubes in groups of 20 with 100µl of mineral water, then placed in a circulating cooler (setup described above). Once all samples were loaded into the

circulating cooler, the temperature was decreased until it reached the target temperature, at which point the time 0 sample was immediately removed from the circulating cooler, and further time points were removed at 2, 4, 8, 12, 24, 48, 72 or 120h after achieving the target temperature, with 3 replicate pools per time point (performed in 2 separate batches, for a total of 6 samples, per condition). A handling control of N = 3 pools of tardigrades was treated similarly except instead of being placed in a circulating cooler was placed at room temperature (temperature +/- 2°C) in constant darkness, for the corresponding amount of time.

Immediately upon being removed from the circulating cooler, the water state of the sample (frozen or liquid) was recorded via manual visual inspection, and the tardigrades were stained in their original sample tubes with 1μM of SYTOX Green, following the protocol described in the prior section. Individuals were scored for survival based on the presence or absence of SYTOX Green uptake (using methods described above), and the proportion of survival was calculated for each pool of tardigrades (Figure 1.2A).

We tested the effects of cold exposure temperature and duration on survival using a generalized linear mixed model fit by maximum likelihood (Laplace Approximation) using the 'glmerMod' package in RStudio (Version 1.3.1073), whereby temperature, duration of the cold exposure, and their interaction were fixed effects, and replicate and batch number were random effects. Individual survival was the response variable, with a binary response of live/dead. Exposure time (duration of cold exposure) was a fixed factor, and we fit 1st, 2nd, and 3rd degree polynomials to describe the effect of exposure time, determining the best fit using AIC (delta AIC < 2 indicated the simpler model was preferred, Supplementary Figure 1.3). Statistical significance for the impact of factors was determined using 1st degree polynomials of tardigrade survival.

The linear mixed-effects model described continuous survival rates between 0 and 120 hours of cold exposure was plotted in ggplot2 for our various low-temperature exposures, with SEMs calculated from the 6 replicates per condition. We used this model to predict a cold hardiness metric we define as the "lethal time at low temperature" (LLt50), which is the time at which 50% of the sample population is predicted to experience mortality, at a given low temperature. We used Pearson's Chi-squared tests with Yate's continuity correction to determine if overall survival differed in each low temperature, compared to our 20°C control temperature.

To determine the impact of water state (frozen vs. liquid) on the survival of animals at each temperature (on average, across all time points), we conducted non-parametric Kolmogorov-Smirnov tests, calculating approximate P-values for significance between the proportion survival of liquid vs. frozen sample replicates at each temperature (GraphPad Version 9.3.1).

1.4.4 Ice-inoculation assays

We next assessed how raising the freezing point of water would impact tardigrade survival of freezing, using the ice-nucleating bacteria *Pseudomonas syringae* (bacterial colony provided by Steven E. Lindow). Groups of tardigrades (n=50) were aspirated into 1.5mL Eppendorf tubes in 200μL mineral water, and inoculated with a small swab of *P. syringae* (picked from a single colony from a cultured dish, per experimental replicate) before being cooled to -10°C, -15°C, -20°C, or a control temperature of 20°C (N=6 pools

of ~20 individuals per temperature/time combination, conducted with N=3 in 2 batches). Control tardigrades were treated identically but without the addition of *P. syringae* (N=6, of ~20 individuals per temperature/time combination). Immediately upon thawing, the water state of each sample was recorded (frozen/unfrozen) and tardigrades were stained with SYTOX Green to score mortality as described above. Because *P. syringae* nucleates ice formation at -1.8 to -3.8°C (Maki et al. 1974), we predicted that tardigrade samples containing *P. syringae* would freeze at all subzero temperatures, whereas control samples without *P. syringae* would supercool (thus remaining liquid) to -10°C and sometimes supercooled to -15°C, based on the prior experiment. Thus, we partitioned data from this experiment into three groups "Control (no addition of *P. syringae* bacteria): Frozen," "Control (no addition of *P. syringae* bacteria): Liquid," and "Inoculated (with the addition of *P. syringae* bacteria): Frozen" since all cold exposed samples with *P. syringae* experienced freezing and some in the control group merely supercooled. We conducted multiple Kolmogorov-Smirnov tests, calculating approximate or exact P-values for significance between the proportion survival of sample replicates in each of the three groups at each temperature (GraphPad Version 9.3.1).

1.4.5 Thermal acclimation assays

To explore if tardigrade cold tolerance may be impacted by thermal acclimation prior to cold exposure, we cultured tardigrades (as described above) in PHCBI Panasonic MIR-154-PA incubators set at 1°C, 4°C, 15°C, or on the benchtop (at 20°C) for 3 weeks. Tardigrades cultured in incubators were in constant darkness, whereas tardigrades cultured on the benchtop were in constant dim ambient light. After this 3-week acclimation period, groups of n≈20 tardigrades were extracted from individual culture dishes, thrice washed, and placed into 1.5mL Eppendorf tubes with 100µl of mineral water. N=3 samples were prepared from each acclimation temperature, and were then exposed to -20°C for 24 hours and 25 minutes (the time where 50% of animals died at -20°C in Figure 1.2). An additional N=6 samples were prepared from 20°C acclimated tardigrades (standard culture conditions, used in all prior experiments) and also exposed to -20°C for 24 hours and 25 minutes. All samples were stained with SYTOX Green post-cold exposure, as described above, and scored for tardigrade mortality rates based on the presence or absence of SYTOX Green uptake. We conducted multiple two-sided Fisher's exact tests, calculating P-values for significance between the percent survival of each of the three temperatures compared to room temperature controls (GraphPad Version 9.3.1).

1.5 Results

1.5.1 Uptake of SYTOX Green is a more accurate measure of cold-induced mortality than lack of locomotion

To determine the best metric for scoring mortality in tardigrades post-cold exposure, we compared the accuracy of locomotion vs. SYTOX Green uptake (a live/dead cell marker) to predict long-term survival of *H. exemplaris* (n=173 animals) after a 4 to 48 hour long -15°C cold exposure (Figure 1.1A). Among 69/173 tardigrades that

experienced uptake of SYTOX Green, we found three common staining patterns (Figure 1.1B): ii. Staining of the posterior (around the ovaries and malpighian tubules) iii. Staining of the anterior and posterior (head and trunk rejoin), or iv. whole-body stain (where many storage cells throughout the animal also took up stain). All three of these staining patterns were marked as SYTOX Dead (69/173 individuals), and individuals without any visible staining were marked as SYTOX Alive. We determined that 98.8% of tardigrades with any staining pattern of SYTOX Green Uptake were confirmed to have died, with SYTOX Green Uptake predicting mortality with 97.75% specificity (compared to 61.80% specificity in the case of using lack of locomotion as a marker of mortality) (Figure 1.1C). In the case where animals did not uptake SYTOX Green, we found that the absence of SYTOX Green uptake had a false negative rate of 2.25% but a low sensitivity of 79.76% (compared to locomotion's sensitivity of 97.62%). Thus, SYTOX Green uptake was a highly sensitive marker of mortality, but it was a scoring metric would sometimes miss observation of lethal damage in non-stained individuals (Figure 1.1D). Using locomotion, however, as a marker for mortality has dramatically lower sensitivity, and would falsely classify many non-moving individuals as dead (Figure 1.1E). There was not a significant difference in mortality scoring accuracy in water-state specific (frozen or liquid) samples (Supplementary Figure 1.1), although analysis may have been limited by small sample size for partitioned data. When survival data are partitioned by exposure time, SYTOX Green performed significantly better at the longest exposure time (48 hours, Supplementary Figure 1.2).

Overall, we determined that SYTOX Green uptake was more accurate at predicting mortality outcomes (Accuracy = 89.01%), compared to the absence of locomotion on Day 0 (Accuracy = 79.19%.). An Exact McNemar test (with central confidence intervals) determined that SYTOX Green uptake was a significantly more accurate marker of mortality than lack of locomotion (p-value = 0.01315). These data provide evidence that SYTOX Green uptake is a more accurate metric for scoring mortality outcomes of *H. exemplaris*, and is preferable scoring methods relying on observation of locomotion after cold exposure, where organismal activity is likely to be temporarily diminished, due to sublethal damage or other physiological changes. We thus used SYTOX Green uptake as our measure of survival for subsequent experiments.

1.5.2 Tardigrade mortality increases with lower subzero temperatures and longer exposure time

Temperature and exposure time significantly interacted to determine tardigrade survival (Figure 1.2A), when 1st degree polynomials for exposure duration were fit to survival data in a binomial generalized linear mixed model fit by maximum likelihood (Laplace Approximation), with survival based on SYTOX Green uptake as the dependent variable, duration and temperature as fixed effects, and replicate batch as a random effect (error df=2910). Both the effect of temperature, duration, and the interaction of the two factors significantly impacted survival at -15°C vs -20°C (temperature: z-value=4.055; p-value=5.02e-05; duration: z-value=-15.507; p-value<2e-16); and the interaction of the two factors (z-value=7.925, p-value=2.27e-15) as well as between -10°C vs -20°C (temperature: z-value=9.003; p-value=<2e-16); and the interaction of the two factors (z-value=2.677; p-value=0.00742). More so, we found that overall survival at -15°C and

-20°C was significantly different compared to that of our room temperature control (-20°C vs 20°C: p-value<2e-16, df=1; -15°C vs 20°C p-value<2.2e-16; df: 1; Pearson's Chi-squared test with Yates continuity correction) whereas -10°C vs 20°C was not (p-value=0.1439, df=1). Survival of room temperature controls also varied significantly with time (z-value=-13.671, p-value<2.2e-16), according to the generalized linear mixed model fit by maximum likelihood (Laplace Approximation), with duration as a fixed effect and replicate number as a random effect), although the average survival rate of the control was high at 99.50% (SEM: 0.54%).

Likewise, the survival of *H. exemplaris* was uniformly high across all durations of exposure to -10°C, with an average percent of 97.82% survival (SEM: 1.75%). The water in nearly all -10°C samples remained unfrozen at the end of each trial (Figure 1.2B), which we predict contributed to their high survival under these exposure conditions.

When groups of tardigrades were exposed to an intermediate temperature of -15°C, survival rates did not diminish over time in a unidirectional fashion (Figure 1.2A). Instead, overall survival was lowest at 12 hours (30.01% survival, SEM: 7.08%), with an average percent of survival increasing to 86.78% (SEM: 5.52%) after 120 hours of -15°C cold exposure. In the case of -15°C cold exposures, there was variation in whether a given sample supercooled or spontaneously froze, especially at shorter exposure times (less than 72 hours). We subsequently predicted that variation in tardigrade survival at -15°C may be related to the sample's water state (frozen or liquid). Indeed, survival was significantly higher in unfrozen (liquid) samples compared to frozen samples, for tardigrades subjected to -15°C (approximate p-value <0.0001 Kolmogorov-Smirnov test) as well as for -20°C (exact p-value 0.0282 Kolmogorov-Smirnov test) (Figure 1.2C).

Survival of *H. exemplaris* exposed to -20°C diminished with increased exposure time (Figure 1.2A). An average of 98.6% (SEM: 0.88%) of animals survived after immediately reaching the low temperature of -20°C, but tardigrade survival decreased to 7.05% (SEM: 2.31%) for tardigrades exposed for the maximum duration of 120 hours. At ~24 hours, 50% of tardigrades were dead after exposure to -20°C. We observed that the water in all but two samples exposed to -20°C froze. In Supplementary Table 1.5, we also observed shifts in staining patterns of SYTOX Green uptake whereby the rates of whole-body staining (compared to localized anterior or posterior staining) increased with exposure time.

In summary, these data demonstrate that *H. exemplaris* are sensitive to both intensity and duration of cold exposure, with survival decreasing precipitously with exposure time under -20°C conditions (Full data available in Supplementary Tables 1.2-4). Importantly, the role of ice-formation on tardigrade mortality depended on the final low temperature. In the next experiment, we thus induced ice formation at higher subzero temperatures using ice-nucleating bacteria, to explore the impact of ice formation dynamics vs. temperature alone.

1.5.3 Ice-formation by ice-nucleating bacteria does not result in organismal mortality, indicating freeze tolerance

We seeded ice-nucleating bacteria *Pseudomonas syringae* into tardigrade samples and then exposed them to -10°C, -15°C, and -20°C for 120 hours and compared survival against samples without ice-nucleating bacteria, to determine the impact of controlled ice-inoculation. Without the addition of *P. syringae* into tardigrade samples, we

predicted that samples exposed to -10°C would remain liquid (with high tardigrade survival), samples exposed to -20°C would freeze (with low tardigrade survival), and samples exposed to -15°C would exhibit high variation in water-state (with survival dependent on water-state)—as we observed in the large-scale survival study above (Figure 1.2A). Because *P. syringae* has been documented to induce ice-nucleation with high efficacy at temperatures as high as -1.8°C, we predicted that all tardigrade samples seeded with *P. syringae* before cold exposure would freeze, regardless of final low temperature (Cochet and Widehem 2000; Maki et al. 1974; Arny et al. 1976).

The addition of *P. syringae* compared to regular handling controls did not cause any observed mortality after 120h (0%) under standard culturing conditions (20°C). All cold-exposed samples seeded with *P. syringae* froze, regardless of final exposure temperature or time. Tardigrade survival was uniformly high (average 94.11%) in inoculated frozen samples across all low temperatures (Figure 1.3A-C). At -10°C, unfrozen controls and frozen inoculated samples had similar high survival (Figure 1.3B), with no statistically significant difference (p-value >0.9999, Kolmogorov-Smirnov test). At -15°C, unfrozen and frozen controls had similar high survival to inoculated frozen samples (Figure 1.3D), with no statistically significant difference (p-value >0.9999, Kolmogorov-Smirnov test). At -20°C, frozen controls had considerable mortality (60.99%), while survival of inoculated frozen samples remained close to 100% and was significantly higher (p-value 0.0152, Kolmogorov-Smirnov test). This illustrates that ice-formation alone does not result in tardigrade mortality, when it occurs in the presence of ice-nucleating bacteria.

1.5.4 Three-week thermal acclimation at 15°C improves cold tolerance

Tardigrades were acclimated at three temperatures (1°C, 4°C, 15°C, 20°C) in constant darkness for 3 weeks before being exposed to -20°C for ~24 hours (near the LLt50 for room temperature acclimated tardigrades: 24 hours and 25 minutes), to gauge the impact of thermal acclimation on cold tolerance. While 3-week acclimation at 1°C and 4°C had no significant impact on tardigrades' survival (p-values = 0.8868 and 0.6709 respectively, Fisher's exact test), tardigrades acclimated to 15°C had a significantly higher survival compared to room temperature controls (p-value = <0.0001, Fisher's exact test).

1.6 Discussion

Prior to this work, tardigrades were widely viewed as tolerant to virtually any environmental extreme, including low temperatures and freezing (Hengherr and Schill 2018). Using novel methods to score mortality, we demonstrate that survival of hydrated *Hypsibius exemplaris* is highly variable after exposure to low temperatures, depending on the interaction of duration and intensity of cold exposure, exposure to external microbial ice-nucleators, and thermal acclimation. We found that there was a threshold temperature (-20°C), at which survival declines exponentially with increasing exposure time. Above that temperature, increased exposure time did not have clear directional impacts on tardigrade survival. At this damaging low temperature, the addition of ice-nucleating bacteria to induce freezing at higher subzero temperatures dramatically increased survival, suggesting that the dynamics of ice formation and ecological conditions are critical to tardigrade cold tolerance. We established several instances where active adult

tardigrades can survive external freezing of external water, without relying on anhydrobiosis. Taken in whole, we found evidence that tardigrades are not universally tolerant to environmental extremes such as cold, but given the right conditions, tardigrades can survive freezing for our longest timelines tested, without relying on tun or cyst formation. Furthermore, we provide a new framework to assay thousands of tardigrades in large-scale physiological or phenotypic screens, with improved accuracy by relying on visualization of SYTOX Green uptake.

Cold exposure duration and intensity interact to determine tardigrade mortality

Exploring cold tolerance in hydrated, not desiccated, tardigrades is crucial to understanding the impacts of cold under more ecologically-relevant conditions. Here, we examined the survival rates of thousands of hydrated, fed, and active *H. exemplaris*. This work is the first to compare the impact of ecologically-feasible low temperature, time spent at low temperature (duration), and the interaction of these two factors on the survival of any tardigrade species. As a novel insight, we found that survival of *H. exemplaris* decreased exponentially with time when exposed to our lowest experimental temperature of -20°C (in the absence of external bacterial ice nucleators). The survival of tardigrades exposed to -20°C was high for short durations of exposure time (90.02% at the 2-hour time point), even when surrounding water froze in the tardigrade samples. Survival of tardigrades exposed to -20°C decreased, however, to an average of 45.36% after 24 hours and 7.05% after 120 hours (where all samples froze). In contrast, we found that tardigrades could tolerate temperatures of -10°C and -15°C with high survival (up to 100% depending on duration), as long as the surrounding water remained in a liquid, presumably super-cooled state. From these data alone, it appeared that *H. exemplaris* may survive low temperatures by adopting a freeze-avoidant strategy, surviving cold until exposed to a thermal threshold between -15°C and -20°C, and succumbing to freeze damage when exposed to -20°C for periods of time longer than ~24 hours. In this work, we did not observe whether ice formed in the tissues directly, due to the methodological constraint of not being able to easily visualize tardigrades' bodies while animals were encapsulated in opaque frozen water.

These findings are most comparable to the previously described survival rate of 55.6% for the sister species *Hypsibius dujardini*, when adult tardigrades were starved but hydrated and were cooled to -20°C for six days at a rate of 0.35°C min−1 (Guidetti et al. 2011). Guidetti et al also exposed cohorts of hydrated *H. dujardini* to final low temperatures of -9°C and -80°C, where they observed survival rates of 72.5% and 18.8% respectively (although cooling rates differed with each temperature) Overall, the authors concluded that *H. dujardini* had "moderate" cryobiotic abilities, which is consistent with our findings of *H. exemplaris* on average (with survival ranging from 7.05% to 100%, at various low temperatures and durations, in the absence of additional ice-nucleating bacteria). Our study uniquely illustrates that although *H. exemplaris* is only moderately cold-tolerant on average, it ranges from being robustly tolerant to sensitive to cold, depending on temperature and duration of cold exposure.

This work was the first study to assess the combined impacts of low temperature and duration of time spent at low temperature on tardigrade survival while holding the cooling rate roughly constant. Cooling rate has strong effects on the cold tolerance of a range of tardigrade species (Hengherr et al. 2009) and the use of a cooling circulator

allowed us to control the rate of cooling during cold exposures, regardless of the final low temperature. In Guidetti *et al*, hydrated tardigrades were chilled to their target temperatures at rates that differed by 2-3x fold, which additionally impacted total time spent at low temperature and thus prevented authors from more exhaustively separating the impact of low temperature vs. duration of cold exposure (Guidetti et al. 2011). A productive avenue for future research would be to vary the rate of cooling and thawing independently of the duration and intensity of cold exposure, to allow us to assess the relative importance of each factor in determining survival.

External ice-inoculation at higher temperatures dramatically improves survival

Initially, we found that tardigrades had higher survival of a -15°C cold exposure when animals were suspended in unfrozen water (96.1%) compared to when samples spontaneously froze (53.4%) (Figure 1.2C). We thus used ice-nucleating bacteria, *P. syringae*, to induce ice formation at high subzero temperatures, and to separate the effects of freezing from the effects of duration and intensity of cold exposure (Figure 1.3). The addition of this ice-nucleating bacteria to hydrated tardigrade samples improved tardigrade survival at the lowest exposure temperature, -20°C, significantly when frozen (99.9% compared to 58.5% for control samples; p-value >0.9999, Kolmogorov-Smirnov tests, Figure 1.3C). Ice-nucleation by *P. syringae* also improved survival at higher temperatures (-10°C and -15°C), where tardigrade survival averaged 97.4% and 85.1% respectively (Figure 1.3A & 1.3B). The addition of this ice-nucleating bacteria allows for ice-formation to occur at higher sub-zero temperatures, allowing a slower and more controlled rate of ice formation (Maki et al. 1974), compared to that found in tardigrade-containing samples alone. Freezing at moderate speeds (such that may occur without external ice-nucleating agents) is more likely to result in mortality, due to the predicted formation of larger ice crystals, resulting in freeze damage (Hengherr and Schill 2018).

These observations suggest that *H. exemplaris* may be tolerant of freezing when it occurs under controlled conditions of ice formation (such as at higher temperatures ranging from -1.8 to -3.8°C). This supports conclusions from several past studies, which inferred that tardigrades may experience a diversity of cold tolerance strategies including freeze avoidance, rapid cold hardening, and/or freeze tolerance, varying in accordance with the species' natural habitat and rate of freezing (Hengherr and Schill 2018). Likewise, recent work from (Møbjerg et al. 2022) suggested that the extraordinary freeze-tolerance of *Ramazzottius varieornatus* likely relies on controlled ice formation, as suggested by observation of a significant decrease in viability following rapid cooling. However, we caution that we were not able to directly observe the freezing of the body tissues, and it is possible (though unlikely) that tardigrades were supercooled within the frozen water. Conclusively determining the cold tolerance strategy of tardigrades has remained elusive due to the destructive nature of calorimetry experiments or the methodology of scoring survival. This constraint limited the ability to discern if low temperature, external ice-formation, or ice-formation within the animal was responsible for tardigrade mortality. In future work, we will utilize micro-CT scans of cold-exposed tardigrades to visualize density shifts of intra- and extracellular freezing events.

This is the first published work to indicate that tardigrade survival may be enhanced by the presence of other cold-hardy microbes, potentially found in their shared habitats. Thus, in nature *H. exemplaris* is likely tolerant of freezing in the presence of ice

inoculators. The importance of external ice nucleators is emerging as an important determinant of cold tolerance strategy in invertebrates: Even classically “freeze avoidant” species such as the Linden bug, *Pyrrhocoris apterus*, are freeze-tolerant when ice formation is inoculated externally at high sub-zero temperatures, suggesting that supercooling and freezing are not distinct strategies but rather ecophysiological alternatives, depending on the presence of external ice nucleators (Rozsypal and Košťál 2018). The role of environmental microbes on tardigrade cold tolerance and ice-formation has been absent from the literature, until data presented here.

Expanding the design of the initial study to also include examining the impact of time and temperature on the survival of tardigrades at various life history stages would be an important next step. Hengherr *et al* found no ice-nucleation events in any of the five distinct developmental stages of embryos and uniform temperatures of ice crystallization, suggesting that tardigrade embryos have similar freezing and survival patterns as adults (Hengherr et al. 2010). Yet, substantial literature in the nematode field has indicated that early-stage *C. elegans* are capable of surviving freezing via entering a daur stage, potentially by relying on the use of ice-binding proteins, demonstrating variation in cold tolerance across the life-history stages for some aquatic microorganisms (Gade et al. 2020; Kuramochi et al. 2019). Exploring whether any combination of cold exposure conditions, along with the addition of external ice-nucleating agents like *P. syringae,* shifts the survival dynamics of cold-exposed tardigrades across various life stages would better contextualize the universality of this organism’s cold tolerance.

15°C acclimation improves tardigrade survival rates, indicating the importance of environmental conditions for organismal growth prior to stress exposures

Few prior studies explored the impact of thermal acclimation on tardigrade stress tolerance, with the limited existing work focusing on the impact of acclimation at warmer temperatures in surviving high heat or impacting locomotor performance (Neves et al. 2020; Li and Wang 2005). Here, we found that only one of our three thermal acclimation temperatures tested (15°C) was beneficial for improving survival to sub-zero temperatures in *H. exemplaris*. This temperature of 15°C may indeed induce beneficial acclimation mechanisms prior to winter-like cold exposures, or 15°C may be a more ideal temperature to culture *H. exemplaris* for overall organismal fitness, compared to 20°C. The lack of a strong acclimation response at 1 and 4°C suggests that seasonal acclimatization might not be an important mechanism through which tardigrades survive winter cold, but further work is required to test more ecologically relevant acclimation treatments.

SYTOX Green improves throughput and accuracy of physiological assays in tardigrades, enabling large-scale phenotypic screens

Methodologically, one of the most exciting aspects of this work was the ability to innovate on a more tractable method of scoring tardigrade mortality—via visualization of uptake of the cellular live/dead dye SYTOX Green. Virtually all prior work scored tardigrade survival by the presence of any bodily movement or locomotion, after variable amounts of time post-experiment. Our data suggest that replacing locomotion-based scoring methods with the observation of SYTOX Green uptake predicts survival-related

outcomes with greater accuracy, especially in data sets such as our own, where numerous animals are initially non-mobile but subsequently recovered days or weeks after an environmental stressor. The low-false positive rate of SYTOX Green uptake as a marker of mortality will increase the utility of future physiological assays or screens, where sublethal damage (resulting in lack of initial organismal activity), or delayed onset of locomotion due to dormancy, occurs. Visualization of SYTOX Green uptake allows for mortality scoring within several hours after staining, compared to locomotion, which must be observed at precise times immediately post-cold exposure to ensure optimal accuracy and reproducibility.

In future work, SYTOX Green uptake as a metric for improved mortality scoring should be validated across a broader set of environmental stressors and, in the case of cold stress, a wider range of low temperature temperatures and exposure times. More so, additional validation studies can be conducted to ensure that SYTOX Green staining does not increase mortality in damaged animals. In Chapter 2 of this thesis, we stain tardigrades exposed to low temperatures that result in sublethal damage (-4°C for 120h, Figure 2.2) and see no significant increase in mortality compared to non-cold exposed tardigrades. While these additional findings indicate that SYTOX Green staining does not likely induce mortality in mildly damaged animals, validation studies of SYTOX Green's accuracy and innocuous impacts on tardigrade health across a wider range of cold exposures (and thus extents of underlying damage) could better address these questions.

Nonetheless, findings here provide a pipeline to explore patterns of cold tolerance in a wide diversity of tardigrade species, in a more quantitative and high-throughput manner. This improved methodology for scoring mortality provided here serves as a foundation to further automate phenotypic screens in tardigrades, which could rely on automated imaging collection techniques seen in other microscopic invertebrates or cells, rather than relying on manual inspection alone (Pulak 2006; Dravid et al. 2021). The majority of prior studies examined the survival of dozens to hundreds of tardigrades (Hengherr and Schill 2018), but these improved methods enable the study of thousands of individuals within a single experiment, enabling a higher standard for robust sample sizes in future work.

Conclusions

By relying on visualization of SYTOX Green uptake to score tardigrade mortality, our work examined the effects of several ecologically-relevant environmental factors on cold tolerance at large-scale, with improved accuracy and speed, compared to prior studies that rely on scoring mortality based on locomotion alone. In contrast to the popular science narrative of tardigrades as universally tolerant to all environmental extremes, we found that the survival of *Hypsibius exemplaris* is significantly decreased with lower subzero temperatures and prolonged exposure times, unless animals are frozen alongside external ice-nucleating agents like the bacteria *P. syringae* or prior thermal acclimation at 15°C. This work challenges the narrative that tardigrades are universally tolerant to all environmental stressors, and furthermore demonstrates a more nuanced view of how more ecologically relevant conditions impact tardigrade survival and performance. Our work emphasizes the importance of external ice nucleators on cold tolerance and suggests that bacteria present in the environment of tardigrades likely improve cold tolerance markedly over survival measured in pure water in the laboratory.

This illustrates the importance of considering external ice nucleators more generally in invertebrate cold tolerance strategies.

This work provides key scaffolding for other large-scale phenotypic assays that rely on scoring survival in tardigrades, across a wide range of environmental stressors. More so, we provide a framework for studying stress tolerance across a wide range of tardigrade species, enabling researchers to explore tardigrade physiology through a comparative lens with improved throughput. These advancements further solidify tardigrades as an increasingly tractable emerging model organism, across a growing set of biological disciplines.

1.7 Acknowledgements

Our work was partially supported by several Walker Grants from the Essig Museum of Entomology (2017-2021), Summer Research Awards from the Department of Integrative Biology, UC Berkeley (2017-2022), and an IB Dissertation Completion Award (2021). Kevin T. Roberts performed GLM modeling and consulted in data analysis. Daisy Stock and Kylie Cheng aided in tardigrade viability in Figure 1. Déjenaé See, Kylie Cheng, Lily Shang, and Daisy Stock assisted in tardigrade husbandry. Steven Lindow generously provided *P. syringae* cultures. Michael Shapira generously provided use of fluorescent microscopy equipment. Caroline Williams provided helpful comments in crafting and editing this chapter.

1.8 Figures

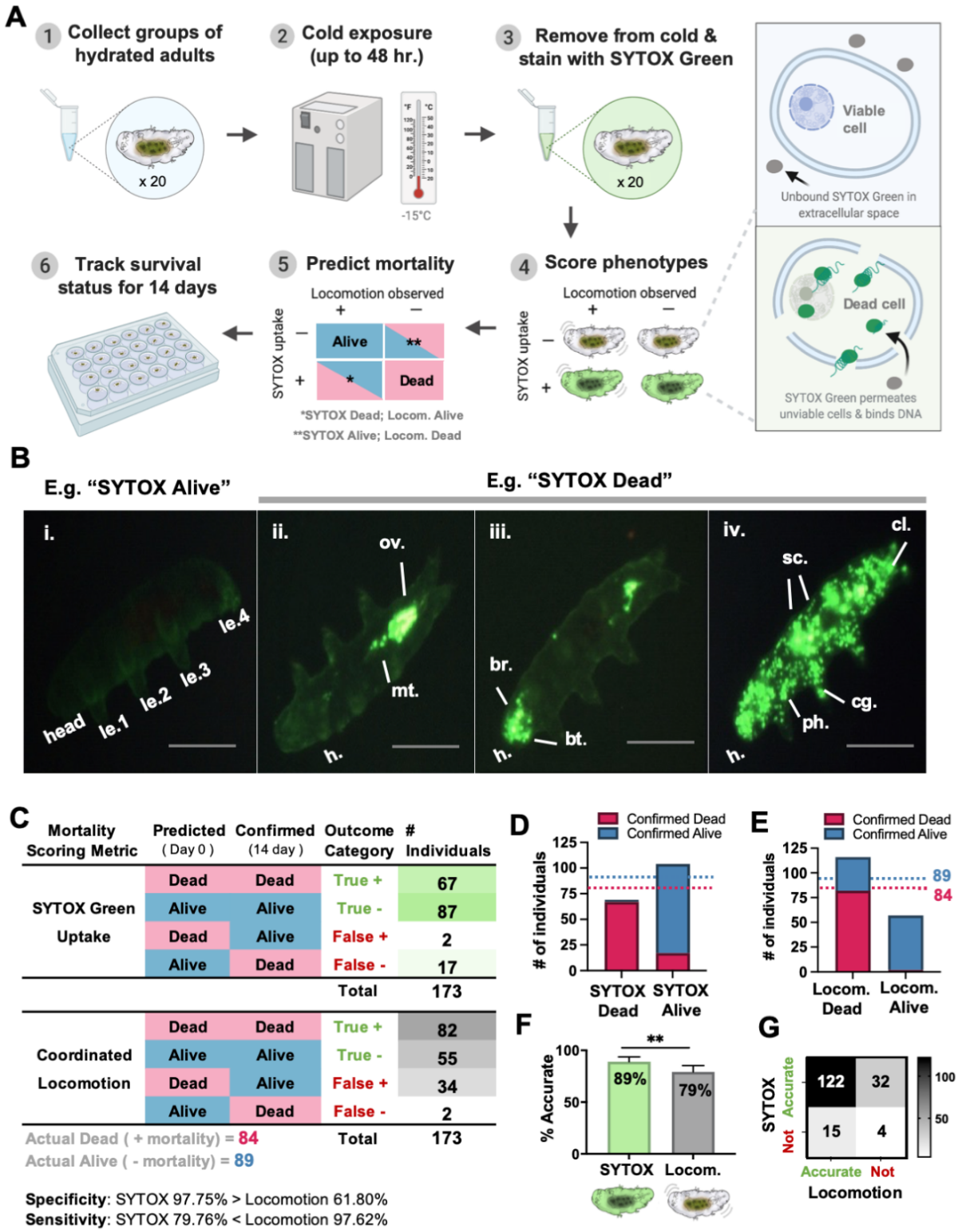

Figure 1.1 Uptake of SYTOX Green stain predicts mortality outcomes of tardigrades after cold exposure more accurately than locomotion

Figure 1.1 continued

(A) Experimental design of the preliminary study to compare the accuracy of SYTOX Green uptake vs. the absence of locomotion in predicting mortality outcomes of cold exposed tardigrades.

(B) Representative staining patterns of SYTOX Green uptake. All tardigrades are shown with heads in the lower-left corner and hind legs in the upper right, although the exact orientation varies. Le: leg, ov: ovaries, mt: malpighian tubules, br: brain, sc: storage cells, cl: cloaca. The scale bar is approximately 10 microns. Tardigrades without any staining (i) were recorded as SYTOX Alive, while those with posterior (ii), anterior and posterior (ii), or whole-body (iv) staining were recorded as SYTOX Dead.

(C) Summary of predictions of long-term survival status based on SYTOX uptake and locomotion on Day 0 ("Predictions") vs. confirmed mortality status after 14 days of observation ("Confirmed").

(D) Bar graph summarizing proportions of tardigrades predicted as dead or alive using SYTOX Green uptake, compared to confirmed values after 14 days (dotted lines: blue = 89 confirmed dead, and pink = 84 confirmed alive).

(E) Bar graph summarizing proportions of tardigrades predicted as dead or alive using locomotion, compared to confirmed values after 14 days (dotted lines: blue = 89 confirmed dead, and pink = 84 confirmed alive).

(F) Bar graph comparing percent accuracy (TP+TN/total) for each mortality scoring metric. SYTOX Green performed significantly better at predicting mortality according to an Exact McNemar test (p-value = 0.01315).

(G) Accuracy matrix for SYTOX Green uptake and locomotion for predicting mortality, used to compute significance levels using the Exact McNemar test.

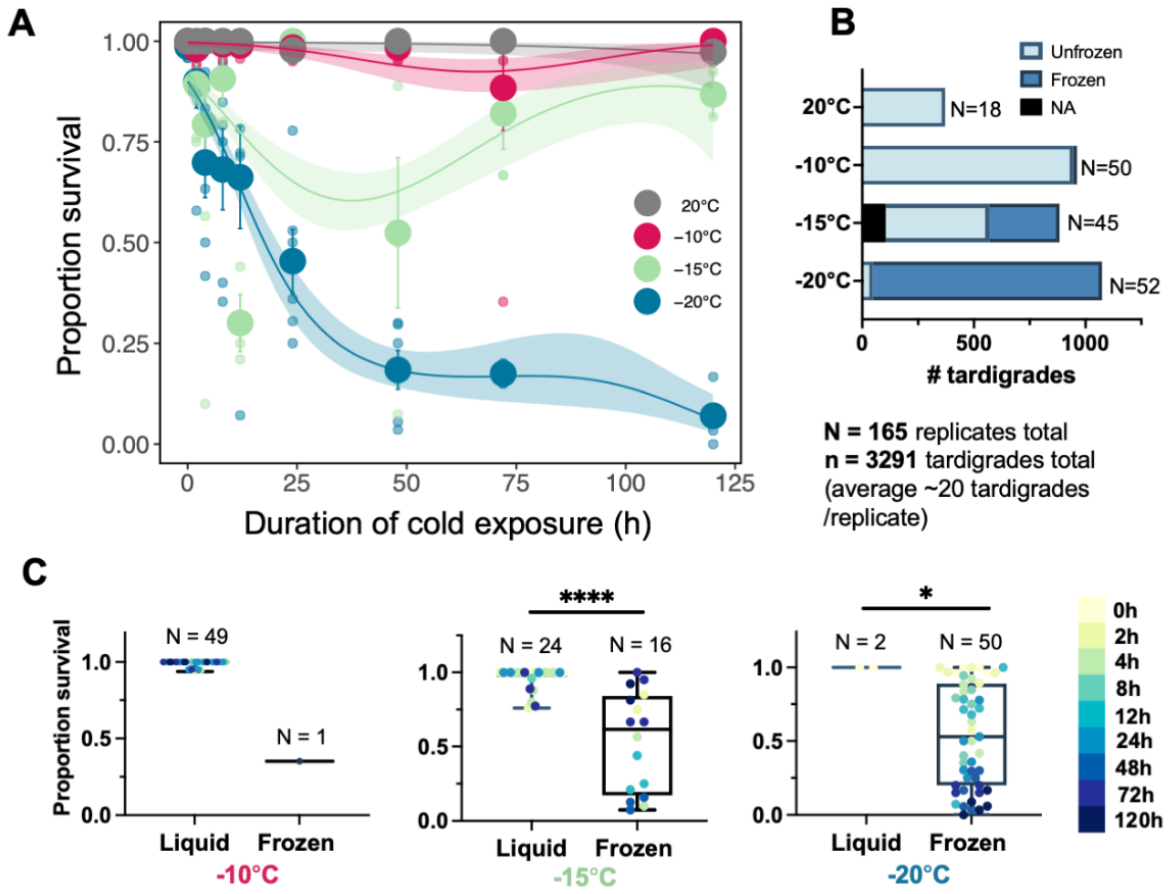

Figure 1.2. Survival of tardigrades decreases with increasing duration and intensity of cold exposure

(A) Proportion survival of tardigrades at a given intensity and duration of cold exposure. Small circles indicate the proportion of survival for each replicate (out of ~20 individuals in a sample group), and large circles indicate the average proportion of survival between six replicates (mean ± SEM). Trendlines represent the best-fit binomial linear mixed model for that temperature (third-degree polynomial) and shading indicates 95% CI on the model predictions. Colors indicate experimental or control temperature.

(B) Numbers of tardigrades among all replicates in each temperature exposure that remained liquid (light blue), froze (dark blue), or whose water status was not recorded (NA=black). N = number of sample replicates (groups of n=~20 tardigrades in a single Eppendorf tube). The majority of samples at -10°C remained unfrozen, whereas nearly all samples froze at -20°C. The freezing status of samples at -15°C was mixed.

(C) Proportion survival of samples exposed to -10°C, -15°C, or -20°C that remained liquid vs. froze. Boxes indicate median and upper and lower quartiles, with whiskers indicating the range of data. Individual data points are colored according to cold exposure time (legend right). Survival of liquid vs. frozen samples was significantly higher, at cold exposures of -15°C and -20°C (p-values=<0.0001 and p-value=0.0282, respectively, according to paired Kolmogorov-Smirnov tests).

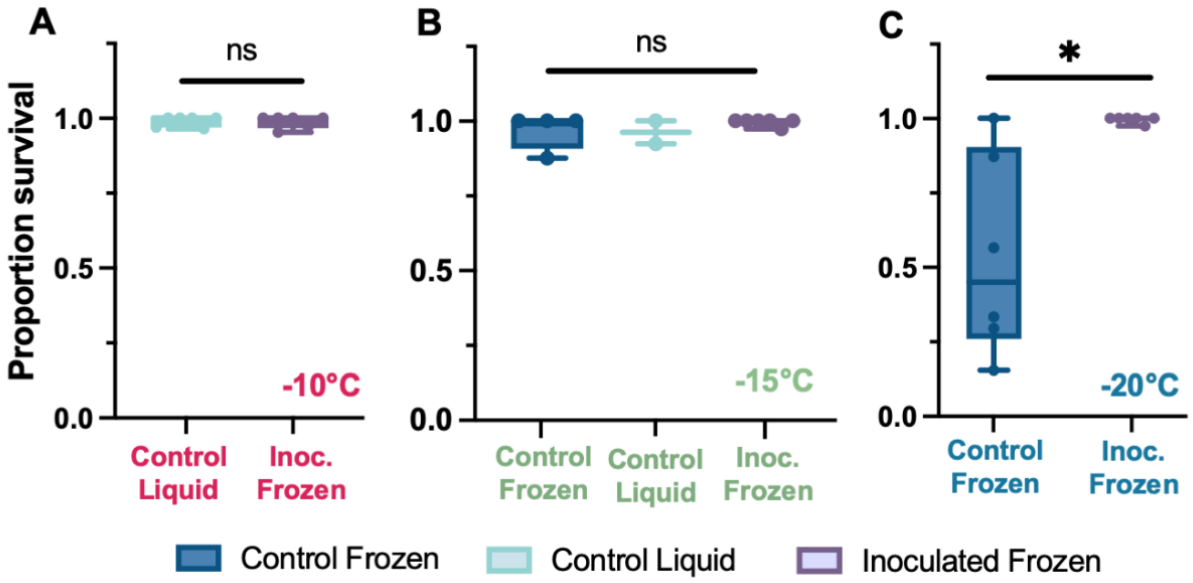

Figure 1.3. Ice-nucleating bacteria seed sample freezing but tardigrade survival remains high

(A-C) Proportion of tardigrades that survived 120 hours of cold exposure, separated by whether they received the ice-nucleating bacteria or not (Inoculated or Control) and whether the water in their tube was frozen or liquid at the end of the cold exposure (Control Frozen = dark blue, Control Liquid (unfrozen) = light blue, Inoculated Frozen = purple). Boxes indicate median and upper and lower quartiles, with whiskers indicating range of data. Individual data points represent sample replicates (tubes of ~20 tardigrades).

(A) Proportion survival of tardigrades exposed to -10°C was not significantly different among control samples that remained unfrozen and froze due to inoculation (p-value >0.9999, Kolmogorov-Smirnov test), indicating that freezing did not result in significant mortality at when induced by inoculation.

(B) Proportion survival of tardigrades exposed to -15°C was not significantly different among control samples that remained unfrozen, control samples that froze, and samples that froze due to inoculation (p-value >0.9999, Kolmogorov-Smirnov tests).

(C) Proportion survival of tardigrades exposed to -20°C was significantly different among control samples that froze and samples that froze due to inoculation (p-value 0.0152, Kolmogorov-Smirnov test). This indicates that the act of freezing alone does not result in mortality, but rather whether freezing is inoculated and at what temperature.

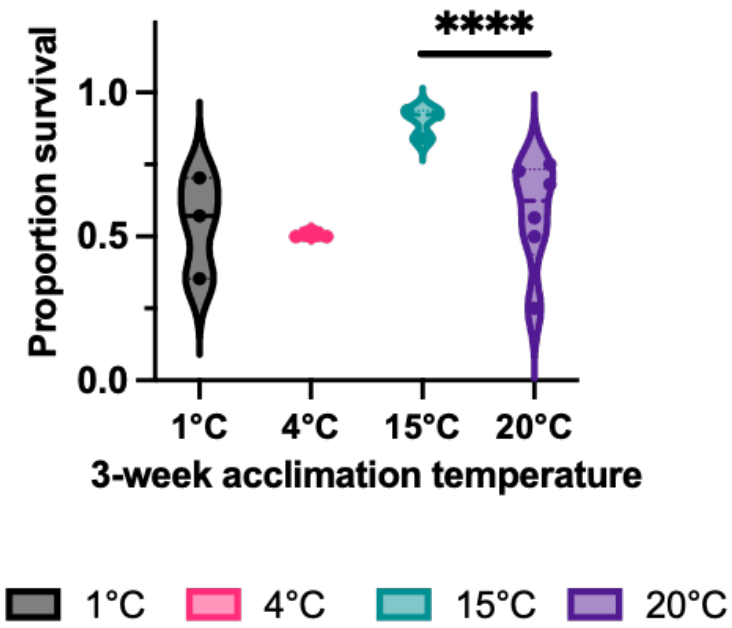

Figure 1.4. Four-week acclimation at 15°C improves tardigrade cold tolerance
Groups of tardigrades were cultured at 1°C, 4°C, 15°C or the standard 20°C culture temperature for 3 weeks and subjected to a cold exposure of -20°C for 24 hours and 25 minutes (~50% survival in Fig 1) and scored for survival using SYTOX Green uptake. Tardigrades acclimated to 1°C and 4°C did not have significantly higher survival than 20°C control conditions (Fisher's exact test, p=0.8868 and p=0.6709, respectively). Tardigrades acclimated to 15°C had higher survival than all other experimental thermal acclimation conditions (p= <0.0001, Fisher's exact test). Boxes indicate median and upper and lower quartiles, with whiskers indicating the range of data.

1.9 Supplementary Materials

A FROZEN SAMPLES

i

Mortality Scoring Metric	Predicted (Day 0)	Confirmed (14 day)	Outcome Category	# Individuals
SYTOX Green Uptake	Dead	Dead	True +	61
	Alive	Alive	True -	26
	Dead	Alive	False +	1
	Alive	Dead	False -	8
			Total	96
Coordinated Locomotion	Dead	Dead	True +	68
	Alive	Alive	True -	13
	Dead	Alive	False +	14
	Alive	Dead	False -	1
			Total	96

Actual Dead (+ mortality) = 69
Actual Alive (- mortality) = 27

Specificity: SYTOX 92.30% > Locomotion 48.15%
Sensitivity: SYTOX 88.41% < Locomotion 98.56%

ii

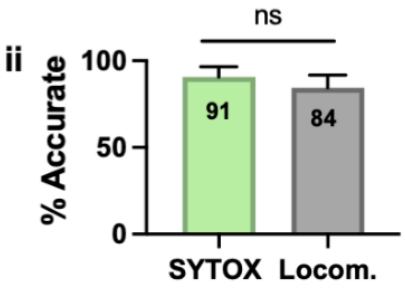

iii

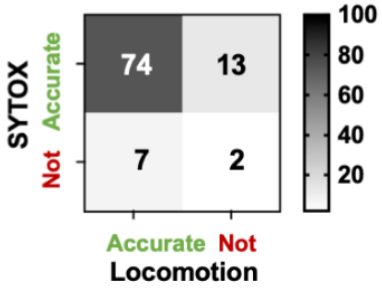

B

i NOT FROZEN SAMPLES

Mortality Scoring Metric	Predicted (Day 0)	Confirmed (14 day)	Outcome Category	# Individuals
SYTOX Green Uptake	Dead	Dead	True +	6
	Alive	Alive	True -	61
	Dead	Alive	False +	1
	Alive	Dead	False -	9
			Total	77
Coordinated Locomotion	Dead	Dead	True +	14
	Alive	Alive	True -	42
	Dead	Alive	False +	20
	Alive	Dead	False -	1
			Total	77

Actual Dead (+ mortality) = 15
Actual Alive (- mortality) = 62

Specificity: SYTOX 98.39% > Locomotion 67.74%
Sensitivity: SYTOX 40% < Locomotion 93.33%

ii

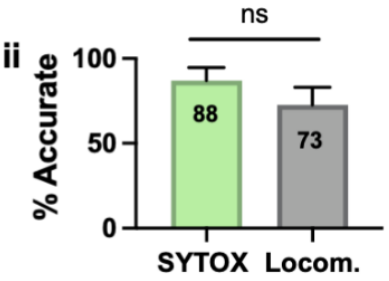

iii

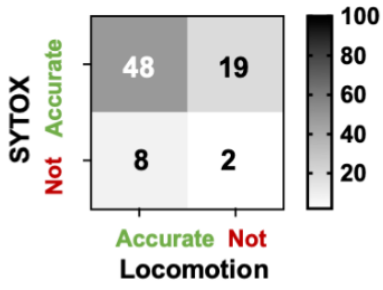

Supplementary Figure 1.1 Accuracy of mortality scoring metrics by water-state (frozen vs. not frozen)

Supplementary Figure 1.1 continued
(A) i. Table summarizing predictions of long-term survival status based on SYTOX uptake and locomotion on Day 0 (“Predictions”) vs. confirmed mortality status after 14 days of observation (“Confirmed”), for samples that froze in Fig 1.
ii. Bar graph comparing percent accuracy (TP+TN/total) for each mortality scoring metric, for frozen samples from Figure 1.1. SYTOX Green did not perform significantly better at predicting mortality according to an Exact McNemar test (p-value = 0.2632).
iii. Accuracy matrix for SYTOX Green uptake and locomotion for predicting mortality in frozen samples, used to compute significance levels using the Exact McNemar test.
(B) i. Table summarizing predictions of long-term survival status based on SYTOX uptake and locomotion on Day 0 (“Predictions”) vs. confirmed mortality status after 14 days of observation (“Confirmed”), for samples that remained liquid in Fig 1.
ii. Bar graph comparing percent accuracy (TP+TN/total) for each mortality scoring metric, for liquid samples from Figure 1.1. SYTOX Green did not perform significantly better at predicting mortality according to an Exact McNemar test (p-value = 0.05224).
iii. Accuracy matrix for SYTOX Green uptake and locomotion for predicting mortality in liquid samples, used to compute significance levels using the Exact McNemar test.

A

Mortality Scoring Metric	Predicted (Day 0)	Confirmed (14 day)	Outcome Category	# Individuals 4 hours	# Individuals 8 hours	# Individuals 12 hours	# Individuals 48 hours
SYTOX Green Uptake	Dead	Dead	True +	11 (18)	5 (13)	28 (30)	23 (23)
	Alive	Alive	True -	24 (25)	30 (30)	8 (9)	25 (25)
	Dead	Alive	False +	1	0	1	0
	Alive	Dead	False -	7	8	2	0
			Total	43	43	3	48
Coordinated Locomotion	Dead	Dead	True +	17 (18)	12 (13)	30 (30)	23 (23)
	Alive	Alive	True -	22 (25)	11 (30)	8 (9)	14 (25)
	Dead	Alive	False +	3	19	1	11
	Alive	Dead	False -	1	1	0	0
Actual Dead (+ mortality)			Total	43	43	39	48
Actual Alive (- mortality)							

B

SYTOX Green Uptake	4 hours	8 hours	12 hours	48 hours
% Accuracy	81.4	81.4	92.31	100
% Specificity	96	100	88.89	100
% Sensitivity	61.11	38.46	93.33	100

Coordinated Locomotion	4 hours	8 hours	12 hours	48 hours
% Accuracy	90.7	53.49	97.44	77.08
% Specificity	88	36.67	88.89	56
% Sensitivity	94.44	92.31	100	100

Exact McNemar test (SYTOX vs. Locomotion accuracy matrix)

	4 hours	8 hours	12 hours	48 hours
p-values	0.2891	0.02896	0.25	0.0009766
Significance	NS	*	NS	***

C

4 hours	Locomotion	
Sytox	Accurate	Inaccurate
Accurate	33	6
Inaccurate	2	2

8 hours	Locomotion	
Sytox	Accurate	Inaccurate
Accurate	16	19
Inaccurate	7	1

12 hours	Locomotion	
Sytox	Accurate	Inaccurate
Accurate	36	0
Inaccurate	2	1

48 hours	Locomotion	
Sytox	Accurate	Inaccurate
Accurate	37	0
Inaccurate	11	0

Supplementary Figure 1.2. Accuracy of mortality scoring metrics across timepoints (regardless of freezing status)

(A) Table summarizing predictions of long-term survival status based on SYTOX Green uptake and locomotion on Day 0 ("Predictions") vs. confirmed mortality status after 14 days of observation ("Confirmed"), for samples in Fig 1 according to -15°C exposure time (4-48 h).

(B) Tables summarizing accuracy metrics and p-values (Exact McNemar tests) of SYTOX Green uptake vs. locomotion, for samples in Fig 1 according to -15°C exposure time (4-48 h).

(C) Accuracy matrix for SYTOX Green uptake and locomotion for predicting mortality in time course-separated samples, used to compute significance levels using the Exact McNemar test.

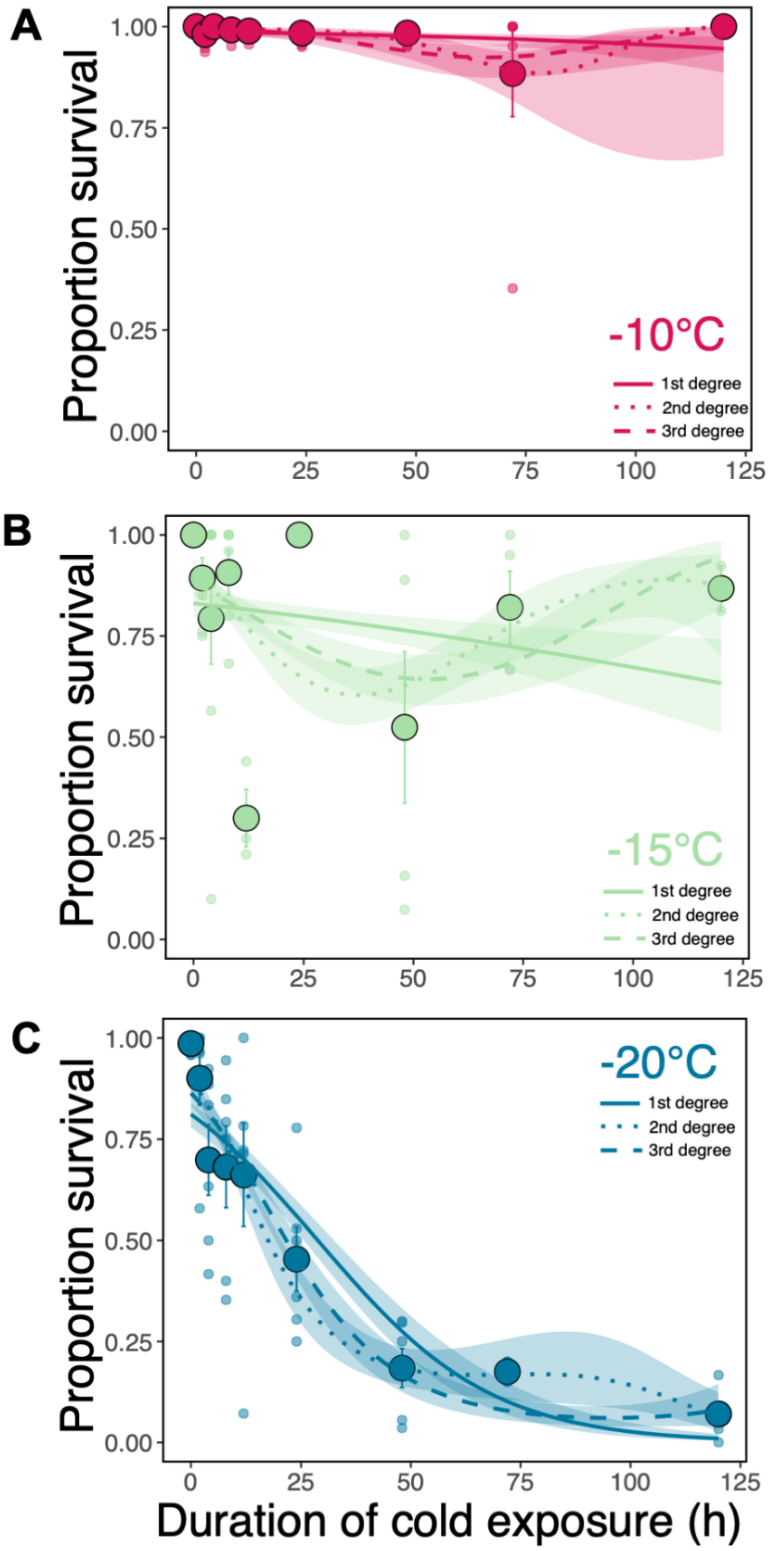

Supplementary Figure 1.3. Selection of best-fit for proportion survival across timepoints for general linear model

Supplementary Figure 1.3. continued
(A) Binomial polynomial fit for the -10°C treatments for first, second, and third-degree polynomials. Best-fit based on AIC is third-degree polynomial (AIC=171.5718) vs AIC values for second-degree (AIC=175.837) or first-degree polynomials (AIC=192.7941). Second-degree polynomial is the best fit for -10°C survival data according to BIC (190.444), compared to first- and third-degree (BIC=202.5322 and 191.0479, respectively).
(B) Binomial polynomial fit for the -15°C treatments for first, second, and third-degree polynomials. Best-fit based on AIC is third-degree polynomial (AIC=845.1951) vs AIC values for second-degree (AIC=853.8989) or first-degree polynomials (AIC=884.2961). Third-degree polynomial is the best fit for -15°C survival data according to BIC (864.333), compared to first- and second-degree (BIC=893.8651 and 868.2523, respectively).
(C) Binomial polynomial fit for the -20°C treatments for first, second, and third-degree polynomials. Best-fit based on AIC is third-degree polynomial (AIC=1017.132) vs AIC values for second-degree (AIC=1028.914) or first-degree polynomials (AIC=1067.566). Third-degree polynomial is the best fit for -20°C survival data according to BIC (1037.049), compared to first- and third-degree (BIC=1043.851 and 1077.524, respectively).

Proportion Survival (non-repeated measurements)

	Replicate	0 hrs.	2 hrs.	4 hrs.	8 hrs.	12 hrs.	24 hrs.	48 hrs.	72 hrs.	120 hrs.
–20°C Survival among reps.	1	1	1	0.63	0.35	0.71	0.3	0.3	0.15	0.09
	2	1	0.58	0.42	0.4	1	0.36	0.17	0.2	0.03
	3	1	1	0.83	0.85	0.68	0.53	0.06	0.15	0
	4	1	0.89	0.5	0.94	0.78	0.25	0.04	0.2	0.17
	5	0.96	0.97	0.88	0.79	0.72	0.5	0.3	NA	0.06
	6	0.96	0.96	0.92	0.75	0.07	0.78	0.25	NA	NA
Overall average by time		**0.99**	**0.9**	**0.7**	**0.68**	**0.66**	**0.45**	**0.19**	**0.18**	**0.07**
Liquid average by time		**1**	NA	NA	NA	NA	NA	NA	NA	NA
Frozen average by time		**0.98**	**0.94**	**0.77**	**0.8**	**0.58**	**0.5**	**0.17**	**0.18**	**0.08**

Overall **liquid** average	**1**
Overall **frozen** average	**0.54**

# of Tardigrades Scored

	Replicate	0 hrs.	2 hrs.	4 hrs.	8 hrs.	12 hrs.	24 hrs.	48 hrs.	72 hrs.	120 hrs.
–20°C # Tardigrades among reps.	1	25	6	30	17	21	23	27	20	23
	2	22	19	12	25	18	25	24	15	30
	3	11	18	30	33	25	17	18	20	18
	4	18	28	32	18	23	16	28	15	12
	5	24	31	26	24	18	18	10	NA	17
	6	24	26	26	24	14	9	8	NA	NA
Total by time		**124**	**128**	**156**	**141**	**119**	**108**	**115**	**70**	**100**
Overall total, all times		**1061**								

Supplementary Table 1.1. Summary of survival data and # of tardigrades used for -20°C samples Light blue indicates samples that froze, whereas Green or red gradients represent variation in the proportion of survival or the number of tardigrades used in each sample, respectively. Grey NA boxes indicate experimental conditions that were not measured, due to human or instrument error.

Proportion Survival (non-repeated measurements)

	Replicate	0 hrs.	2 hrs.	4 hrs.	8 hrs.	12 hrs.	24 hrs.	48 hrs.	72 hrs.	120 hrs.
	1	1	1	1	0.96	0.44	1	0.89	0.67	0.81
–15°C	2	1	0.76	1	1	0.25	1	0.77	0.67	0.92
Survival	3	1	1	1	1	0.21	1	1	0.95	NA
among reps.	4	1	1	1	0.68182	NA	1	0.16	1	NA
	5	1	0.85	0.8	0.8	NA	NA	0.13	NA	NA
	6	1	0.75	0.88	1	NA	NA	0.07	NA	NA
	7			0.1						
	8			0.57						
Overall average by time		**1**	**0.89**	**0.79**	**0.91**	**0.3**	**1**	**0.5**	**0.82**	**0.87**
Liquid average by time		1	0.94	0.95	0.96	NA	1	0.89	NA	NA
Frozen average by time			0.8	0.34	NA	0.3	NA	0.12	NA	NA

Overall **liquid** average	1
Overall **frozen** average	0.79
Overall unknown avg.	0.9

# of Tardigrades Scored

	Replicate	0 hrs.	2 hrs.	4 hrs.	8 hrs.	12 hrs.	24 hrs.	48 hrs.	72 hrs.	120 hrs.
	1	25	15	20	25	25	19	18	24	16
–15°C	2	16	25	20	25	24	25	22	18	13
# Tardigrades	3	20	16	18	10	19	19	27	20	NA
among reps.	4	15	16	19	22	NA	21	19	24	NA
	5	12	20	15	25	NA	NA	16	NA	NA
	6	12	16	25	23	NA	NA	27	NA	NA
	7			10						
	8			23						
	Total	**100**	**108**	**150**	**130**	**68**	**84**	**129**	**86**	**29**
Overall total, all times		**884**								

Supplementary Table 1.2. Summary of survival data and # of tardigrades used for -15°C samples Light blue indicates samples that froze, whereas Green or red gradients represent variation in the proportion of survival or the number of tardigrades used in each sample, respectively. Grey NA boxes indicate experimental conditions that were not measured, due to human or instrument error.

Proportion Survival (non-repeated measurements)

	Replicate	0 hrs.	2 hrs.	4 hrs.	8 hrs.	12 hrs.	24 hrs.	48 hrs.	72 hrs.	120 hrs.
	1	1	1	1	0.95	0.96	0.95	0.95	0.35	1
–10°C	2	1	1	1	1	1	1	0.95	1	1
Survival	3	1	0.95	1	1	1	0.95	1	1	1
among reps.	4	1	0.94	1	1	1	1	1	0.95	1
	5	1	1	1	1	NA	1	1	1	NA
	6	1	1	1	1	NA	1	1	1	NA
Overall average by time		**1**	**0.98**	**1**	**0.99**	**0.99**	**0.98**	**0.98**	**0.88**	**1**
Liquid average by time		1	0.98	1	0.99	0.99	0.98	0.98	0.99	1
Frozen average by time		NA	NA	NA	NA	NA	NA	NA	0.35	NA

Overall **liquid** average	**0.99**
Overall **frozen** average	**0.98**

# of Tardigrades Scored

	Replicate	0 hrs.	2 hrs.	4 hrs.	8 hrs.	12 hrs.	24 hrs.	48 hrs.	72 hrs.	120 hrs.
	1	23	22	21	21	23	20	20	17	18
–10°C	2	23	17	19	21	19	18	22	19	23
# Tardigrades	3	26	19	16	18	22	22	17	21	27
among reps.	4	21	16	17	21	19	16	15	21	25
	5	19	18	16	19	NA	21	16	10	NA
	6	15	16	19	25	NA	12	17	14	NA
Total by time		**127**	**108**	**108**	**125**	**83**	**109**	**107**	**102**	**93**
Overall total, all times		**962**								

Supplementary Table 1.3. Summary of survival data and # of tardigrades used for -10°C samples Light blue indicates samples that froze, whereas Green or red gradients represent variation in the proportion of survival or the number of tardigrades used in each sample, respectively. Grey NA boxes indicate experimental conditions that were not measured, due to human or instrument error.

Proportion Survival (non-repeated measurements)

	Replicate	0 hrs.	2 hrs.	4 hrs.	8 hrs.	12 hrs.	24 hrs.	48 hrs.	72 hrs.	120 hrs.
20°C	1	1	1	1	1	1	0.95	1	1	0.95
Survival	2	1	1	1	1	1	1	1	1	1
Overall average by time		**1**	**1**	**1**	**1**	**1**	**0.98**	**1**	**1**	**0.98**
Liquid average by time		1	1	1	1	1	0.98	1	1	0.98
Frozen average by time		NA	NA	NA	NA	NA	NA	NA	0.35	NA

Overall **liquid** average	**0.99**
Overall **frozen** average	**NA**

# of Tardigrades Scored

	Replicate	0 hrs.	2 hrs.	4 hrs.	8 hrs.	12 hrs.	24 hrs.	48 hrs.	72 hrs.	120 hrs.
20°C	1	21	18	28	21	20	22	22	15	38
# Tardigrades	2	21	19	21	8	20	19	22	16	30
Total by time		**42**	**37**	**49**	**29**	**40**	**41**	**44**	**31**	**68**

Overall total, all times	**381**

Supplementary Table 1.4. Summary of survival data and # of tardigrades used for 20°C control samples Light blue indicates samples that froze, whereas Green or red gradients represent variation in the proportion of survival or the number of tardigrades used in each sample, respectively. Grey NA boxes indicate experimental conditions that were not measured, due to human or instrument error.

–20°C

		# of Tardigrades Scored									
SYTOX Uptake	**Status**	**0 hrs.**	**2 hrs.**	**4 hrs.**	**8 hrs.**	**12 hrs.**	**24 hrs.**	**48 hrs.**	**72 hrs.**	**120 hrs.**	**Total**
None	**Alive**	122	115	112	98	90	44	19	12	9	621
Anterior	**Dead**	0	0	1	1	0	0	2	0	0	4
Posterior	**Dead**	1	2	4	4	7	7	14	2	20	61
Ant.-Post.	**Dead**	1	5	2	0	0	3	8	0	10	29
Whole-body	**Dead**	0	6	37	35	21	52	67	56	72	346
	Total	**124**	**128**	**156**	**138**	**118**	**106**	**110**	**70**	**111**	**1061**

–15°C

		# of Tardigrades Scored									
SYTOX Uptake	**Status**	**0 hrs.**	**2 hrs.**	**4 hrs.**	**8 hrs.**	**12 hrs.**	**24 hrs.**	**48 hrs.**	**72 hrs.**	**120 hrs.**	**Total**
None	**Alive**	100	94	125	117	20	84	69	71	25	705
Anterior	**Dead**	0	2	0	1	2	0	0	0	0	5
Posterior	**Dead**	0	4	3	1	0	0	20	15	1	44
Ant.-Post.	**Dead**	0	0	0	0	0	0	0	0	0	0
Whole-body	**Dead**	0	8	22	11	46	0	40	0	3	130
	Total	**100**	**108**	**150**	**130**	**68**	**84**	**129**	**86**	**29**	**884**

–10°C

		# of Tardigrades Scored									
SYTOX Uptake	**Status**	**0 hrs.**	**2 hrs.**	**4 hrs.**	**8 hrs.**	**12 hrs.**	**24 hrs.**	**48 hrs.**	**72 hrs.**	**120 hrs.**	**Total**
None	**Alive**	127	106	108	123	82	107	107	90	93	943
Anterior	**Dead**	0	0	0	0	0	0	0	0	0	0
Posterior	**Dead**	0	0	0	0	0	1	0	7	0	8
Ant.-Post.	**Dead**	0	0	0	0	0	0	0	0	0	0
Whole-body	**Dead**	0	2	0	2	1	1	0	5	0	11
	Total	**127**	**108**	**108**	**125**	**83**	**109**	**107**	**102**	**93**	**962**

Supplementary Table 1.5. Summary of # of tardigrades exhibiting various SYTOX Green uptake patterns, across each cold exposure's timecourse Green gradients represent variation in the number of tardigrades that did not uptake any SYTOX Green stain (and were scored to survive). Red gradients represent variation in the number of tardigrades that exhibited one of the four SYTOX Green staining patterns (and were scored to have died), according to those shown in Figure 1.1B.

Chapter 2

Plasticity of chill coma in tardigrades (*Hypsibius exemplaris*) in response to cold exposure and photoperiod

2.1 Key Findings

- Tardigrades experience a reversible state of paralysis in response to sublethal cold (12 hours and above, at temperatures between 1°C to -4°C), similar to that seen during chill coma in insects, suggesting loss of neuromuscular function at low temperatures.
- Recovery time from chill coma (chill coma recovery time or CCRT) depends on both exposure time and temperature. We observe a threshold temperature of 0°C, where CCRT decreases with longer cold exposure times, suggesting potential beneficial acclimation. CCRT increases with longer cold exposure times of -3°C and below, suggesting potential sublethal damage.
- Tardigrades recover from chill coma quickly (on average 2-3 minutes) given the length of the cold exposures explored here (up 60 hours), compared to insects.
-A 2-week acclimation to long ("summer") or short day-length ("winter") photoperiod significantly impacts CCRT, with longer photoperiod summer-like days increasing CCRT and shorter winter-like days decreasing CCRT, compared to standard culture-condition controls (constant dim light).

2.2 Abstract

Tardigrades are capable of surviving subzero temperatures, but no reports have been made on their susceptibility to chill coma. Chill coma is a reversible state of paralysis induced by cold but non-freezing temperatures, resulting from ionoregulatory collapse and loss of neuromuscular function. Using *Hypsibius exemplaris* as a model species, we determine the impact of low temperature and duration on the plasticity of chill coma recovery time (CCRT). We exposed *H. exemplaris* to temperatures ranging from -4°C to 1°C for times ranging from 12 to 60 hours and recorded the amount of time required for animals to resume movement at room temperature (CCRT). Below -2°C, tardigrades recovered from chill coma more slowly with increasing cold exposure times (requiring up to ~15 minutes), suggesting some damage may accumulate at those low temperatures. Conversely, tardigrades recovered from chill coma more quickly with increasing time above 0°C, with recovery times as little as ~10 seconds. In a second set of experiments, we explored the impact of a 2-week photoperiod-acclimation (16 hours light: 8 hours dark "summer" or 8 hours light: 16 hours dark "winter") on CCRT. Winter-like photoperiods significantly decreased CCRT compared to summer-like photoperiods as well as constant dim light (lab conditions). Short day ("winter") photoperiods were associated with the fastest CCRTs out of all treatment groups. Establishing methods for CCRTs assays represents crucial foundational work needed to dissect how specific molecular mechanisms underlie cold tolerance strategies in tardigrades, as well as demonstrating the sensitivity of neuromuscular function in an otherwise remarkably tolerant organism.

2.3 Introduction

Nearly all studies examining the impacts of cold on tardigrades measure survival but neglect characterization of other non-lethal, ecologically-relevant phenotypes and behaviors (Hengherr and Schill 2018). Survival of tardigrades to subzero temperatures is highly variable depending on environmental conditions, degree of cold exposure, and species, and the primary focus of numerous prior studies has been on the survival of inactive tardigrades (often desiccated) at extremely low temperatures (Hengherr et al. 2009; Møbjerg et al. 2022; Tsujimoto et al. 2016) with the exception of few studies (Guidetti et al. 2011). While tardigrades are typically form protective tuns or cysts in response to desiccation, radiation, and other environmental stress, it is not well understood how their morphology and behavior is impacted by low temperatures (Guidetti et al. 2011), absent tun formation (Hengherr and Schill 2018). How the physiology of tardigrades is impacted by non-lethal cold temperatures is entirely uncharacterized, and the impact of mild low temperatures, such as those often seen by temperate species in winter months, can provide insight into the ecology and life history of tardigrades during shifts in seasons—as well as illuminating their basic biology and evolutionary history.

While tardigrades are classified in their own distinct phylum, they share some similarities with their sister taxa *Arthropoda* (Smith et al. 2016; Koziol 2018; Campbell et al. 2011). Whether tardigrades' nervous system is impacted to sublethal cold in ways similar to insects, however, remains unknown (Hengherr and Schill 2018). Like insects, tardigrades have a centralized nervous system that controls complex neuromusculature that runs through the periphery of their bodies (Gross and Mayer 2019). This neuromusculature connects to four pairs of legs and allows tardigrades to push off of a variety of surfaces with their claws (Bertolani and Biserov 1996; Gross and Mayer 2019; Martin et al. 2017), mirroring gait patterns seen in insects thousands of times larger (Nirody et al. 2021). Prior studies have proposed that tardigrades may have miniaturized throughout their evolutionary history, which may translate into their remarkable neuromuscular dexterity (Gross et al. 2019). Recent work observing tardigrade gait patterns has hypothesized that tardigrades and arthropods may share common neural circuits that allow for similar gait patterns, due to a common ancestor, despite millions of years of divergent evolution (Mapalo et al. 2021; Guil and Giribet 2012; Jørgensen et al. 2018; Yoshida et al. 2017). A major goal of the work presented here is to determine how cold temperatures impact tardigrade's ability for movement, and whether these impacts may reflect what is seen in the dysregulation of insect neurological function at low temperatures (MacMillan and Sinclair 2011).

In many insect species, individuals lose neuromuscular function at low temperatures by entering a state of reversible paralysis known as chill coma (MacMillan and Sinclair 2011; Overgaard and MacMillan 2017). Chill coma has ecological consequences due to loss of organisms' ability to locomote, feed, reproduce, and evade predators at low temperatures (Findsen et al. 2014; Hazell and Bale 2011). Alternatively, chill coma may otherwise serve as an involuntary mechanism of energy conservation and preservation during winter conditions (Cobb et al. 2021; Lubawy et al. 2022). Chill coma is caused by an inability to maintain ion balance at low temperature, thus affecting the function of ATPases, ion channel gating, the lipid membrane, and ultimately muscle excitability and the proper function of neuromusculature (MacMillan and Sinclair 2011;

MacMillan 2013). The time it takes for organisms to recover from chill coma once returned to permissive temperatures is known as the chill coma recovery time (CCRT), and CCRT is a convenient, widely used, and sensitive assay for neuromuscular function of insects (Hazell and Bale 2011; Andersen and Overgaard 2019; MacMillan et al. 2012). Chill coma recovery time may be determined as the first, involuntary movement of an organism regaining neurological control, or the first signs of full-body or goal-directed movement; and these different end-points likely represent different stages in physiological recovery (MacMillan and Sinclair 2011). There have not yet been any studies investigating chill coma in tardigrades, on any scale.

Chill coma phenotypes display plasticity, in response to environmental factors like temperature, cold exposure, and acclimatization (Overgaard and MacMillan 2017). In *Drosophila melanogaster*, increasing duration and decreasing temperature of cold exposure interacted to increase recovery times (Macdonald et al. 2004). More so, there was a thermal and time-dependent threshold that resulted in flies sustaining chill-injury, beyond reversible chill coma (Macdonald et al. 2004; MacMillan and Sinclair 2011). Insect chill coma can be influenced by acclimation to lower temperature and shifts in photoperiod, such as those seen in winter conditions (longer nights, shorter days) (Bauerfeind et al. 2014; Fischer et al. 2012; Papadopoulos et al. 2022). In particular, these studies have suggested that insects benefit from shorter-day photoperiod acclimation to improve chill coma phenotypes (such as quicker recovery from chill coma)—potentially by allowing for preparation of protective mechanisms (Overgaard and MacMillan 2017).

Here, we explore if *Hypsibius exemplaris* enter and recover from a state of chill coma by developing new methods to measure CCRT, in these microscopic, aquatic organisms. *H. exemplaris* is widely considered to be a cosmopolitan tardigrade species (globally distributed), and individuals inhabit a diversity of limno-terrestrial (moss, leaf-litter, lichen) and limnic habitats (freshwater bodies of water), where locomotion in films of water is required for survival (Goldstein 2018). The type specimen of *H. exemplaris* was collected from a benthic sample from a pond in Darcy Lever, Bolton, Lancashire, England (latitude 53.566166, longitude -2.3925272; British National Grid Ref. SD741078) (McNuff 2018) where animals presumably experience fluctuating low temperatures throughout the wintertime. Although not focused on the species *H. exemplaris*, a field-study conducted in British Columbia detected a high abundance of snow algae genetic material in eutardigrade gut contents during winter months, indicating snow algae consumption and activity of species of tardigrades like *H. exemplaris* at low temperatures (Yakimovich et al. 2020). Thus, maintaining neuromusculature function under cold conditions—or quickly recovering from loss of function, in the case of chill coma—is likely important to tardigrade survival, to allow for locomotion and foraging for food in wintertime months.

By subjecting mixed-staged adult *H. exemplaris* to a range of temperatures (-4°C to 1°C) and exposure times (12 to 60 hours), we characterize the plasticity of chill coma recovery time (CCRT) in tardigrades in response to cold exposure time, low temperature, and these factors' interaction. Because tardigrades are microscopic and difficult to observe using traditional CCRT methods, we utilize video recordings and randomize (blind) video analysis, to accurately calculate CCRT with minimal bias. Video analysis also allows us to document the overall morphology of cold-exposed tardigrades, to infer if tardigrades forgo tun formation, but rather experience chill coma. To determine that chill

coma does not result in mortality in tardigrades, we visualize SYTOX Green uptake in cold-exposed tardigrades (under conditions inducing chill coma). Finally, we subject groups of tardigrades to 2-week photoperiod acclimations (keeping temperature constant, at 20°C), mimicking long summer-like days (18h light: 6h dark) or short winter-like days (6h light:18h dark), to explore if tardigrades recover from chill coma more quickly in winter photoperiodic conditions. Overall, this study is the first to identify that tardigrades experience chill coma, and that recovery of chill coma is plastic depending on time, temperature, and photoperiod.

2.4 Methods

2.4.1 Tardigrade culture

Experiments were conducted on the cosmopolitan eutardigrade species *Hypsibius exemplaris* Z151, purchased from Sciento (Manchester, United Kingdom). Tardigrades were cultured as previously described (Chapter 1) under constant conditions of 20°C (+/- 2°C) and dim light.

2.4.2 Chill coma recovery time assay

To establish whether the chill coma recovery time (CCRT) of *H. exemplaris* is impacted by temperature and duration of cold exposure, we exposed groups (n=50) of hydrated, active mixed-stage adult tardigrades to one of six temperatures (-4°C, -3°C, -2°C, -1°C, 0°C, 1°C, or our control temperature of 20°C) and for one of five exposure times (12, 24, 36, 48, or 60 hours), for a total of 30 treatment groups. Tardigrades (Sciento, Manchester, UK) were collected from culture Petri dishes via manual microaspiration and washed thrice in mineral water (Crystal Geyser), before being placed into a single well of a flat bottom 4-well tissue culture plate (Thermo Scientific). 24 hours prior to the addition of tardigrades, the wells of the 4-well plate were coated with Gorilla Super Glue, using the brush applicator to create a textured surface for tardigrades to freely locomote on, once the glue had thoroughly dried. Once dried, 300µm of mineral water and 150µm of freshwater *Chlorococcum sp.* algae (Sciento, Manchester, UK) were added to each well of the 4-well plate, along with tardigrades, and then parafilm was applied to the perimeter of the plate, sealing the lid to the base. Each time point per temperature had a separate 4-well plate that was prepared with a Thermocron iButton (DS1921G-F5#, Maxim Integrated) set to record temperature every 120 seconds, to determine the ramping rate and final low temperature.

Once prepared in respective 4-well plates, tardigrade samples were placed into a clean, empty 1-pint paint tin (weighted down by a 10lb scuba weight) that served as a secondary container to place the tardigrades into the chilled cooling circulator (Scientific 1167P Heating/Cooling Recirculating Water Bath, VWR, Radnor, Pennsylvania, United States), which was filled with 1 part Ethylene Glycol: 1 part distilled water). For each run of the cooling circulator, 5 plates were stacked in reverse chronological order into the can (1 for each time point), with the longest time points towards the bottom, to allow for quick removal of each plate from the cooling circulator at the designated time. Once tardigrade samples were loaded, the can was carefully lowered in the cooling circulator set to 20°C.

The cooling circulator was then set to the designated temperature, and time point 0 was set as the time that the desired temperature was achieved.

Upon reaching a time point, the designated tardigrade-containing plate was removed from the described apparatus and immediately video recorded at 35X magnification using a digital microscope with camera (Opti-Tekscope OT-M HDMI Microscope Macro Camera Magnifier) for 30 minutes. Exact numbers of tardigrades captured for CCRT measurement varied between recordings, because the number of tardigrades in the 35X magnified field used for video analysis depended on how many tardigrades were in the initial frame of view (random) (Supplemental Tables 2.1 and 2.2). Subsequently, N = 315 individual tardigrades were analyzed in total, for this experiment. Videos recorded from this post-cold exposure observation period were manually viewed and analyzed in QuickTime Player (Version 10.5 (935.5)) using timestamps of movement events, to determine the CCRT of each tardigrade visible in the video frame. Videos among all trials were randomized in filename and order of collection, for blind analysis. Two metrics of CCRT were identified: “full-body movement” (where all legs on a given tardigrade regained movement and the body demonstrated the ability to rotate) or “first movement” (where an initial 1 leg showed movement), to represent what may be physiologically distinct events in chill coma recovery. Some treatment conditions were excluded from analysis (producing missing values for CCRTs), due to failure to capture chill coma recovery time prior to the video recording (human error).

CCRT data were analyzed in R, using a general linear model in RStudio (Version 1.3.1073), with fixed effects of time and temperature and the response variable of CCRT (either full body movement or first movement). In total, 26 of 30 treatment group videos were collected and analyzed (with 4 timepoints and temperature conditions not successfully captured). Tardigrades with CCRTs greater than 900 seconds were removed from the dataset (N=2 of 315 tardigrades), as they likely represented outliers. P-values were computed using one-sided ANOVA tests in R. An additional 5 videos of 20°C controls were likewise collected and analyzed.

2.4.3 Survival assay of cold-treated tardigrades

To determine if chill coma resulted in mortality, we stained tardigrades with SYTOX Green after a 120h cold exposure to a range of chill-coma inducing temperatures, using methods described in Chapter 1 (-4°C: N=25, 1°C: N=25, 20°C: N= 50). Animals were examined under a Leica DMRXA2 upright fluorescent microscope equipped with a Leica I3 long-pass GFP filter and a Leica DC500 camera (Leica Microsystems, Wetzlar, Germany) and scored as alive if there was no visible SYTOX Green uptake, and dead if SYTOX Green was visible. Data were analyzed via a non-parametric Kolmogorov-Smirnov test, calculating approximate P-values for significance between the proportion survival of tardigrades in each cold exposure vs. the 20°C control (GraphPad Version 9.3.1).

2.4.4 Chill coma recovery time assay with photoperiod acclimation

To investigate the plasticity of CCRT in response to photoperiod, we placed standard culture dishes of tardigrades under custom-made light boxes set to timers of either 16 hours light: 8 hours dark (simulating long summer-like photoperiods) or 8 hours light: 16 hours dark (simulating short winter-like photoperiods) for an acclimation period

of two weeks (both conditions held at ambient culture temperatures of 20°C). Once the 2-week photoperiod acclimation was completed, tardigrades were processed for CCRT assays as described above. Groups of tardigrades (n=50) were subjected to one of five cold exposure times used in prior experiments (12, 24, 36, 48, 60 hours), at a single cold exposure temperature of -3°C. This temperature was selected as our single post-photoperiod acclimation cold exposure temperature because it induced a pattern of increasing CCRT with exposure time in prior experiments, and we hoped to explore if winter-like photoperiod acclimation could minimize these damaging effects. As in prior CCRT experiments, exact numbers of tardigrades captured for CCRT measurement varied between recordings, because the number of tardigrades in the 35X magnified field used for video analysis depended on how many tardigrades were randomly in the initial frame of view (Supplemental Tables 2.3 and 2.4). Subsequently N = 197 individual tardigrades were analyzed in total, for this photoperiod acclimation experiment. Unlike in the prior CCRT experiments, iButtons were not used to monitor the precise temperature of the cooling circulator—although the prior experiment suggested that the actual temperature varies roughly +/-1 degrees from the set low temperature.

CCRT data from photoperiod-acclimated tardigrades were analyzed in R, using a general linear model in RStudio (Version 1.3.1073) (lm function), with main effects of time and photoperiod and the response variable of CCRT. P-values were computed using one-sided ANOVA tests with Tukey post-hoc comparisons.

2.5 Results

We found that *Hypsibius exemplaris* exhibits reversible paralysis after exposure to 1°C and below (down to -4°C) for exposure times ≥12 hours (Figure 2.1B and 2.1C), suggesting that they experience chill coma. As inferred by visualization of video recordings, tardigrades did not form tuns (a dormant state, that results in a change in the overall morphology of their body-shapes) in response to cold-exposure but rather their bodies elongated and ceased all movement, indicating chill coma.

Two metrics of movement were used to score the amount of time tardigrades needed to recover from chill coma: Full-body movement (Fig 2.1B) or first-movement (Fig 2.1C). Tardigrades recovered from chill coma by both metrics, although the plasticity of time required to recover varied by metric. Scoring chill coma recovery time (CCRT) using full-body movement as the metric required tardigrades to show movement of all legs, as well as movement in the epicenter of the whole organism, as an indication of voluntary locomotion. Scoring chill coma recovery time (CCRT) using first-movement required tardigrades to move only one leg, as an initial indicator of neuromuscular recovery.

Chill coma recovery times (CCRT) were plastic and ranged from as short as 34 seconds (after 60 hours at 0°C) to as long as 814 seconds (after 60 hours at -3°C) (Supplementary Table 2.1), when using full body movement as the CCRT metric. CCRT was significantly impacted by the interaction of low temperature and duration of cold exposure, for both full-body movement recovery (Figure 2.1B; $F_{311,1} = 7.530$, p-value < 0.001) and first-movement (Figure 2.1C; $F_{299,1} = 14.565$, p-value < 0.001), as determined by one-way ANOVA tests. Lower temperatures generally led to longer CCRT, for recovery of both full movement ($F_{311,1} = 92.884$, p-value < 0.001) and first movement ($F_{299,1} = 9.094$, p-value = 0.003).

When using full-body movement as our metric of CCRT (Figure 2.1B), tardigrade CCRTs became longer with increasing exposure time for the two lowest temperatures (-4°C and -3°C). At the two moderate temperatures (-2°C and -1°C), tardigrade recovery times remained constant at an average of 150.8 seconds regardless of exposure time. At the two mildest temperatures (0°C and 1°C), tardigrade CCRTs decreased with cold exposure time. Statistical trends and conclusions were identical when using first-body movement as our recovery metric for CCRT (Figure 2.1C), although the variation in CCRT across the time course was less pronounced compared to full-body movement.

We observed that chill coma in tardigrades requires multiple hours to induce and resulted in no mortality. Preliminary experiments (data not shown) suggested that tardigrades do not enter chill coma for periods equal to or less than 12 hours at 4°C. Chill coma in these tardigrades was reversible and resulted in no mortality in any animals recorded (N = 315 individuals exposed to experimental conditions), regardless of cold exposure, based on their recovery of locomotion. All control 20°C exposed tardigrades (N = 120) did not experience chill coma and had a CCRT of 0 seconds (data not shown). In an additional experiment to validate the lack of mortality in tardigrade chill coma, visualization of SYTOX Green uptake indicated that tardigrades did not experience significant mortality after even the longest cold exposure of 120h to -4°C or 1°C, compared to tardigrades held at standard room temperature culture conditions (Figure 2.2, Kruskal-Wallis test, $p = 0.41$).

In photoperiod acclimation experiments, we found that CCRT based on full-body movement was significantly quicker among short-day “winter” photoperiod acclimated tardigrades (6 hour light: 18 hour dark) and long-day “summer” photoperiod acclimated tardigrades (18 hour light: 6 hour dark) (Tukey’s HSD, p-adj. < 0.001) (Figure 2.3). CCRTs were significantly shorter in 8h light: 16h dark (“winter”) acclimated tardigrades compared to non-acclimation tardigrades (Tukey’s HSD, p-adj. < 0.001), but not between 16h light: 8h dark (“summer”) and non-acclimation tardigrades (Tukey’s HSD, p-adj. = 0.977). None of these comparisons showed significance when using “first-movement” as the CCRT metric (Supplementary Figure 2.1, Tukey’s HSD, winter vs. summer: p-adj. = 0.45; winter vs. non-acclimated: p-adj. = 0.17; summer vs. non-acclimated: p-adj. = 0.89).

2.6 Discussion

This study is the first to document and characterize chill coma, a phenotype of cold-induced but reversible paralysis, in any species of tardigrade. Chill coma can be highly plastic in various insect species, depending on environmental conditions like cold exposure time and low temperature (Macdonald et al. 2004; Macmillan and Sinclair 2011). While focusing on a single tardigrade species *Hypsibius exemplaris*, we determined that CCRT of tardigrades also exhibits significant plasticity according to exposure time, low temperature, and their interaction, at exposure times between 12-60 hours and at temperatures between -4°C to 1°C. At a thermal threshold of ≥0°C, tardigrades required less time to recover from chill coma in response to longer cold exposure times, suggesting improved cold-hardiness with time. These trends of decreasing CCRTs at ≥0°C suggest potential beneficial acclimation to low temperature with time, which may allow for the production or acclimation of protective biochemical mechanisms to chill coma and cold.

Examples of general biochemical mechanisms that may improve chill coma recovery times are those that help maintain or restore cation concentrations in neuromusculature, activate voltage dependent channels, maintain or restore membrane resting potentials in muscles and lipid membrane fluidity, prevent oxygen-related limitations, and improve performance of ion-motive ATPases at low temperatures (Overgaard and MacMillan 2017). Alternatively, we observed that tardigrades required more time to recover from chill coma at a thermal threshold of ≤ -3°C, in response to longer cold exposure times, suggesting decreased cold-hardiness beyond these low temperatures. These trends of increasing CCRTs (reduced cold hardiness) could suggest the accumulation of sublethal damage and/or dampening of repair mechanisms at the thermal threshold of -3°C or below. More specifically, examples of sublethal damage that may prolong CCRTs include deficiencies in the function of any of the biochemical mechanisms listed above. These trends in shifting plasticity of CCRTs remained consistent among both chill coma recovery metrics: full movement (all legs move and torso rotates) and first movement (one leg initially moves), which may represent distinct physiological aspects of chill coma recovery (Overgaard and MacMillan 2017).

The observation of chill coma is entirely absent in prior tardigrade literature (Hengherr and Schill 2018), and it fills a gap in understanding the physiological responses of tardigrades to cold. Furthermore, study of chill coma in tardigrades provides new insight into how their neurological architecture and function may overlap or differ with sister taxa, such as insects, especially in response to cold. The range of chill coma recovery times in *Drosophila*, for example, can be very broad: Spanning from under 2 minutes to over an hour after exposure to 0°C, depending on exposure time (Macdonald et al. 2004; Gibert et al. 2001). Here we see that chill coma recovery time in *H. exemplaris* remained under 15 minutes in all treatment groups tested for the recovery of full body movement, and less than 3 minutes for first movement in all treatment groups. Macdonald et al. 2004 furthermore observed the impact of time and low temperature interacting to influence CCRT recovery in time in *Drosophila*, by observing a steep increase in coma recovery times in the longest cold exposure times (6-7 hours), increasing CCRT to over 40 minutes on average (from 5-20 minutes, at lower temperatures and exposure times). Alternatively, we observed this trend in lengthening CCRT with tardigrades' increased cold exposure time at or below -3°C, but with CCRT reaching comparatively lower CCRTs reaching maximums of less than 15 minutes. Macdonald et al. 2004 additionally observed a plateau in chill coma recovery times at intermediate cold exposure temperature (between -1°C and 1°C)—similar to our observations of such a plateau at the lower temperatures -2°C and -1°C.

Thus, while tardigrades apparently share the susceptibility to experience chill coma in fashion that is dependent on both time and low temperature, we can predict that they may utilize unique mechanisms for restoring ion balance and neuromuscular function at a more rapid pace, or have unique benefits due to their microscopic size, allowing them to recover from chill coma more quickly, compared to insects. Tardigrades' microscopic size may be especially important in enabling rapid CCRTs, as the distribution of ion channels and ion flux may scale with surface area, vs. volume of impacted cells. More directly measuring how ion balance, neuron function, and muscle function is impacted by low temperature in tardigrades, and thus orchestrates chill coma, will be crucial for making

further comparisons of the physiology and molecular mechanism underlying chill coma in these sister-taxa.

Specimens of *H. exemplaris* are likely exposed to temperatures studied here (ranging from -4°C to 1°C) during winter months in their natural habitats, as they are globally distributed temperate species (Goldstein 2018) and their type-specimen originates from a seasonally cold climate, in the United Kingdom (McNuff 2018). Observation of chill coma in tardigrades offers a proposed mechanism for how individuals can rapidly cycle in and out of activity during winter months (Ono et al. 2021; Yakimovich et al. 2020; Guidetti et al. 2011; Guidetti and Møbjerg 2018) and survive long term storage at 4°C without the addition of new food source, for months at a time, for use in laboratory settings (McNuff 2018). The thermal thresholds of 0°C for predicted beneficial acclimation and -3°C for predicted damage accumulation in CCRTs may hold some currently unknown ecological or physiological relevance. In *Drosophila*, shorter CCRTs represent a more cold-hardy organism and improved fitness in winter conditions (Kristensen et al. 2008), and such changes in CCRTs may confer similar fitness changes to tardigrades in winter-months. It is worth noting, however, that the practical impact of a several minute faster chill coma recovery in tardigrades may not confer a notable ecological advantage. Likewise, these shortened CCRTs may not represent a true beneficial acclimation, without further investigation of the tardigrades' downstream fitness after CCRTs (Woods and Harrison 2002). Additionally, these trends of plastic CCRTs may differ depending on the species and ecological habitat of the tardigrade, which should be explored in future work for a more complete understanding of the ecophysiology of the phylum as a whole. For example, CCRT has been shown to vary among evolutionary distinct populations of numerous insects, and has been proposed to influence the geography of species distribution (Gibert et al. 2001; Castañeda et al. 2005; Andersen et al. 2015), which may also hold true in the wide diversity of tardigrade species.

As an additional source of plasticity, we observed that 2-weeks acclimations of tardigrades to short-day winterlike photoperiods (8h light: 16h dark) significantly reduces CCRT, compared to long-day summer-like photoperiods (16h light: 8h dark) or no photoperiod acclimation (standard lab conditions, constant dim light). These findings suggest that tardigrades may become more cold-hardy with seasonal shifts in daylength, although the mechanism is unknown. Tardigrades may respond to photoperiod cues with their primitive eyespots or through some other uncharacterized, light-sensitive physiological mechanism (Fleming et al. 2021). This is the first study in tardigrades to look at the impact of photoperiod or environmental acclimation on any thermal performance or environmental stress response. Our findings mirror findings in several insect species, whereas cold tolerance improves with decreasing daylength (Wallingford et al. 2016; Bauerfeind et al. 2014). More rigorously acclimatizing tardigrades to winter conditions with additional environmental cues, such as gradually reducing temperature with daylength, or subjecting tardigrades to fluctuating thermal regimes (Colinet et al. 2018), may consequently yield more pronounced adaptations to low temperatures.

Lastly, this study joins a growing body of literature that utilizes video recordings to quantify changes in tardigrade physiology and behavior (Shcherbakov et al. 2010; Nirody et al. 2021; Hering et al. 2016; Heikes and Goldstein 2018). Without methods to record tardigrade movement immediately after removal from low temperatures, it would not have been possible to quantify CCRT in the quantity of animals studied here. Yet, future

iterations of CCRT in tardigrades could be further improved by automating video analysis, using tools such as DeepLabCut (Mathis et al. 2018), which would increase throughput and likely improve standardization of measurements across experiments and research groups.

In summary, this work is the first to observe chill coma in any species of tardigrade. Unlike the morphological changes in response to desiccation or other better-studied environmental stressors, we found that tardigrades of the species *Hypsibius exemplaris* do not form protective tuns or cysts in response to non-freezing low temperatures, but rather experience a total cessation of movement known as chill coma. Like in insects, we found that recovery time from chill coma is plastic depending on environmental conditions (temperature, duration of cold exposure, photoperiod). But unlike many insect species, we found that chill coma is induced in tardigrades at 12+ hour exposures to low temperature and recovery from chill coma is rapid (on the order of seconds, rather than minutes or hours). The exact conditions required for chill coma onset should be explored in future work.

More specifically, we determined that CCRT of *H. exemplaris* depends on both exposure time and exposure temperature, and we identified thermal thresholds where CCRT shortens with exposure time (≥0°C) or becomes longer (≤-3°C). Likewise, we found that 2-week acclimations of tardigrades to shorter day lengths (mimicking winter conditions) can also significantly decrease CCRT: a potential sign of improved cold-adaptation. Virtually all prior studies of cold tolerance in tardigrades have focused on measuring survival alone, but here we present a new assay and phenotype to further characterize tardigrade cold tolerance, applicable to a wide range of species and habitats. Work in the thermal physiology of insects suggests that chill coma can be one of several phenotypes to gauge the overall thermal performance of species, but should not necessarily be the only sublethal phenotype characterized (Davis et al. 2021). Overall, these findings suggest similar behaviors of the neuromuscular function of tardigrades in response to cold, as seen in insects. The precise molecular mechanisms and evolutionary origins of chill coma in tardigrades is an exciting avenue for future research.

2.7 Acknowledgements

Our work was partially supported by a Walker Grant from the Essig Museum of Entomology (2017), the NSF REU @ UC Berkeley Integrating Biology from Molecules to Ecosystems, and a Summer Research Award from the Department of Integrative Biology, UC Berkeley (2017). Paige Byassee and Ananya Krishnapura helped perform CCRT assays and tardigrade husbandry. Caroline Williams and Paige Byassee assisted in data analysis of Figure 2.1, and Caroline Williams provided helpful comments in crafting and editing this chapter. Michael Shapira generously provided use of fluorescent microscopy equipment, needed for SYTOX Green uptake visualization.

2.8 Figures

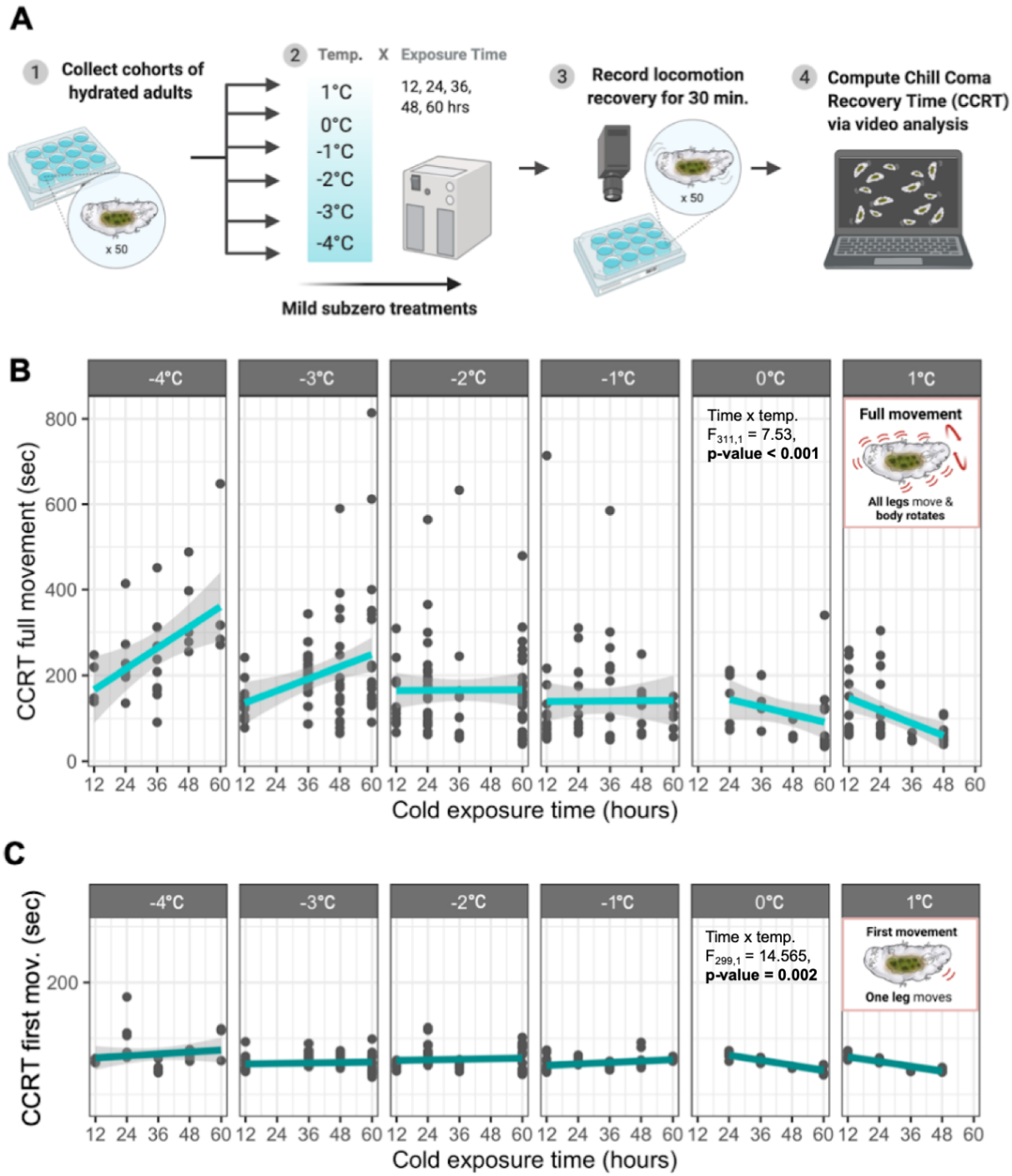

Figure 2.1. Chill coma recovery time assay (CCRT) illustrates that tardigrades recover quickly from cold-induced paralysis (in less than 15 minutes), but at rates depending on exposure time and low temperature

A) Experimental design of CCRT assay. Groups of 30-50 adult tardigrades are collected and exposed to a cold treatment (with a final low temperature between -4°C to 1°C) or ambient temperature (20°C) for up to 60 hours, where after their recovery from

Figure 2.1. continued
cold-induced paralysis to “fully-body movement” (B) or “first-movement” (C) is recorded (computing the “Chill coma recovery time” or CCRT).
B) Time observed for tardigrades to transition from a state of chill coma to full-body movement (when all visible legs show movement, as well as the epicenter of the body, as an indication of voluntary locomotion), across cold exposure times and temperatures. Trendlines represent the linear fit for that temperature and shading indicates 95% confidence intervals. CCRT increases with exposure time, for temperatures at or lower than -3°C. CCRT decreases with exposure time, for temperatures at or above than 0°C. The interaction of time and temperature impacting full-body CCRT is significant ($F_{311,1}$ = 7.53, p-value < 0.001), as well as the impact of temperature ($F_{311,1}$ = 26.112, p-value < 0.001) but not the impact of time ($F_{311,1}$ = 1.737, p-value = 0.189), as determined by one-way ANOVA tests.
C) Time observed for tardigrades to transition from a state of chill coma to first- movement (when one leg shows movement, as an initial indicator of neuromuscular recovery), across cold exposure times and temperatures. The interaction of time and temperature impacting first-body CCRT is significant ($F_{299,1}$ = 14.565, p-value = 0.002), as well as the impact of temperature ($F_{299,1}$ = 9.094, p-value = 0.003) but again not the impact of time ($F_{299,1}$ = 0.124, p-value = 0.724), as determined by one-way ANOVA tests.

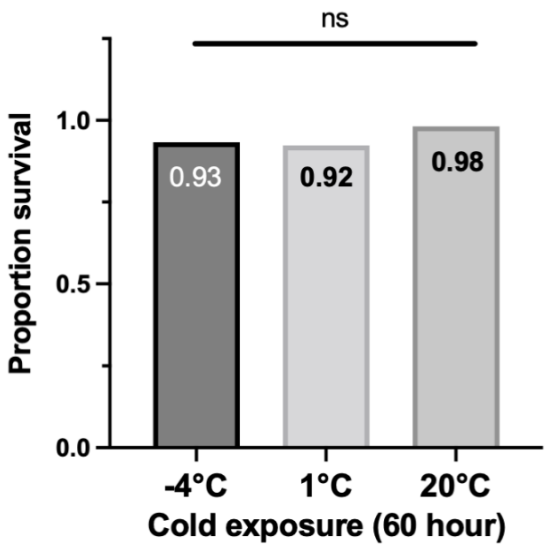

Figure 2.2. Exposure times and temperatures that induce chill coma in tardigrades do not result in significant mortality

Groups of ~15-50 adult tardigrades are collected and exposed to a cold treatment (-4°C, -1°C) or ambient temperature (20°C) for 120 hours, and their proportion of subsequent survival is measured by visualizing the presence or absence of SYTOX Green stain (indicating mortality or survival, respectively). Survival of cold treated tardigrades, recovered from chill coma, do not significantly differ from those kept at standard culture conditions (20°C) (p-value = 0.410, Kruskal-Wallis test). The treatment groups consisted of these number of tardigrades: 15 (-4°C), 26 (-1°C), 55 (20°C).

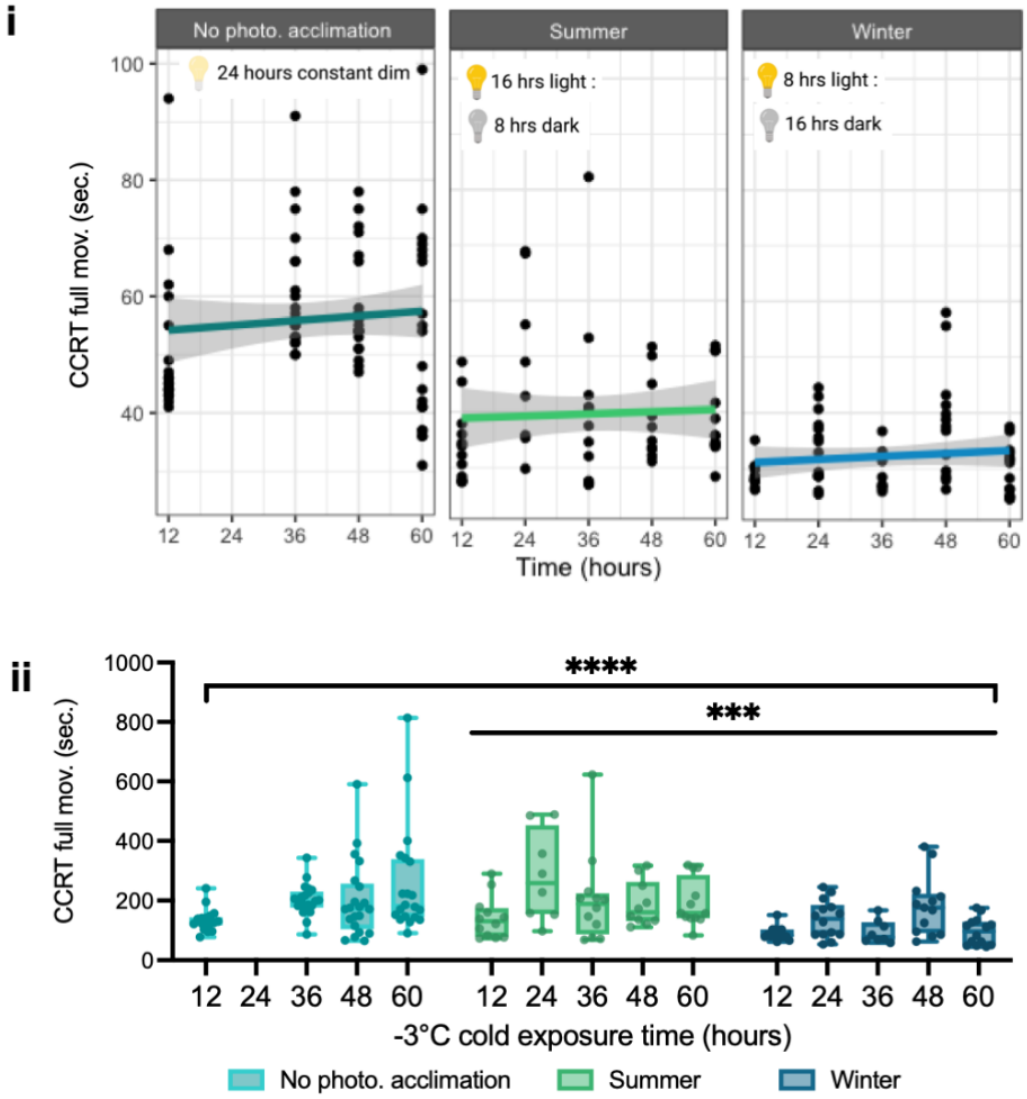

Figure 2.3. Two week acclimation to photoperiods mimicking seasonal long or short-days significantly impacts full-body movement CCRT

i) Tardigrades were acclimated to 16h light: 8h dark ("summer"), 8h light: 16h dark ("winter"), or no photoperiod (constant dim 24 hours, standard culture conditions) for two 2 weeks (keeping a culture temperature of 20°C constant for all photoperiods). Tardigrades were then exposed to -3°C for 12-60 hours, from which CCRT was measured according to "full-body movement." CCRT was significantly shorter among short-day "winter" photoperiod acclimated tardigrades vs. long-day "summer" photoperiod acclimated tardigrades (Tukey's HSD, p-adj. < 0.001). CCRTs were significantly shorter in "winter" photoperiod acclimated tardigrades compared to non-acclimation (Tukey's HSD, p-adj. < 0.001), but not between "summer" and non-acclimation tardigrades (Tukey's HSD, p-value = 0.977).

ii) Same dataset, visually illustrating p-values of corresponding comparisons.

2.9 Supplementary Materials

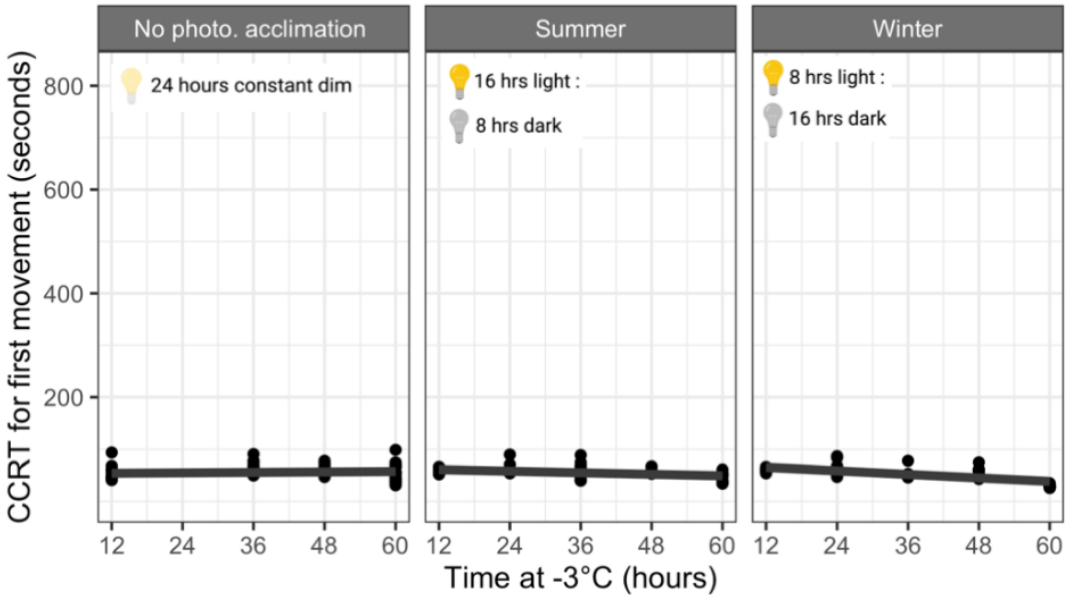

Supplementary Figure 2.1. Acclimation to winter or summer-like photoperiod conditions does not significantly impact first-movement CCRT
Tardigrades were acclimated to 16h light: 8h dark ("summer"), 8h light: 16h dark ("winter"), or no photoperiod (constant dim 24 hours, standard culture conditions), and exposed to -3°C for 12-60 hours, from which there CCRT was then measured according to "first-movement." No comparisons between acclimation types showed significance when using "first-movement" as the CCRT metric (Tukey's HSD, winter vs. summer: p-adj. = 0.45; winter vs. non-acclimated: p-adj. = 0.17; summer vs. non-acclimated: p-adj. = 0.89).

A

 # Tardigrades per treatment group

Temp. (C)	12 hrs.	24 hrs.	36 hrs.	48 hrs.	60 hrs.	Total by temp.
-4	4	7	10	5	4	30
-3	18	NA	21	21	20	80
-2	12	26	11	NA	27	76
-1	19	13	11	11	8	62
0	NA	7	6	3	12	28
1	11	11	5	12	NA	39
Total by time	64	64	64	52	71	315

B

Average CCRT for full movement (sec)

Temp. (C)	12 hrs.	24 hrs.	36 hrs.	48 hrs.	60 hrs.	Avg. by temp.
-4	187.8	236.3	215	343.6	380	272.5
-3	134.8	NA	202.3	200.4	202.3	185
-2	142.9	180.3	157.3	NA	164.3	161.2
-1	122.3	137.8	202.5	135.5	104.1	140.4
0	NA	144.7	133.7	70.3	96.7	111.4
1	136.8	140.8	52.8	62.5	NA	98.2
Avg. by time	144.9	168	160.6	162.5	189.5	

C

Minimum CCRT for full movement (sec)

Temp. (C)	12 hrs.	24 hrs.	36 hrs.	48 hrs.	60 hrs.	Total by temp.
-4	138	135	91	255	271	178
-3	78	NA	87	65	91	80.3
-2	67	62	54	NA	40	55.8
-1	52	66	50	61	57	57.2
0	NA	73	70	53	34	57.5
1	61	60	47	39	NA	51.8
Avg. by time	79.2	79.2	66.5	94.6	98.6	

D

Maximum CCRT for full movement (sec)

Temp. (C)	12 hrs.	24 hrs.	36 hrs.	48 hrs.	60 hrs.	Total by temp.
-4	247	414	451	488	648	449.6
-3	241	NA	343	590	814	497
-2	309	564	633	NA	479	496.3
-1	714	310	585	249	151	401.8
0	NA	211	201	98	340	212.5
1	258	304	67	110	NA	184.8
Avg. by time	353.8	360.6	380	307	486.4	

Supplementary Table 2.1. Summary of # of tardigrades used and full movement CCRT data for Fig. 2.1A Full movement is defined by all legs showing movement and the whole-body rotating when tardigrades are restored to 20°C, after cold-induced paralysis (chill coma) (A) # of tardigrades per treatment group (B) Average chill coma recovery time (CCRT) in seconds per treatment group (C) Minimum CCRT time in seconds per treatment group (D) Minimum CCRT time in seconds per treatment group.

A

 # Tardigrades per treatment group

Temp. (C)	12 hrs.	24 hrs.	36 hrs.	48 hrs.	60 hrs.	Total by temp.
-4	4	7	10	5	4	30
-3	18	NA	21	21	20	80
-2	12	26	11	NA	27	76
-1	19	13	11	11	8	62
0	NA	7	6	3	12	28
1	11	11	5	12	NA	39
Total by time	64	64	64	52	71	315

B

Average CCRT for first movement (sec)

Temp. (C)	12 hrs.	24 hrs.	36 hrs.	48 hrs.	60 hrs.	Avg. by temp.
-4	58.75	95.86	50.6	67.2	101.75	74.8
-3	51	NA	60.33	58.43	53.65	55.9
-2	51.25	180.27	51.7	NA	64.52	86.9
-1	50.21	59.92	49.11	59.36	63.57	56.4
0	NA	70.43	60.4	49	42.63	55.6
1	67.5	59	44.6	43	NA	53.5
Avg. by time	55.7	93.1	52.8	55.4	65.2	

C

Minimum CCRT for first movement (sec)

Temp. (C)	12 hrs.	24 hrs.	36 hrs.	48 hrs.	60 hrs.	Avg. by temp.
-4	56	66	39	59	60	56
-3	41	NA	50	47	31	42.3
-2	42	52	41	NA	36	42.8
-1	40	53	44	48	59	48.8
0	NA	59	55	47	35	49
1	61	56	41	40	NA	49.5
Avg. by time	48	57.2	45	48.2	44.2	

D

Maximum CCRT for first movement (sec)

Temp. (C)	12 hrs.	24 hrs.	36 hrs.	48 hrs.	60 hrs.	Avg. by temp.
-4	64	174	68	80	117	100.6
-3	94	NA	91	78	99	90.5
-2	61	119	62	NA	102	86
-1	79	70	59	93	68	73.8
0	NA	78	66	50	53	61.8
1	78	65	48	48	NA	59.8
Avg. by time	75.2	101.2	65.7	69.8	87.8	

Supplementary Table 2.2. Summary of # of tardigrades used and first movement CCRT data for Fig. 2.1B First movement is defined by a single leg showing movement when tardigrades are restored to 20°C, after cold-induced paralysis (chill coma) (A) # of tardigrades per treatment group (B) Average chill coma recovery time (CCRT) in seconds per treatment group (C) Minimum CCRT time in seconds per treatment group (D) Minimum CCRT time in seconds per treatment group.

A

 # Tardigrades per treatment group

Acclimation	12 hrs.	24 hrs.	36 hrs.	48 hrs.	60 hrs.	Total by temp.
Winter	14	14	8	13	14	63
Summer	12	8	12	10	12	54
No acclim.	18	NA	21	21	20	80
Total by time	44	22	41	44	46	197

B

Average CCRT for full movement (sec)

Acclimation	12 hrs.	24 hrs.	36 hrs.	48 hrs.	60 hrs.	Avg. by acclim.
Winter	89.9	138	95.1	181.7	96.6	120.3
Summer	142	282.3	205.3	188.3	192.2	202
No acclim.	134.8	NA	202.3	200.4	202.3	185
Avg. by time	122.2	210.2	167.6	190.1	163.7	

C

Minimum CCRT for full movement (sec)

Acclimation	12 hrs.	24 hrs.	36 hrs.	48 hrs.	60 hrs.	Avg. by acclim.
Winter	62	54	59	63	45	56.6
Summer	74	98	69	111	84	87.2
No acclim.	78	NA	87	65	91	80.3
Avg. by time	71.3	76	71.7	79.7	73.3	

D

Maximum CCRT for full movement (sec)

Acclimation	12 hrs.	24 hrs.	36 hrs.	48 hrs.	60 hrs.	Avg. by acclim.
Winter	151	245	167	380	175	223.6
Summer	290	489	623	317	319	407.6
No acclim.	241	NA	343	590	814	497
Avg. by time	227.3	367	377.7	429	436	

Supplementary Table 2.3. Summary of # of tardigrades used and full movement CCRT data in response to 2-week photoperiod acclimation (Figure 2.2) Winter photoperiod refers 8 hours light: 16 hours dark; summer photoperiod refers 16 hours light: 8 hours dark; No acclimation refers 24 hours of constant dim light (standard lab conditions), with all acclimations occurring at 20°C. Full movement is defined by all legs showing movement and the whole-body rotating when tardigrades are restored to 20°C, after cold-induced paralysis (chill coma). (A) # of tardigrades per treatment group (B) Average chill coma recovery time (CCRT) in seconds per treatment group (C) Minimum CCRT time in seconds per treatment group (D) Minimum CCRT time in seconds per treatment group.

A

 # Tardigrades per treatment group

Acclimation	12 hrs.	24 hrs.	36 hrs.	48 hrs.	60 hrs.	Total by temp.
Winter	14	14	8	13	14	**63**
Summer	12	8	12	10	12	**54**
No acclim.	18	NA	21	21	20	**80**
Total by time	**44**	**22**	**41**	**44**	**46**	**197**

B

Average CCRT for first movement (sec)

Acclimation	12 hrs.	24 hrs.	36 hrs.	48 hrs.	60 hrs.	Avg. by acclim.
Winter	60.5	61.5	54	56.9	29.2	**52.4**
Summer	57.7	62.1	55.3	57.6	45.1	**55.6**
No acclim.	51	NA	60.3	58.4	53.7	**55.9**
Avg. by time	**56.4**	**61.8**	**56.5**	**57.6**	**42.7**	

C

Minimum CCRT for first movement (sec)

Acclimation	12 hrs.	24 hrs.	36 hrs.	48 hrs.	60 hrs.	Avg. by acclim.
Winter	54	47	46	43	26	**43.2**
Summer	52	54	40	53	34	**46.6**
No acclim.	18	0	21	21	20	**16**
Avg. by time	**41.3**	**33.7**	**35.7**	**39**	**26.7**	

D

Maximum CCRT for first movement (sec)

Acclimation	12 hrs.	24 hrs.	36 hrs.	48 hrs.	60 hrs.	Avg. by acclim.
Winter	66	87	78	75	35	**68.2**
Summer	66	90	89	67	61	**74.6**
No acclim.	41	NA	50	47	31	**42.3**
Avg. by time	**57.7**	**88.5**	**72.3**	**63**	**42.3**	

Supplementary Table 2.4. Summary of # of tardigrades used and first movement CCRT data in response to 2-week photoperiod acclimation (Supplementary Figure 2.1) Winter photoperiod refers 8 hours light: 16 hours dark; summer photoperiod refers 16 hours light: 8 hours dark; No acclimation refers 24 hours of constant dim light (standard lab conditions), with all acclimations occurring at 20°C. First movement is defined by a single leg showing movement when tardigrades are restored to 20°C, after cold-induced paralysis (chill coma) (A) # of tardigrades per treatment group (B) Average chill coma recovery time (CCRT) in seconds per treatment group (C) Minimum CCRT time in seconds per treatment group (D) Minimum CCRT time in seconds per treatment group.

Chapter 3

Comparative proteomics of cold-treated tardigrades reveals shifts in key biological processes and identifies putative ice-binding proteins

3.1 Key Findings

- High-sensitivity data-independent acquisition (DIA) mass-spectrometry on cold-treated *Hypsibius exemplaris* identified 2776 unique proteins, with 89 proteins being differentially abundant compared to tardigrades kept at ambient temperatures.
- Twenty-two of these differentially abundant proteins in response to cold are unique to tardigrades and functionally unannotated.
- Enrichment of gene ontology (GO) annotations of proteins significantly more abundant after cold illustrates changes in neuron and neuromuscular function, calcium ion balance, cell division processes (such as apoptosis), and glucose metabolism.
- Enriched GO annotations of proteins significantly less abundant after cold demonstrate changes in lipid metabolism, cuticle production, development, and redox.
- Ice-affinity purification and a bioinformatics pipeline identified a ranked list of novel candidate ice-binding proteins that tardigrades may utilize to survive freezing.
- This study is the first comparative proteomics study exploring the impacts of cold stress, in any animal.

3.2 Abstract

Little is known about the molecular mechanisms that allow tardigrades to survive subzero temperatures, especially in terms of biological processes and the utilization of tardigrade-specific proteins related to cold tolerance. Here we explore shifts in proteins found in a model tardigrade species (*Hypsibius exemplaris*) in response to a mild, ecologically-feasible cold exposure, using comparative proteomics methods, as well as a specialized affinity purification method used to enrich for putative ice-binding proteins (IBPs). Thousands of adult tardigrades were exposed to cold (-10°C) or ambient temperatures (20°C) and both whole-body lysate and proteins incorporated into the ice fraction after ice-affinity purification were analyzed using DIA mass-spectrometry. First, we identified differentially abundant proteins between the whole-body lysate of cold-treated and room temperature cultured tardigrades (N=3, per thermal treatment). We found a total of 2776 proteins identified among all samples, with 28 proteins being significantly more abundant after cold treatment and 61 proteins being significantly less abundant after cold treatment (q-value < 0.1, between cold-treated and room-temperature treated samples). Of these 89 differentially abundant proteins, 41 (46%) were unannotated in the tardigrade genome, with 58 (65%) having no significant pBLAST homologs among other taxa (E-value 0.05 or less). GO enrichment analysis illustrated several terms which were significantly enriched in proteins differentially abundant in response to cold. For example, GO terms related to neuron and neuromuscular function, calcium ion balance, cell division processes (such as apoptosis), and glucose metabolism were significantly enriched in proteins more abundant in cold-treated tardigrades. Conversely, GO terms related to lipid metabolism, cuticle production, development, and redox were significantly enriched in

proteins less abundant in cold. As our second experimental goal, we conducted ice-affinity purification on pools of thousands of cold-treated and room temperature cultured tardigrades (N=3, per thermal treatment), with the aim of enriching for proteins with a physical affinity to bind to ice (predicted to act as protective antifreeze proteins). PCA suggested high variation in the proteomic profiles of these ice-affinity purified samples compared to whole-body samples (PC1 49.9%), suggesting the impact of the selective protein enrichment. We ranked proteins found in the final ice-affinity fractions according to protein abundance, size, and known characteristics of ice binding proteins (ice-binding motifs found in proteins of other organisms, predictions based on previously published machine learning methods, *de novo* protein structure modeling). We subsequently identified a list of top candidate ice-binding proteins (IBP) that we predict to help prevent damage by ice-formation in *H. exemplaris*, and which are otherwise currently uncharacterized. Four of these proteins were heterologously expressed and purified for future *in vitro* functional verification via thermal hysteresis assays and are unique to tardigrades. In summary, this study represents the first-ever high-sensitivity comparative proteomics study in response to cold stress in tardigrades, or any eukaryotic animal, where GO annotation enrichment of differentially abundant proteins suggested the role of key biological processes in response to subzero temperatures. The putative ice-binding proteins identified here are novel and promising candidates for playing a functional role in tardigrade freezing tolerance, and may shed light on the evolution of ice-binding proteins in this unique phylum.

3.3 Introduction

Tardigrades are increasingly appreciated for their unique role as an emerging model organism, with the potential to illuminate new frontiers in molecular mechanisms underlying environmental stress tolerance (Goldstein 2018; Jönsson 2020). Both translational applications and an improved evolutionary understanding of *Panarthropoda* are expected to culminate from this growing field of research, as illustrated by recent studies focusing on tardigrade comparative genomics, desiccation tolerance, radiation tolerance, and osmotic stress (Yoshida et al. 2017; Møbjerg and Neves 2021; Förster et al. 2012; Mali et al. 2010; Boothby et al. 2017; Yoshida et al. 2021; Heidemann et al. 2016). The molecular mechanisms that underlie tolerance to cold and freezing in tardigrades, however, are less understood than these other environmental stressors (Hengherr and Schill 2018). Cold stress and potential ice-formation represent a unique set of physical, biochemical, and physiological challenges that tardigrades must overcome, in order to survive winter conditions in their often unforgiving aquatic habitats. It is plausible that tardigrades may employ a unique arsenal of protective biochemical mechanisms, tailored to enable survival in subzero temperatures, where temperature-induced metabolic suppression and ice-formation may occur (Schill et al. 2009).

Numerous studies have demonstrated that tardigrades range from being moderately to robustly cold-tolerant, depending on the species and native habitat (Guidetti et al. 2011; Hengherr et al. 2009; Tsujimoto et al. 2016; Somme and Meier 1995). Prior work on tardigrade cold stress has primarily focused on organismal-level phenotypes, such as cold tolerance strategy (varying between freeze avoidant or freeze-

tolerant), super-cooling point, and survival (Hengherr and Schill 2018). This work has suggested that some tardigrade species can likely tolerate extracellular ice formation, although the molecular mechanisms that allow this are largely unknown (Guidetti et al. 2011; Hengherr et al. 2009; Hengherr et al. 2010). As one proposed mechanism to assist in tardigrade cold tolerance, a recent bioinformatics study identified a series of predicted cold-shock proteins in several lineages of tardigrades (1 heterotardigrade species and 7 eutardigrade species), which authors predict to function as RNA chaperones capable of reducing cold-induced damage (Kamilari et al. 2019)—although this temperature-related function is not yet experimentally demonstrated. It has been suggested that tardigrade species may rely on the production of cryoprotectants (such as glycerol, sorbitol, mannitol, or trehalose) or ice-binding proteins, to reduce lethal damage caused by ice-formation, but neither of these molecular mechanisms have been directly observed in response to cold in any tardigrade species (Wright 2001). For example, low molecular weight osmolytes (capable of behaving as cryoprotectants) have been found in the active state of desiccated tardigrades (Halberg et al. 2013), but not at higher rates in cold-exposed animals. More so, tardigrades such as *Hypsibius exemplaris* lack critical proteins in the molecular pathway needed produce to trehalose, the most prominent osmolyte attributed to tardigrade desiccation tolerance (such as trehalose-6-phosphatase synthase) (Yoshida et al. 2017). Differential scanning calorimetry experiments detecting the crystallization temperature (defined as the first freezing isotherm observed in a cooling experiment) of the tardigrade species *Adorybiotus coronifer* suggested the likely presence of ice-nucleating or ice-binding proteins, but these proteins have remained unidentified throughout recent decades (Westh et al. 1991).

Alternatively, a growing number of studies have focused on the molecular response of tardigrades to high temperature—of which they are weakly tolerant (Neves et al. 2020)—involving a wide range of differentially expressed genes relating to DNA protection, heat shock, and tardigrade disordered proteins (such as the Cytosolic Abundant Heat-soluble ‘CAHS’ and Secretory Abundant Heat Soluble ‘SAHS’ proteins; types of late embryogenesis abundant LEA proteins, specific to tardigrades) (Neves et al. 2022; Yamaguchi et al. 2012). Prior work in other organisms such as plants has shown the important role of such LEA proteins in response to low temperatures, by stabilizing protein and membrane structure during water loss (Abdul Aziz et al. 2021; Kosová et al. 2021). LEA proteins play important roles in anhydrobiotic midges at low temperatures, by offsetting protein aggregation and acting as a molecular shield (Toxopeus et al. 2014; Hatanaka et al. 2013). Yet, a brief transcriptomics analysis of CAHS proteins in tardigrades suggested that transcription of these tardigrade disordered LEA proteins is not significantly induced by cold exposure (Boothby et al. 2017). Recent work in the tardigrade species *Ramazzottius varieornatus* suggested remarkable levels of cold tolerance yet minimal changes in transcriptional profiles in response to extreme cold (-80 and -120°C) (Møbjerg et al. 2022). Only two unannotated transcripts were differentially expressed in response to extreme cold in this study, with none being involved in LEA protein production or other known stress tolerance proteins (such as heat shock proteins, HSPs), although this may have been largely impacted to the effect of extreme cold stopping most biochemical processes. Nonetheless, mechanisms of cold tolerance in tardigrades are predicted to not rely on large transcriptional shifts in LEA or HSP

transcription, but rather the protective function of newly translated or existing proteins, or other biomolecules.

While there is a limited description of molecular mechanisms that underlie cold tolerance in tardigrades, such mechanisms are better understood in numerous sister taxa—such as various insect and nematode species (Sinclair et al. 2003; Perry and Wharton 2011; Toxopeus and Sinclair 2018; Overgaard and MacMillan 2017). To avoid mechanical injury due to freezing, insects and many other taxa rely on biochemical strategies to avoid freezing or tolerate freezing, or induce cryoprotective dehydration, as seen in Antarctic nematodes (Denlinger and Lee 2010; Wharton et al. 2005). Regardless of cold tolerance strategy, it is hypothesized that nearly all winter-exposed taxa will eventually come into contact with environmental ice or ice-nucleators, and many may benefit from mechanisms to induce or tolerate inoculative freezing (Denlinger and Lee 2010; Rozsypal and Košťál 2018).

To overcome the challenges of freezing, a suite of proteins has been observed to play a role in insect cold tolerance. Heat shock proteins (HSPs) have been observed to play a role in diapause and larval development of the Antarctic midge *Belgica antarctica* at low temperatures (Rinehart et al. 2007; Rinehart et al. 2006). Proteins preventing reactive oxygen species, modifying ATPase activity, as well as desaturases involved in membrane restructuring have been observed in cold-exposed insects (McMullen and Storey 2008; Kayukawa et al. 2007). Comparative -omics studies in insects such as *Drosophila melanogaster* have additionally illustrated shifts in various pathways that respond to low temperature, often relating altered thermal sensitivity of ion channels, altered membrane composition, recruitment of ion transporters in nerve and muscle cells, and regulation of paracellular permeability (MacMillan et al. 2016; Williams et al. 2014). Shifts in protein processing (misfolded protein regulation, retrotranslocation, ubiquitination, stabilizing/folding, and protein degradation) may also play an important role in extreme cold tolerance, as illustrated by a comparative transcriptomics study of the drosophilid species *Chymomyza costata* where larvae were plunged into liquid nitrogen after a several-week long cold acclimation (Des Marteaux et al. 2019).

Although there currently exist no proteomics studies describing the impact of cold in any animal species, a growing body of literature describes the proteomic-level impacts of cold stress in model plant species and crops (Jan et al. 2019). These studies generally indicate shifts in abundances and localization of proteins related to protein degradation, protein processing, stress response, mitochondria function, sugar catabolism, plasma membrane restructuring, antifreeze function, heat shock, and LEA proteins (Takahashi et al. 2013; Martinez-Seidel et al. 2021; Gharechahi et al. 2016; Yuan et al. 2019; Neilson et al. 2011; Janmohammadi et al. 2015). Whether any of these mechanisms play a role in tardigrade cold tolerance remains unknown and differential expression of related transcripts was not observed in prior transcriptomic studies (Møbjerg et al. 2022).

In addition to the wide range of biological processes listed above, many organisms utilize a diverse class of proteins known as “ice-binding proteins” (IBPs) to survive subzero temperatures (Bar Dolev et al. 2016). IBPs confer protection against freeze-damage by binding and inhibiting the growth of ice crystals in organisms exposed to subzero temperatures. Since their initial discovery, a diversity of structurally and functionally distinct IBPs have been described among various taxa across the tree of life (Davies 2022, Davies 2014), including eight orders of arthropods (Duman 2015).

Nonetheless, additional IBPs with unique structures, functions, evolutionary histories, and prospective biomedical and agricultural applications likely remain undescribed (Voets 2017; Chen et al. 2021; Cid et al. 2016; Białkowska et al. 2020; Mangiagalli et al. 2020; Mahatabuddin and Tsuda 2018). Recent work has not established whether any species of tardigrades produce IBPs, despite their ability to remain active in winter conditions and viable in extreme subzero temperatures (Hengherr and Schill 2018; Møbjerg et al. 2022). Because IBPs' function is often co-opted from existing proteins (Davies 2022) or horizontally transferred among species (Arai et al. 2019; Raymond 2014; Raymond and Remias 2019), discovering novel IBPs in previously unstudied organisms is often challenging: many false-positives are identified when looking for homologs of knowns IBPs using bioinformatic sequence-similarity tools alone, due to instances of neofunctionalization of otherwise well-conserved paralogs (Deng et al. 2010). Thus, experimental methods involving protein extraction and functional purification are often required to discover and verify novel IBPs in organisms such as tardigrades (Marshall et al. 2016; Adar et al. 2018; Kuiper et al. 2003).

Here, we use a comparative proteomics pipeline and ice-affinity purification on cold-treated tardigrades to characterize shifts in the proteomic profile and production of novel candidate tardigrade ice-binding proteins, in response to subzero temperatures. In particular, we explore shifts in the proteomic profile of the globally distributed eutardigrade species *Hypsibius exemplaris*, in response to an ecologically-feasible but non-lethal cold exposure (-10°C). We have demonstrated in prior work that this species of tardigrade has a large dynamic range of tolerance to subzero temperatures, depending on the extent and duration of cold exposure, as well as the presence of ice-nucleation events. Thus, we predict that *H. exemplaris* may experience shifts in protein abundance in response to changes in temperature (as indicated by their variability in cold tolerance, depending on the duration and extent of cold exposure), as well as utilizing ice-binding proteins, to survive freezing conditions.

As our first experimental goal, we compare protein abundances between cold-treated and room temperature cultured adult *H. exemplaris*, as well as GO annotation enrichment in differentially abundant proteins after cold exposure, using functional proteomics. As a second experimental goal, we conduct a type of protein purification known as ice-shell purification on cold-treated and room-temperature tardigrades to experimentally enrich for proteins that have a biochemical affinity to bind ice, and thus may function as physiologically protective ice-binding proteins (Marshall et al. 2016). Once identified via proteomics and verified by downstream *in vitro* thermal hysteresis assays, these previously uncharacterized proteins may constitute novel structures of ice-binding proteins, unique to tardigrades, with future industrial and biomedical applications. Even if annotated, any proteins identified in this study will contribute to the long-elusive question of how tardigrades survive cold.

3.4 Methods

Cold treatment and sample preparation

3.4.1 Tardigrade culture

Experiments were conducted on the cosmopolitan eutardigrade species *Hypsibius exemplaris* Z151 (reclassified from *Hypsibius dujardini* in 2017), purchased from Sciento (Manchester, United Kingdom). Tardigrades were cultured as previously described (Chapter 1).

3.4.2 Thermal treatments for comparative proteomics

To establish whether the proteome of *H. exemplaris* shifts in response to subzero temperatures, we exposed groups of 1000 hydrated, active adult tardigrades to a mild non-lethal exposure (a protocol spanning 41 hours total, with a final low temperature of -10°C for 24 hours) or our control temperature of 20°C (N=3 sets of 1000 tardigrades, per thermal treatment group, for a total of 6 samples). For both thermal treatments (cold -10°C or room temperature 20°C), groups of 200 mixed-staged adult *Hypsibius exemplaris* were collected from culture dishes (at 20°C) via manual microaspiration, washed in mineral water thrice to remove algae sediments in secondary petri dishes, and collected into a 1.5mL Eppendorf tubes with 100ul of mineral water (Crystal Gyster). Five (5) tubes of 200 tardigrades were treated at a time in batches of 1000 animals, which were subsequently pooled together during the preparation of tardigrade lysate, to constitute each complete sample.

Tardigrades designated for cold treatment were exposed to a final low temperature -10°C after a ramping and hold period, in a cooling circulator (Lauda RP2045) via placement into a secondary metal container submerged into Ethylene Glycol (1 part Ethylene Glycol: 1 part distilled water). The full cold treatment consisted of the following 4 steps, which were implemented by the Lauda RP2045 as a custom program: 1) a ramp from 20°C to 0C at a rate of 0.1°C/min (3 hours, 20 minutes), 2) a 12-hour hold at 0°C, 3) a ramp from 0°C to -10°C at a rate of 0.1°C/min (1 hour, 40 minutes), and a final hold at -10°C for 24 hours. This subjected the tardigrades to a total thermal treatment time of 41 hours, including a 12 hour accurate acclimation at 0°C and a final hold -10°C for 24 hours.

After cold treatment, cooled tardigrade samples were removed from the cooling circulator, pooled to obtain the designated number of animals (1000 per replicate), spun at low speed, and as much supernatant was removed as possible without disturbing the animals' pellet. Samples were then immediately flash frozen and stored at -80°C to euthanize the tardigrades, before further sample processing. A parallel set of tardigrade samples (N = 3) were not cooled, held at 20°C for the same period of time (41 hours), and were similarly combined, flash-frozen in liquid nitrogen, and stored at -80°C. In total, 6000 tardigrades were required for this comparative proteomics experiment.

3.4.3 Thermal treatments for ice-affinity purification (IAP)

An additional set of tardigrade samples were designated for downstream ice-affinity purification (with and without cold treatment), with the goal to experimentally enrich for novel candidate ice-binding proteins from the model tardigrade species. N=3 tardigrade samples were prepared following the protocol and cold-treatment described above, except for a total of 2000 animals were used per biological replicate (pooling together ten tubes of 200 tardigrades, post-cold treatment). Lastly, a thermal control set of N=3 tardigrade samples was also prepared (2000 tardigrades per sample), with animals being exposed to 20°C and no cold treatment. Because of the exploratory nature

of the experiment—not knowing whether candidate tardigrade ice-binding proteins might be constitutively expressed at room temperature or induced by cold exposure—we prepared these parallel sets of tardigrade ice-affinity purification samples with and without cold treatment.

3.4.4 Preparation of tardigrade lysate and protein extraction

Protein was extracted from tardigrade samples prepared above by thawing samples on ice, with the addition of a designated lysis buffer (depending on the designated downstream analysis). Samples allocated for comparative proteomics analysis (N=3 “cold-treated whole-body tardigrade samples" and N=3 “room-temperature whole-body tardigrade samples”) then received the addition of 500µl of a 5% SDS, 50mM TEAB lysis buffer, prepared with cOmplete ™, Mini, EDTA-free Protease Inhibitor Cocktail at 1X final concentration. Samples allocated for downstream ice-affinity purification (N=3 “cold-treated ice-affinity purification tardigrade samples” and N=3 “room-temperature ice-affinity purification tardigrade samples”) received the addition of 1000µl of a physiological 50 mM Tris-HCl (pH 7.6), 100 mM NaCl buffer, prepared with cOmplete ™, Mini, EDTA-free Protease Inhibitor Cocktail at 1X final concentration. Samples were then transferred to fresh 1.5mL tubes designed for use in a Bioruptor® sonication device and sonicated in the Bioruptor® at high power for 30 cycles (Sonication cycle: 30 sec ON, 30 sec OFF; protocol modified from Walther et al. 2015). Sonicated samples were spun 1000g for 1 min, and clarified lysates were transferred to fresh 1.5mL Eppendorf tubes. “Whole-body” comparative proteomics samples were flash-frozen in liquid nitrogen and stored at -80°C, until transported on dry ice for subsequent sample preparation for mass spectrometry. Samples designated for ice-affinity purification were immediately processed as described below.

3.4.5 Ice-affinity purification (IAP)

To experimentally enrich tardigrade proteins that have a biochemical affinity to bind ice (candidate ice-binding proteins), we utilized an ice-affinity purification (IAP) protocol using custom-made ice shells, as described by Marshall et al. 2016. Ice shells were prepared inside 100mL bottom flasks, by adding 7.5 mL of chilled HPLC-grade water (Spectrum Chemical) and rotating the flask in a -80°C 95% dry ice-ethanol bath for 45–60 seconds, until the interior of the flask was well coated and the ice formed a series of visible cracks throughout. Two separate ice shells were created (in separate round bottom flasks) for each sample type (cold-treated and room temperature-treated tardigrades, as described in “*Thermal treatments for ice-affinity purification”*), for a total of four ice shells.

All three cold-treated tardigrade samples designated for ice-affinity purification (N=3, a total of 6000-tardigrade protein lysate) were pooled and then suspended in 10 mL of chilled physiological buffer (50 mM Tris-HCl (pH 7.6), 100 mM NaCl buffer, prepared with cOmplete™, Mini, EDTA-free Protease Inhibitor Cocktail at 1X final concentration). This tardigrade lysate solution was chilled to 0°C (cooled to prevent ice-shell melting upon application) and then transferred into the first ice shell. The ice shell was quickly attached to a custom device consisting of a motor (Uxcell 12V DC 40RPM Gear Motor) and Fisherbrand™ Stainless Steel Clamp, which was arranged to allow the ice shell to be half-submerged in a liquid bath of glycerol antifreeze, which was chilled in a cooling circular held at -0.5°C (VWR Scientific 1167P Heating/Cooling Recirculating

Water Bath, filled with Ethylene Glycol). The sample-loaded round-bottom flask was then rotated at 5 RPM for ~15 minutes until roughly half of the chilled tardigrade lysate solution was incorporated into the ice shell (Figure 3.1B). This process was conducted in a 12°C cold room, to prevent condensation formation and the premature melting of the ice shell. At the conclusion of the ~15 minutes, an excess sample that did not incorporate into the ice shell was poured into a 50mL conical centrifuge tube and set aside. Importantly, the ice shell was then allowed to melt, and this ice-shell melt (containing bound tardigrade lysate) was poured into a fresh 50mL conical centrifuge tube to be applied to the second ice shell.

Once this melt was chilled to 0°C, it was applied to the second ice shell (in a new round bottom flask) and this new ice shell was rotated at 5 RPM for ~15 minutes until roughly half of the chilled tardigrade lysate solution was incorporated. The excess sample that did not incorporate into the ice shell was set aside, and the ice shell and bound sample were melted. This final melt was considered the final elution fraction, for tardigrade proteins that may have a biochemical affinity to bind to ice (acting as candidate ice-binding proteins). This cold-treated IAP tardigrade elution fraction was concentrated on a 3kDa Amicon® Ultra filter, to a final volume of 1.5 mL. This concentrated cold-treated IAP tardigrade elution fraction then split into three 500 µl aliquots (in 1.5 mL Eppendorf tubes) to generate three technical replicates for proteomics, which were flash-frozen in liquid nitrogen and stored at -80°C, until transported on dry ice for subsequent sample preparation for mass spectrometry.

This ice-affinity purification process was repeated for the N=3 room-temperature treated tardigrade samples designated for IAP, and a room temperature-treated IAP tardigrade elution fraction was generated as described above. The concentrated room temperature-treated IAP tardigrade elution fraction was likewise split into three 500 µl aliquots (in 1.5 mL Eppendorf tubes) to generate three technical replicates for proteomics, which were flash-frozen in liquid nitrogen and stored at -80°C until further analysis.

3.4.6 Sample preparation for LC-MS/MS

All tardigrade samples (12 in total; 3 cold treated whole-body samples, 3 room temperature treated whole-body samples, 3 cold treated ice-affinity purification samples, and 3 room temperature treated ice-affinity purification samples) were submitted to UC Davis proteomics core for digestion and LC-MS/MS. Protein concentration was determined by BCA assay (Pierce), and 150 µg of proteins were digested on an S-Trap™ Digestion column. Initially, 10 mM dithiothreitol (DTT) was added and incubated at 50°C for 10 min and rested at room temperature for 10 min. Next, 5 mM iodoacetamide (IAA) was added and incubated at room temperature for 30 min in the dark. The samples were acidified with 12% phosphoric acid followed by the addition of freshly made S-trap buffer (90% methanol, 100 mM TEAB, pH 7.1) and mixed immediately by inversion. The entire acidified lysate buffer mix was transferred to the S-trap and centrifuged at 1,000 rcf for 1 min or until all the solution passed through the column. Columns were washed with 400 uL of S-trap buffer and centrifuged at 4,000 rcf until dry. Columns were transferred to a clean elution tube. Trypsin enzyme digest buffer was carefully added (1:25 enzyme: total protein in 120 µL 50mM TEAB, pH 8.0) to the column. After two hours of incubation at 37 C, the same amount of trypsin and TEAB was added to the s-trap as a boost step and the reaction continued overnight at 37 C. The following day peptides were eluted from the

S-trap. Peptide elution steps included 80 µL of 50 mM TEAB (pH 8.0), 80 µL of 0.5% formic acid 80 µL of the solution containing 50% acetonitrile and 0.5% formic acid. The final pooled elution was dried down in a speed-vacuum. Peptides were resuspended in 0.1% TFA 2% ACN and quantified using Pierce™ Quantitative Fluorometric Peptide Assay (Thermo Fisher Scientific).

Mass Spectrometry

3.4.7 LC-MS/MS

LC separation was done on a Dionex nano Ultimate 3000 (Thermo Scientific) with a Thermo Easy-Spray source fitted with a PepSep emitter. The digested peptides were reconstituted in 2% acetonitrile /0.1% trifluoroacetic acid and 5 µl of each sample was loaded onto a Thermo Scientific PepMap 100 C18 5um 0.3 x 5mm reverse-phase trap where they were desalted online before being separated on a PepSep 25cm ID 150 1.5um reverse-phase column. Peptides were eluted using a 120-minute gradient with a flow rate of 0.500 ul/minute. Samples were run an Orbitrap Exploris 480 (Thermo Scientific) in DIA mode; mass spectra were acquired using a collision energy of 30, resolution of 30 K, maximum inject time mode on auto and a AGC target of 1000%, using staggered isolation windows of 45.7 Da in the m/z range 350-1200 m/z.

3.4.8 Data analysis of DIA output

DIA data was analyzed using Spectronaut 15 (Biognosys Schlieren, Switzerland) using the directDIA workflow with the default settings. Briefly trypsin/P Specific was set for the enzyme allowing two missed cleavages. Fixed Modifications were set for Carbamidomethyl, and variable modifications were set to Acetyl (Protein N-term) and Oxidation. For DIA search identification, PSM and Protein Group FDR was set at 0.01%. A minimum of 2 peptides per protein group were required for quantification. Quantification is reported as the sum of the integrated fragment ion peak areas. Hypsibius_dujardini_nHd.3.1.5.proteins (reclassified as *Hypsibius exemplaris*) from Yoshida et al 2017 served as the reference proteome. A report was exported from Spectronaut using the reporting feature and imported into SimpliFi https://simplifi.protifi.com/ for QC and statistical analysis (Protifi, Farmingdale NY).

Comparative & functional proteomics data analysis

3.4.9 Global proteomics assessment

To generate a global snapshot of the number of proteins that were identified among all proteomics sample types (regardless of abundance level), Venn diagrams were created using the VennDiagram package in R (Version 1.6.20; Chen and Boutros (2011)). More specifically, the union of proteins identified in sets of replicates of each distinct sample type (cold whole-body, cold ice-affinity, room temperature whole-body, room temperature ice-affinity) were taken, enabling the creation of a 4-way Venn diagram. To compare variation in proteomic profiles among sample types, a principal components analysis was also conducted in R (taking into account protein abundance levels).

3.4.10 Determination of differentially abundant proteins from whole-body samples & GO enrichment analysis

Proteins were designated as differentially abundant between cold-treated whole-body samples and room temperature-treated whole-body samples if the q-value was <0.1, as calculated by prior Spectronaut data analysis. The value of log2(fold change) between cold-treated and room temperature-treated allowed us to determine if the protein was differentially more abundant or less abundant, in reference to cold-treatment. In our summary table (Figure 3.3B), differentially abundant proteins were designated as "uncharacterized" if the corresponding *Hypsibius exemplaris* annotation was listed as "hypothetical protein." Likewise, abundant proteins were designated as "tardigrade-specific" if the amino acid sequence did not share an E-value of 0.5 or less with any protein or any non-tardigrade organisms in the NCBI non-redundant protein database, using BLASTp. Differentially abundant proteins were labeled as having a "GO-annotation" if they received at least one GO-annotation of any functional category, using Pannzer2.0 (Törönen et al. 2018).

Likewise, GO terms annotations were generated by Pannzer2.0, both on all proteins identified in this proteomics study, as well as the complete Hypsibius exemplaris, predicted proteome (to serve as a resource for future work). Pannzer2.0 output was reformatted with a custom Python script for input into a downstream enrichment analysis.

A series of two Gene Ontology (GO) enrichment analyses were performed on the proteins identified to be differentially (1) more abundant and (2) less abundant, compared to all proteins identified in this complete proteomics study using TopGO version 2.48.0 (Alexa and Rahnenfuhrer, 2022). A Fisher's exact test was conducted to identify significant GO enrichments in all three categories, at an α-level of $p \leq 0.05$ (using the "weightCount" method).

3.4.11 Comparative analysis of ice-shells

Profiles of proteins enriched by ice-affinity purification (cold-treated vs. room-temperature or IAP vs. whole-body) were compared by visualization of log2(fold change) in protein abundance in heat maps generated by GraphPad Prism (Version 9.3.1). Only proteins with an absolute value of log2(fold change)>1 were visualized.

3.4.12 Selection of candidate ice-binding proteins

Proteins designated as novel tardigrade candidate ice-binding proteins were identified in one of three ways: (1) the protein found to be most abundant in the ice-affinity purification fraction of cold-treated tardigrades, after initial filtering (2) the top 25 proteins with the greatest "candidate ice-binding protein score" from the those identified in the ice-affinity purification fraction of cold-treated and/or room-temperature tardigrades, post-filtering.

As an initial filtering step, we removed all proteins based on two preliminary criteria: if they had a negative fold-change in the ice-affinity purification fraction compared to the whole-body proteomics sample (i.e. proteins that were less abundant after conducting ice-affinity purification, and thus did not likely have an affinity to bind ice), or if they were larger than 300 amino acids (as most ice-binding proteins are known to be below roughly this size threshold Bar Dolev et al. 2016).

To generated a “candidate ice-binding protein score,” proteins that passed through this initial filtering step were awarded points as follows, for each given protein: 1 point for each vote of confidence for ice-binding activity by the model machine learning model iAFP (Yu and Lu 2011), 1 point if the log2(fold change) ≥ 1 in the IAP vs. whole-body samples for that thermal condition, 1 point if the log2(fold change) ≥ 2 oin the IAP vs. whole-body samples for that thermal condition, 1 point if the length of the protein was ≤ 100, 1 point if the average protein abundance was at least 10,000 in the IAP for that thermal condition, 1 point if there were at least 2 amino acid motifs shared among known ice-binding proteins in other organisms (as determined by a custom R script; motifs listed in Supplementary Materials), and a final point modification depending on description of the corresponding GO annotations (negative 1 point = proteins which enzymatic, structural, or otherwise highly-conserved non-ice-binding function, 0 point = no known conflict for ice-binding function, and plus 1 point = extracellular space or response to environmental stimuli).

Using this scoring system, lists of filtered proteins for cold-treated IAP proteins and room temperature-treated IAP proteins were independently ranked. From this ranked list, 3 candidates were selected for future functional verification, after manual inspection of their predicted protein structures generated by the open-source web servers provided by TrRosetta and/or Robetta (Du et al. 2021; Su et al. 2021; Yang et al. 2020; Baek et al. 2021; Hiranuma et al. 2021; Song et al. 2013). We considered how predicted tardigrade protein structures compared to known protein structures illustrated in the comprehensive ice-binding protein review Bar Dolev et al. 2016, looking for potential ice-binding domains potentially conferred by similarities in the topology of characteristic beta sheets or alpha helices, with repeating amino acid motifs. Furthermore, final protein candidate selection was determined by the feasibility of synthesizing gene blocks and expression in heterologous systems for downstream analysis (constrained by technical limitations in synthesizing high-repeat sequences beyond a certain length and transfection success). In future work, the thermal hysteresis activity of each protein will be determined by the methods of (Braslavsky and Drori 2013), which will reveal if these proteins cause a gap in the freezing temperature and melting temperature of a solution *in vitro*. An additional list of 15 ranked IBP candidates is also included in Supplementary Materials (SF3.3).

Construction of candidate ice-binding proteins for future downstream analysis

3.4.13 Molecular cloning of tardigrade IBP Candidate 1 and controls

The tardigrade candidate ice-binding protein ‘Tardigrade Candidate IBP 1’ was cloned in *E. coli* for downstream protein expression. The amino acid sequence of this candidate ice-binding protein was run through reverse translation BLAST to obtain the CDS. The CDS was then codon-optimized for *E. coli* expression and ordered as gene blocks from Twist Bioscience. A positive control included the well-characterized fish IBP “AFP3” and negative control of sfGFP was also designed. Gene blocks contained additional linkers to add on restriction enzyme cut sites, along with an sfGFP C-terminal tag and a TEV cut site (ENLYFQG) to be positioned upstream of the 6x-Histidine tag.

The gene blocks were then cloned into pET20b+ using New England Biosciences restriction enzymes BamHI-HF and HindIII-HF. The resulting plasmid construct was transformed into chemically competent BL21(DE3) cells (UC Berkeley Macrolab). Cells transformed with constructs containing the sfGFP tag could be predicted as successful

transformants by observing them fluorescing green under UV light. These fluorescing colonies were picked and grown as 5mL overnight cultures in LB + 1X Ampicillin to generate cell lines, stored as glycerol stocks at -80ºC. A Zymo miniprep kit was used to isolate the plasmid from the transformed cells for verification by sequencing, using primers for the T7 promoter and terminator present on the pET20b+ plasmid. The subsequent modification of plasmid constructs to remove the sfGFP tag used restriction enzymes AvrII and SpeI, which generate compatible sticky ends that can be ligated excluding the fragment containing sfGFP. Successful colonies, in this case, were identified as not displaying green fluorescence.

3.4.14 Protein purification of tardigrade IBP Candidate 1 and controls

Cells containing transformed plasmids were grown as 5 mL overnight cultures in LB + 1X ampicillin to be diluted into larger volumes (1-3L) of LB media containing 1X ampicillin. At OD600 = 0.6–1.0, large cultures were induced with IPTG to 500mM for at least four hours at 37°C, after which the cells were spun down into pellets and the supernatant removed. Pellets were stored at -80°C until later use.

Pellets were resuspended with Lysis buffer (50mM Tris pH 7.6, 100mM NaCl, Roche Protease Inhibitor) and incubated with 1 U/mL DNase I and 1 mg/mL lysozyme for at least 15 minutes. The supernatant from lysis was collected and incubated with Ni-NTA beads for at least 10 minutes to allow binding of the His-tagged proteins, then spun down for the removal of the flow-through. The bead bed was washed twice with wash buffer (20mM Tris pH 8, 500mM NaCl, 50mM imidazole) before protein was eluted from the beads with Elution buffer (20mM Tris pH 8, 500mM NaCl, 500mM imidazole).
Proteins containing a TEV cut site were subsequently dialyzed (Thermo Scientific Slide-A-Lyzer™ Dialysis Cassettes, 10K MWCO, 3 mL) into a 20mM Tris pH 7.6 buffer with protease inhibitor. Dialyzed proteins were processed with TEV protease (UC Berkeley Macrolab) added at 1:20::protease: protein mass ratio, overnight at 4°C. Both the TEV protease and the peptide fragment containing the 6x-His-tag were removed through Ni-NTA bead binding, the same as described in the section above. Proteins of interest were collected in the “flow-through” fractions. Purified and processed proteins were dialyzed overnight into a Physiological buffer (50mM Tris pH 7.6, 100mM NaCl, protease inhibitor) for subsequent in vitro assays.

3.4.15 Production of tardigrade IBP Candidates 2-4

Amino acid sequence of three additional Tardigrade IBP candidates (referred to as “Tardigrade Candidate IBP 2-4” were outsourced to Biointron (Shanghai, China) for expression in CHO mammalian cells and purification, for subsequent measurement of thermal hysteresis (verification of ice-binding protein activity) in future work.

3.5 Results & Discussion

Proteomics summary

In order to evaluate changes in the proteomic profile of *Hypsibius exemplaris* in response to subzero temperatures, we conducted comparative data-independent

acquisition (DIA) mass-spectrometry on groups of thousands of mixed-stage adult tardigrades that were either cold-treated (-10°C for 24 hours, with a custom ramp down protocol) or kept at ambient culture temperatures (20°C). Samples were then processed with one of two protein-purification methods (Figure 3.1A): standard whole-body protein extraction or ice-affinity purification (IAP) (Figure 3.1B)—with the latter aimed at enriching novel tardigrade ice-binding proteins. Among all treatment and sample types, we identified a total of 2,776 unique peptides from our DIA-MS, which corresponds to 13.34% of the predicted *Hypsibius exemplaris* proteins from the genome assembly of Yoshida et al. 2017 (20,815 of predicted proteins) (Figure 3.2A). While our DIA-MS provided modest coverage of the total number of proteins predicted compared to the total set of all predicted proteins predicted from the tardigrade genome, this proteomics output represents a major advance from the only prior proteomic studies of any tardigrade species to date (Schokraie et al. 2010), which identified 144 proteins in total (or 0.74% of the predicted proteome of the tardigrade species studies *Milnesium tardigradum*, of 19,401 predict protein-coding genes in Bemm et al. 2017), using 2D two-dimensional gel electrophoresis and electrospray ionization tandem mass spectrometry. By developing methods to clean and handle large numbers of individual tardigrades (using microaspiration), utilizing updated methods for protein digestions (S-Trap™ by ProtiFi), and using the most-sensitive label-free method of proteomic profiling available to us at the time of experimentation, we increased the percent coverage of predicted-proteins identified by a factor of ~18.

A comparison of proteins identified among our four sample types—cold-treated whole-body, cold-treated ice-affinity purification, room temperature whole-body, and room temperature ice-affinity purification—revealed high overlap among all samples (92.4% overlap, 2,565 of 2,776 proteins were identified in all samples, Fig. 3.2). Notably, this Venn diagram comparison illustrates the number of proteins identified (as a metric of presence or absence), without also comparing the variation in estimates of protein abundance. Beyond the large intersection of proteins identified in all sample types, the next largest overlap was among cold-treated whole-body, room temperature ice-affinity purification, and room temperature whole-body samples, with 120 proteins jointly identified. If candidate ice-binding proteins found in tardigrades are induced by cold exposure, we would then predict that none of these 120 proteins identified in this intersection would likely constitute a viable candidate ice-binding protein in our tardigrade species. Next, the third-largest intersection of proteins identified was among cold-treated whole-body samples and room temperature whole-body samples, with 76 proteins that were uniquely identified. Similarly, these 76 proteins are unlikely to function as candidate ice-binding proteins, as they were identified in neither of the ice-affinity purification sample types.

To more thoroughly compare proteomic outputs of each sample type, we also conducted a principal component analysis of abundance levels of each protein, among all 12 replicates (3 cold-treated whole-body samples, 3 cold-treated ice-affinity purification samples, 3 room temperature whole-body samples, and 3 room temperature ice-affinity purification samples) (Figure 3.2B). Sample types clustered strongly by protein purification method (ice-affinity purification vs. whole-body tardigrade lysates), with PC1 accounting for 49.9% of the variation. Samples also clustered according to thermal treatment, with cold ice-affinity purification especially separating from room temperature

ice-affinity purification on the PC2 (accounting for 13.7% variation). In total, all four sample types formed distinct clusters both by thermal treatment and protein purification method, suggesting some impact on the proteomic profile and impact of ice-affinity purification on the abundance of the various proteins identified in this study. Supplemental Figure 3.1 also displays PCA of samples by thermal treatment or protein purification method.

For statistical analysis of proteomic samples, it is important to highlight differences in the structure of sample replication between whole-body tardigrade samples and ice-affinity purification samples, as illustrated in Figure 3.1A. Cold-treated whole-body samples and room temperature whole-body samples remained full biological replicates throughout the entire sample preparation and proteomics pipeline. In contrast, both types of ice-affinity purification samples were pooled (in parallel, according to thermal treatment) for the ice-affinity purification process, and then split into 3 technical replicates, per prior thermal condition (making a total of 3 cold treated ice-affinity purification samples and 3 room treatment ice-affinity purification samples, post-pooling). Thus, the variation observed in proteomic profiles between the three cold-ice affinity purification replicates on the PCA2 axis may be an artifact of post-protein purification sample preparation or mass-spectrometry. Nonetheless, in downstream analysis of these sample replicates we considered the proteomic profiles of sample-types on average, and we only compared abundance differences between ice-affinity purification replicates (Figure 3.4).

In future implementations of this experimental design, we would recommend conducting separate rounds of ice-affinity purification with larger sets of tardigrades, in order to maintain full biological replicates throughout the entire experimental pipeline. This would clarify the source of variation, and allow for statistical comparison of all sample types.

Determination of differentially abundant proteins after cold treatment reveals many previously uncharacterized and tardigrade-specific proteins

We compared protein abundances (log2 fold change) and quantified statistically significant protein abundance differences (q-values) between cold-treated and room temperature whole-body tardigrade samples, as illustrated in Figure 3.3A, in order to gauge how the tardigrade proteome shifts in response to non-lethal cold exposure (-10°C, for 24 hours). We identified 28 proteins that were differentially more abundant in cold-treated whole-body samples (q-value < 0.1), compared to the 2,776 proteins that were detected overall. Of these 28 proteins found to be more abundant after cold-treatment, 14 (50%) had no functional annotation from the most recent genome assembly Yoshida et al. 2017 and 7 (25%) were unique to tardigrade species (*Hypsibius exemplaris* and *Ramazzottius varieornatus*) in the NCBI non-redundant protein database (BLASTp). Four of these 28 proteins were unique/specific to *Hypsibius exemplaris*, and were absent in *R. varieornatus*. Likewise, we found that 61 proteins were differentially less abundant in cold-treated whole-body samples (q-value < 0.1), compared to the 2,776 proteins that were detected overall. Of these 61 proteins, 27 (44%) were annotated, 15 (25%) were tardigrade-specific, and 10 (16%) were specific to *Hypsibius exemplaris* (Figure 3.3B). Of these 89 differentially abundant proteins, none were annotated as LEA, HSP, or as other tardigrade-specific proteins previously described to be involved in other forms of stress tolerance (Møbjerg and Neves 2021).

To explore whether these differentially abundant proteins were related to shifts in key biological processes, we utilized Pannzer2.0 (Törönen et al. 2018) to annotate all proteins identified in this protein experiment as well as this differentially abundant subset. Of the 2,776 unique proteins identified in this proteomics pipeline, 2,248 proteins (81%) were found to have at least one GO annotation (in any functional category). Of the 28 proteins found to be more abundant after cold treatment, 21 (75%) had at least 1 GO annotation. Only 38 (62%) of the 61 proteins found to be less abundant after cold treatment had at least 1 GO annotation (Figure 3B). All 66 proteins that were differentially abundant with no corresponding GO annotations also were unannotated by the genome assembly. Many of these proteins likewise had homologs via BLASTp with any other non-tardigrade organism currently in the NCBI non-redundant protein database. Complete lists of differentially abundant proteins and information concerning their annotation and conservation can be found in Supplementary Table 3.1. In future work, we suggest exploring other cutting-edge tools to assign GO annotations to the tardigrade proteome, such as the AI-assisted ProteInfer (Bileschi et al. 2022), to achieve even greater annotation coverage. Likewise, it will be especially exciting to further functionally characterize these unknown proteins, as candidate proteins that aid in achieving cold tolerance in tardigrades or other crucial aspects of tardigrade physiology.

In this comparative proteomics study, we found a relatively small proportion of proteins to be differentially abundant in response to our cold treatment (89 out of 2779 proteins identified via DIA-MS, or roughly 3.2%), given our cutoff criteria (q-value < 0.1). However, the overall dynamic range of the tardigrade proteome is not yet well understood, especially in response to stressors that presumably slow down metabolic processes such as cold. For comparison (absent any other existing comparative proteomics study conducted in animals, exploring impacts of cold), a 2016 study explored how a cold acclimation (6°C cold-acclimated for 5 days) reorganizes the *Drosophila melanogaste*r transcriptome and metabolome (MacMillan et al. 2016). This study found that roughly one-third of *Drosophila melanogaste*r transcripts were differentially expressed in response to cold (defined by 2-fold expression difference between acclimation treatments and a Q-value < 0.01). However, how this flux in *Drosophila* transcriptome would correspond to the dynamic range of the proteome after cold acclimation is unknown, as the topic of correlation between transcript abundance and protein abundance is hotly debated and often notoriously poor (Vogel and Marcotte 2012; de Sousa Abreu et al. 2009). Furthermore, this study represents a 15°C warmer cold acclimation that extends roughly three additional days—potentially enabling animals to exhibit a much higher dynamic range of shifts in gene expression. Thus, future work on the proteomic profiles of tardigrades in response to low temperatures should explore a wider range of cold treatments (across a range of temperatures), rapid cold hardening, and winter-like acclimizations for longer periods of time (spanning days, weeks, or months). Exploring how the proteome, metabolome, and/or transcriptome shifts in response to seasonality from field-collected tardigrades would be highly informative, to gauge tardigrades' ecologically relevant response to shifting temperatures across seasons and winter months.

Lastly, the mechanisms of regulation of tardigrade proteins in response to cold are not yet understood: we predict that some combination of regulated protein degradation, cold-induced protein damage, cold-induced protein translation, and reallocation of

ribosomal resources or restructuring likely explains the shifts in protein abundance, similar to what has been observed in cold-exposed plants (Martinez-Seidel et al. 2021; Kazemi-Shahandashti and Maali-Amiri 2018; Ding et al. 2019; Imin et al. 2004). Once functionally important cold tolerance proteins are validated and further characterized, studies interrogating the level of regulation of these proteins (transcriptional, translational, or post-translational) and whether they are actively or passively regulated, will provide key insight into the basic physiology and biochemistry of proteins involved in cold stress tolerance in tardigrades.

GO terms relating to neural function, calcium ion regulation, and cell-cycle processes are significantly enriched in proteins more abundant after cold-treatment

Enriched GO terms of proteins significantly more abundant after cold-treatment reflect numerous alterations to biochemical and physiological pathways, with considerable convergence with insect and plant cold responses (Figure 3.3C) (Kazemi-Shahandashti and Maali-Amiri 2018; Overgaard and MacMillan 2017). Remarkably, 50% of these proteins, however, are from unannotated genes and 25% are tardigrade specific proteins—calling for further functional characterization in future experimental work, as they represent novel candidate tardigrade cold tolerance proteins. Top GO annotations of proteins more abundant in response to cold include those broadly related to neural function and ion-regulation, cell division, and various aspects of metabolism and ER function.

A top GO annotation enriched in tardigrade proteins more abundant in cold is “post regulation of voltage-gated K^+ channel.” Positive regulation of voltage-gated K+ channels is known to be a facilitative process in numerous cold-tolerant insects, as it prevents the spreading of depolarization throughout the organism, allowing the organism to function at lower temperatures and determining the critical thermal minimum CT_{min} (Overgaard and MacMillan 2017; MacMillan 2013). More so, cold stress has been demonstrated to impact the sensitivity of K^+ distribution in muscles, especially when potassium balance is decoupled and membrane potential is lost: Cooling cells have been shown to become progressively depolarized and become functionally silent (Overgaard et al. 2021; Andersen and Overgaard 2019; Findsen et al. 2014). This process is predicted to play a role in not only the onset of chill coma but also likely the recovery (Overgaard and MacMillan 2017), and our results suggest that these processes may also determine cold tolerance in tardigrades.

Likewise “calcium ion transmembrane transport,” “calcium channel activity,” and “ER Ca^{2+} homeostasis” are enriched GO annotations, with proposed functional significance, according to prior studies of cold tolerance in insects. Whereas K^+ depolarizes muscles, blocked calcium release has been shown to result in muscle cell death at cold temperatures in *Locusta migratoria* (Bayley et al. 2018). Thus, proteins that aid in shuttled excess Ca^{2+} are likely important in cold tolerance in tardigrades, as shown here.

Notably, we also observed enrichment of GO annotations related to “engulfment of apoptotic cell” and various GO terms related to cell division. Regulation of cell division is key to regulating apoptosis and cell death, and occurs in cold exposed cells of numerous insects (Yi et al. 2007; Teets and Denlinger 2013). Additional enriched GO

terms spanning a variety of functions suggest future directions for exploration of mechanisms of cold tolerance in tardigrades, beyond those highlighted here.

GO terms corresponding to lipid remodeling, tardigrade-cuticle formation, and metabolism are enriched in less abundant proteins after cold-treatment

GO annotations broadly related to lipid composition and transport, cuticle restructuring, and certain metabolic functions were enriched in proteins less abundant in cold. This is also consistent with changes seen in response to cold in insects and other ectotherms (Overgaard and MacMillan 2017). For example, we observe GO annotations relating to "fatty acid elongation" of saturated and unsaturated fats, as well as "very-long chain fatty acid biosynthesis" enriched in proteins differentially less abundant in cold-exposed tardigrades. These changes may suggest homeoviscous adaptation occurring in cold-exposed tardigrades, whereby lipid membrane composition is modified to maintain membrane fluidity at low temperatures (Sinensky 1974). Homeoviscous adaptation in response to cold occurs in numerous insect species, nematodes, and many other diverse taxa (Overgaard et al. 2008; Kayukawa et al. 2007; Ernst et al. 2016; Sinensky 1974; Wang et al. 2021). Changes in cuticle restructuring (namely upregulation of genes involved in chitin metabolism and cuticle binding), were shown to be significant in cold acclimated *Drosophila melanogaster* and are hypothesized to play the important biological function for enabling the midgut to act as a barrier to cold damage (MacMillan et al. 2016). Changes in GO terms related to collagen production and function, seen here, may have similarly important functions on the barrier of the midgut in tardigrades. As illustrated in our prior work, we observed patterns of localized cell death in the malpighian tubules and midgut of tardigrades (Chapter 1, Figure 1.1B), which is consistent with these findings. Lastly, differential enrichment of GO terms related to lipid vs. glucose metabolism, seen here, may also indicate physiological responses to cold in tardigrades—suggesting additional paths for future investigation.

Determination of candidate tardigrade ice-binding proteins

As shown by PCA (Figure 3.2B), ice-affinity purification resulted in substantial variation in protein abundances captured in downstream proteomics, compared to samples not purified by the ice-affinity method. Using the proteomics output of ice-affinity purification from tardigrades, we implemented a pipeline to rank tardigrade proteins as candidates for ice-binding activity—with the ultimate goal of discovering novel tardigrade ice-binding proteins (Figure 3.5A). Initially, we tabulated all proteins identified in proteomics via ice-affinity purification (of both cold-treated and room-temperature treated tardigrades), and filtered out any protein with a log2 fold change less than 0 in ice-shell fractions vs. whole-body fraction and larger than 300 amino acids in size. The rationale for these filters was that most known ice-binding proteins are ~20 kDA in size or less and by definition, ice-binding proteins should exist in higher concentration in the ice-shell purification fraction than the whole-body control. This left us with a list of 504 proteins, which we ranked by their likelihood to behave as ice-binding proteins, based on factors such as: abundance, degree of enrichment in the ice shell, size, presence of known IBP motifs, and AFP predictions according to (Yu and Lu 2011) (Supplementary Materials). We ultimately selected 4 proteins from this ranked list—based on their ranking as well as their predicted structures compared to known ice-binding proteins and lack of competing

GO annotations (see Methods)—to express and purify for future downstream functional analysis. These proteins include Uncharacterized Protein BV898_07018 (186 amino acids), Uncharacterized Protein BV898_01235 (137 amino acids), Uncharacterized Protein BV898_19509 (115 amino acids), and Uncharacterized Protein BV898_01687 (154 amino acids)—referred to as Candidate Tardigrade IBP 1-4, respectively (bottom row of Figure 3.5). Downstream analysis of these candidate ice-binding proteins will include *in vitro* measurements of thermal hysteresis via a nanoliter osmometer, which is the gold-standard for confirming a protein's ice-binding activity. If confirmed to induce thermal hysteresis (a shift in freezing vs melting temperature, allowing for reduced freeze damage), these proteins would represent the first ice-binding proteins to be described in any tardigrade species.

Conclusions

Prior to this work, few molecular mechanisms underlying cold tolerance in tardigrades were experimentally observed. Using a comparative proteomics pipeline on cold-treated *Hypsibius exemplaris*, we identified 89 proteins that were differentially abundant in response to -10°C cold treatment, while detecting 18 times as many proteins than any prior proteomics study in tardigrades. Nearly half of these proteins are unannotated and specific to tardigrades, meriting future exploration. We did not observe changes in LEA, HSP, or other predicted tardigrade stress-tolerant proteins in our differentially abundant protein dataset. Instead, GO annotation enrichment analysis suggested the importance of regulating ion balance, neuromuscular function, and lipid regulation and transport—among other biological processes—not yet before described in tardigrade stress tolerance, but otherwise consistent with observations in the insect and nematode literature. Prior study of cold tolerance in *Ramazzottius varieornatus* illustrated no significant shifts in transcript abundances in response to extreme subzero temperatures (-80 to -120°C, where biochemical processes are likely haulted), in contrast to our observations to detectible shifts in protein abundances in response to less extreme cold (-10°C), where biochemical responses appear feasible. This suggests that biochemical response to cold in tardigrades may occur on the translational or post-translational level at low temperature, may be taxa-specific, or may only activate in cases of less severe cold. Ice-affinity purification, a custom bioinformatics pipeline, and protein structure modeling identified a set of candidate ice-binding proteins that would be unique to tardigrades, if functionally verified. While there is a rich body of literature describing the proteomics-level response of plants to cold stress, this study represents the first such study in any animal.

3.6 Acknowledgements

Our work was partially supported by several Walker Grants from the Essig Museum of Entomology (2017-2021), Summer Research Awards from the Department of Integrative Biology, UC Berkeley (2017-2022), an IB Dissertation Completion Award (2021), a Berkeley Chapter of Sigma Xi FY 2020 GIAR, and research fellowship funded by the BARD US-Israel Agricultural Research & Development Fund, in collaboration with Prof. Ido Braslavsky at the Robert H. Smith Faculty, Hebrew University of Jerusalem**.** Many remarkable undergraduate researchers must also be thanked for their experimental and

computational contributions to this work: Hannah Ritchie, Walter Wu, Kylie Cheng, Lily Shang, Dejénaé See, Kyla Woyshner, Iris Chow, and Catherine Lu.

3.7 Figures

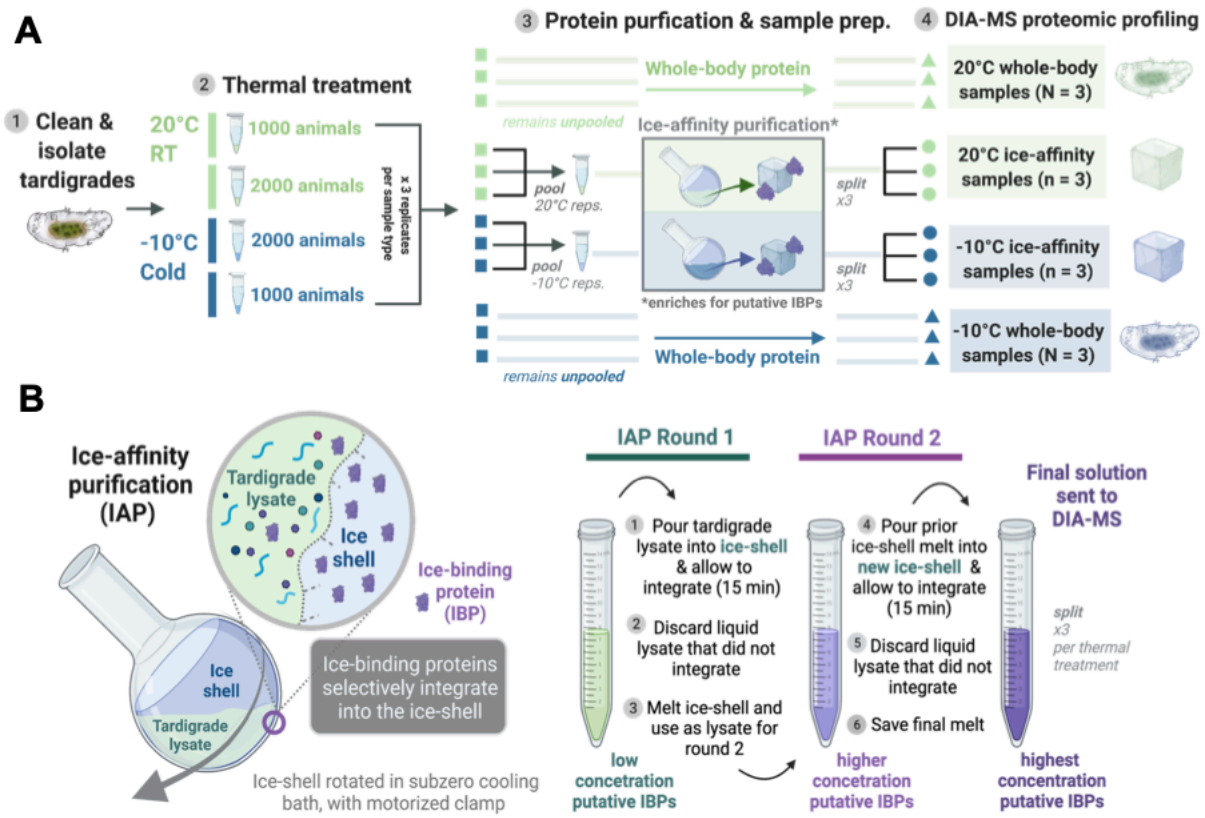

Figure 3.1. Experimental overview for comparative proteomics of cold-treated tardigrades (*Hypsibius exemplaris*)

A) Experimental design of comparative proteomics study. Groups of 1000 (whole-body protein) or 2000 (ice-affinity purification, IAP) adult tardigrades were collected and exposed to cold treatment (with a final low temperature of -10°C) or ambient temperature (20°C) (N=3 for all sample types). Whole-body protein samples were immediately processed for DIA-MS Proteomic Profiling, and IAP samples were pooled prior to undergoing IAP to enrich for novel, candidate ice-binding proteins (IBPs), prior to being split into three technical replicates prior to DIA-MS proteomic profiling.

B) Schematic illustrating the iterative process of ice-affinity purification, with the goal of increasing enrichment of proteins with the biochemical properties to bind to ice. From left to right: Tardigrade lysate (depicted in Green) is poured into a round bottom flask, which is prepared with a thin layer of ice on the internal surface (illustration modified from Marshall et al. 2016). This flask, loaded with tardigrade samples, is rotated at low temperature, to allow candidate ice-binding proteins (purple) to selectively bind to the ice's surface. This ice-shell is melted and the process is repeated for a second time, to result in a higher-concentration of candidate IBPs.

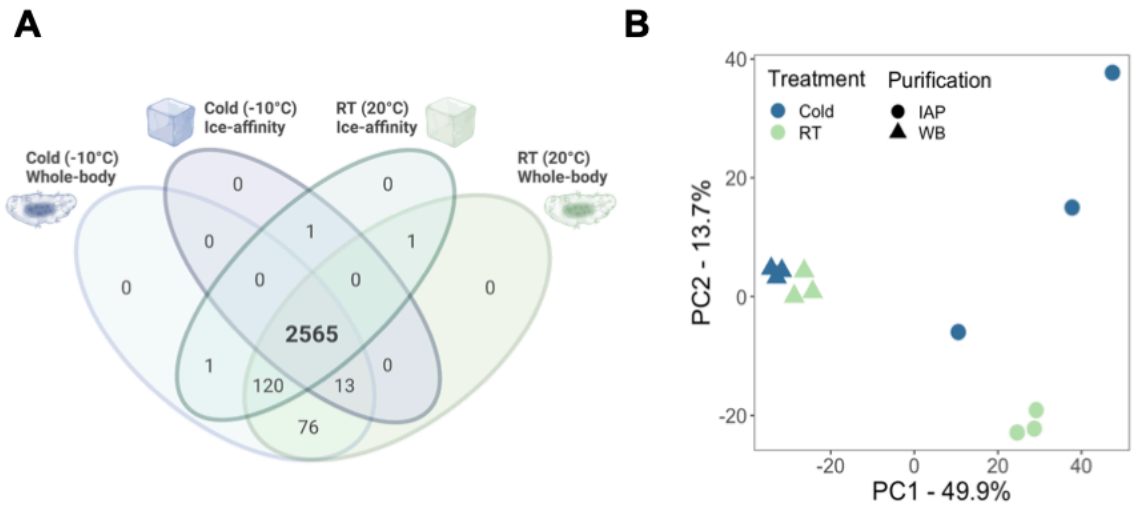

Figure 3.2. Summary of proteins identified via DIA-MS proteomic profiling
A) Number of proteins identified in each sample type (presence or absence). 2776 unique proteins were identified in total, with high coverage across all sample types.
B) Principal components analysis (PCA) on abundances of proteins identified in sample types, based on thermal treatment ("Cold" -10°C = Blue, "RT" Room Temperature 20°C = Green) and protein purification method ("IAP" Ice-affinity Purification = Circle, "WB" whole-body = Triangle). Protein purification method most strongly impacts protein abundance variation (PC1 - 49.9%), and samples further cluster by thermal treatment.

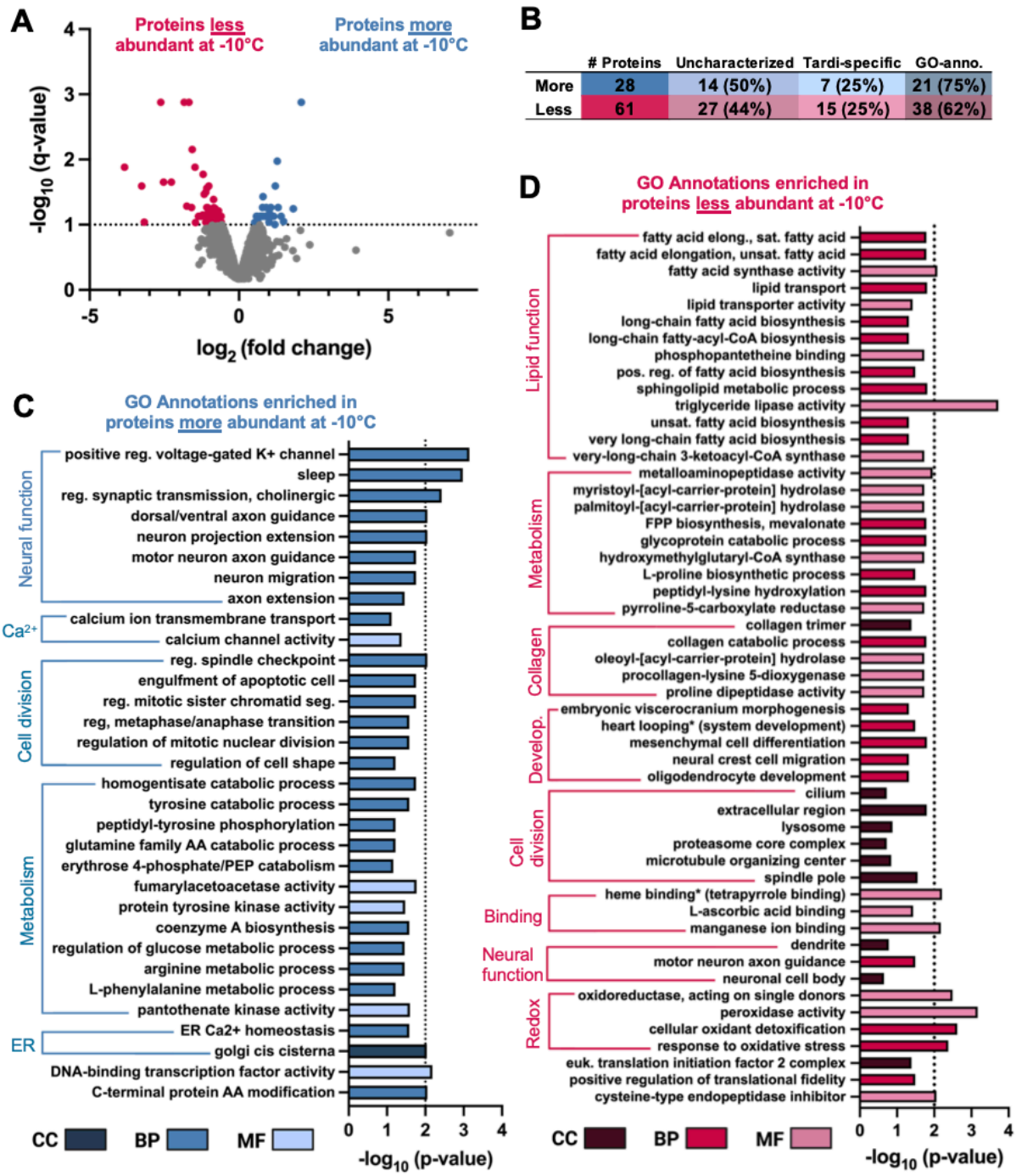

Figure 3.3. Cold treatment of tardigrades affects several key biological processes, as shown by Gene Ontology (GO) enrichment analysis of differentially abundant proteins

Fig. 3.3 continued
A) Volcano plot depicting $\log_2$(fold change) of protein abundance in cold treated (-10°C) whole-body tardigrade samples (blue) vs. room temperature (20°C). Dotted line represents a q-value cutoff of 0.1
B) Description of proteins identified to be differentially more abundant in response to cold treatment (blue) vs. less (pink). # Proteins = number of differentially abundant proteins (q-value < 0.1), Uncharacterized = no annotation for this protein assigned at Yoshida 2017 annotation, Tardi-specific = protein only found in *Hypsibius exemplaris, or H. exemplaris* and the *Ramazzottius varieornatus* genome, but no other taxa in the NCBI non-redundant protein database, GO-anno. = # of proteins with at least 1 GO annotation according to Panzer 2.0
C) GO annotations that are significantly enriched in proteins more abundant or D) less abundant cold-treated animals. Bars denote the –log10(p-value) according to a Fisher's Exact test. All proteins displayed have p-value < 0.05 and dotted line denotes p-value < 0.01. CC= Cellular component, BP = Biological Function, MF = Molecular Function.

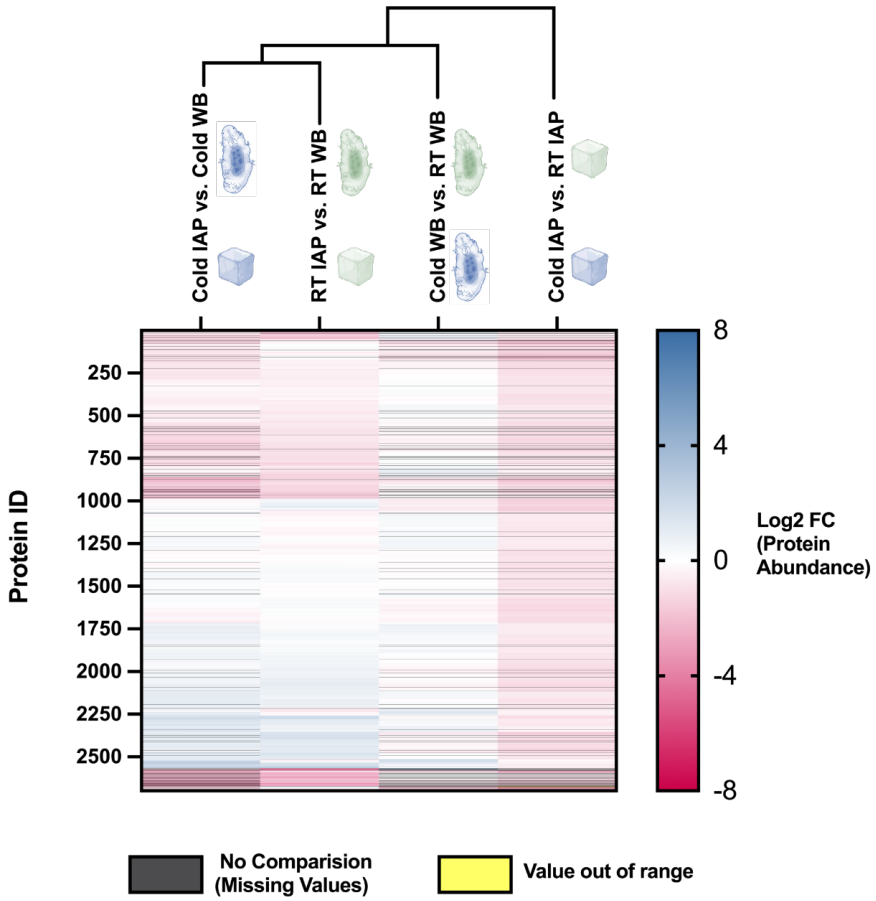

Figure 3.4. Log2 fold changes in protein abundances among ice-affinity purified elution fractions and whole-body tardigrade samples A heatmap represents the log2 fold change in protein abundances of each sample type compared to another, where protein IDs and sample types were hierarchically clustered (using Euclidean distance and averages for linkage). “Cold IAP” = ice-affinity purified protein abundances of cold-treated tardigrades (-10°C); “RT IAP” = ice-affinity purification of room-temperature tardigrades (20°C); “Cold whole-body” = protein abundances from whole-body protein samples from cold-treated tardigrades (-10°C). “RT whole-body” = whole-body protein from room-temperature tardigrades (20°C). Blue depicts an increase in protein abundance of the first sample type listed compared to the second. Magenta depicts a decrease. Black represents proteins where no log2 fold comparison was calculated, due to lack of protein detection during mass-spec in one or both sample types. Yellow represents rare instances where the log2 fold change was greater than or less than the scale bar. Each protein identified in mass spec has been assigned a Protein ID that corresponds with its position on this plot. The cladogram represents similarity among sample-type comparisons, determined by clustering, but is not drawn to scale. Overall, we find that the proteome remains largely stable between experimental conditions, with protein purification method (whole-body or IAP) have the largest global impact on protein abundances—with the exception of proteins discussed in Fig 3.3.

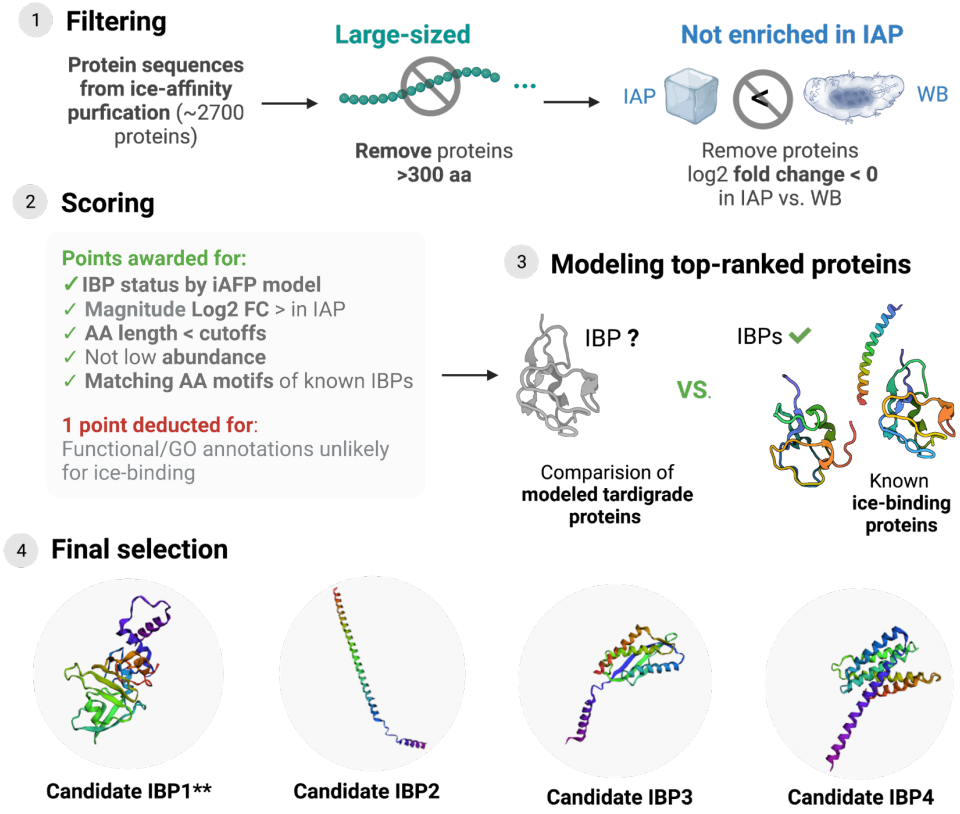

Figure 3.5. Custom bioinformatics pipeline used to select candidate tardigrade ice-binding proteins from ice-affinity purification proteomics data

Pipeline used to select candidate tardigrade ice-binding proteins (IBPs), from ice-affinity purification proteomics data. Step 1 involved removing all proteins from the cold-treated ice-affinity purification proteomics dataset that were over 300 amino acids in length or not selectively enriched in the ice-fraction of ice-affinity purification compared to the whole-body sample (log2 fold change < 0, in ice-affinity purification proteomics output compared to whole-body proteomics output). Most ice-binding proteins found in other organisms are known to be <20kDa in size and have an affinity to bind ice, giving rationale to these filtering steps. In Step 2, remaining proteins in the dataset were scored based on several criteria (listed above; the iAFP model and amino acid motifs are described in methods in greater detail). In Step 3, the structures of the top 25 ranked tardigrade protein sequences were modeled using trRosetta and manually inspected for structural characteristics similar to those seen in known IBPs (see methods). Finally, in Step 4, four tardigrade proteins were selected as top candidate ice-binding proteins for downstream *in vitro* characterization, based on the prior steps. Candidate IBP structures were modeled with trRosetta (Du et al. 2021). *iAFP model implemented is from Yu and Lu 2011. **Candidate IBP1 was selected based on having the highest abundance in the cold-treated ice-affinity purification proteomics output and having predicted ice-binding function from the iAFP model. Other candidates were selected based on all criteria.

3.8 Supplementary Materials

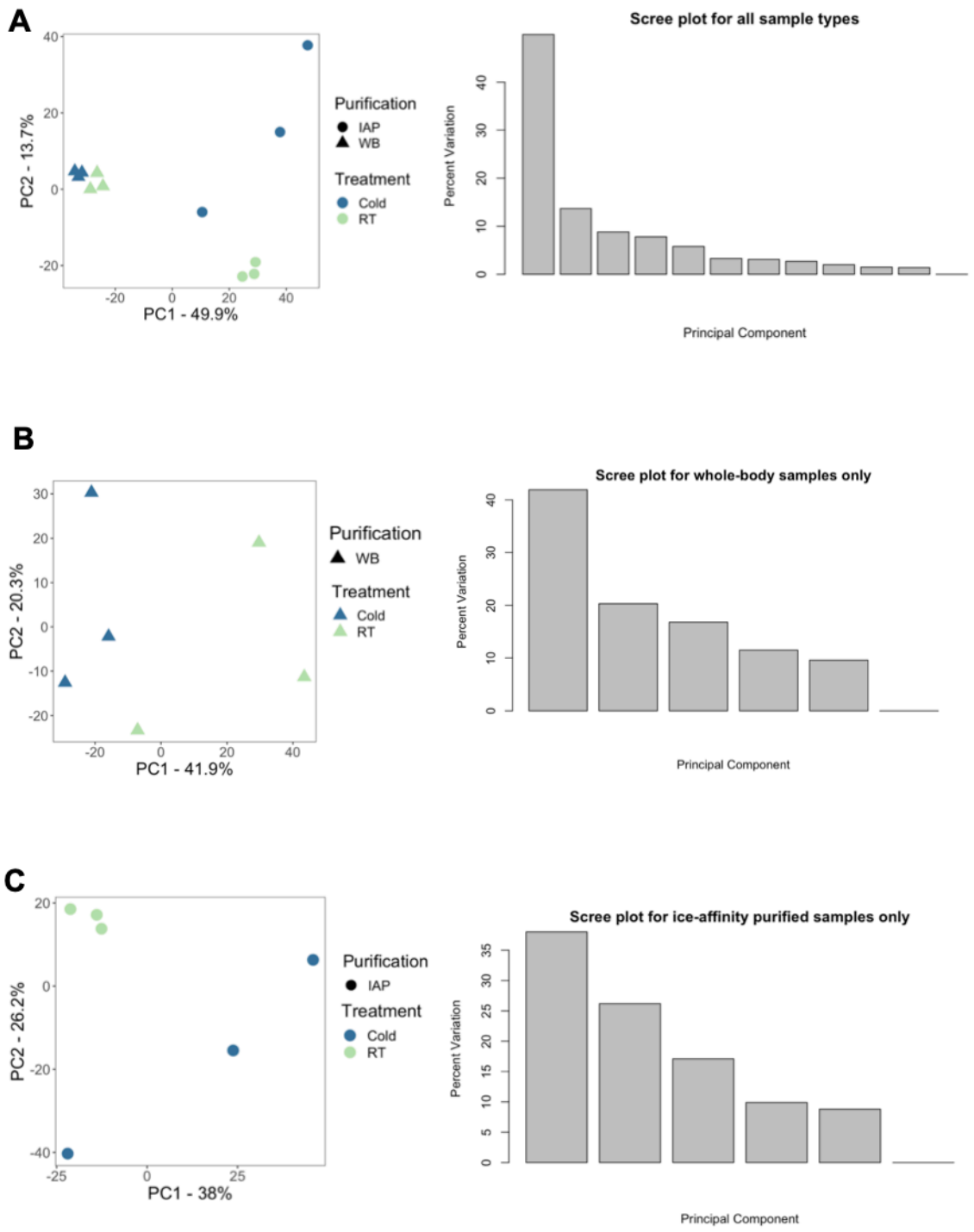

Supplementary Figure 3.1. PCAs of all experimental conditions, further partitioned by purification method

A) Principal components analysis (PCA) on abundances of proteins identified in all sample types, based on both thermal treatment ("Cold" -10°C = Blue, "RT" Room Temperature 20°C = Green) and protein purification method ("IAP" Ice-affinity

Supplementary Fig. 3.1. continued
Purification = Circle, “WB” whole-body = Triangle), also indicating 3-5 principal components in corresponding scree plot.
B) Principal components analysis (PCA) on abundances of proteins identified in whole-body samples, based on thermal treatment (“Cold” -10°C = Blue, “RT” Room Temperature 20°C = Green).
C) Principal components analysis (PCA) on abundances of proteins identified in ice-affinity purification samples, based on thermal treatment (“Cold” -10°C = Blue, “RT” Room Temperature 20°C = Green).

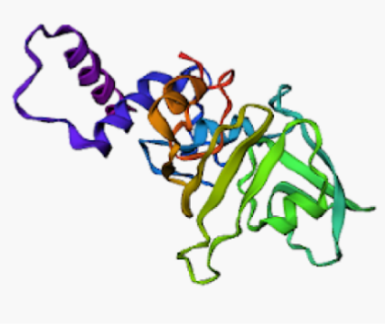

Tardigrade Candidate IBP #1
NCBI Accession number & Genome ID: **OQV18962.1, BV898_07018**
Genome annotation: **Hypothetical protein (unknown function)**
Closest pBLAST annotation: **hypothetical protein RvY_05618 [*Ramazzottius varieornatus*] (e-value 1e-80)**
GO annotations**: fatty acid transport, lipid catabolic process, extracellular region, lipase activity, binding, cellular process**
Length: **186 aa** Molecular weight: **19.94 kDa**
Avg. IAP Abundance: **43,031,400** Log2 fold change in IAP vs WB**: 0.71**
Reason for selection: **iAPF = 1, highest abundance protein in IAP & top candidate in pilot IAP experiment**

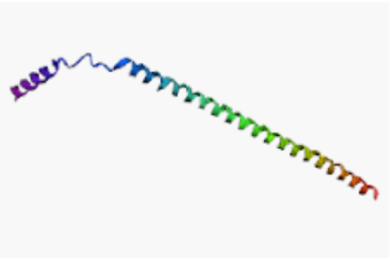

Tardigrade Candidate IBP #2
NCBI Accession number & Genome ID: **none; BV898_09539**
Genome annotation: **Hypothetical protein (unknown function)**
Closest pBLAST annotation: **none**
GO annotations**: nucleosome, nucleosome assembly, nucleus, nucleosomal DNA binding**
Length: **99 aa** Molecular weight: **9.5 kDa**
Avg. IAP Abundance:**2,431,163** Log2 fold change in IAP vs WB**: 0.39**
Reason for selection: **iAPF = 2, large number of IBP-like motifs, high score in ranking system**

Tardigrade Candidate IBP #3
NCBI Accession number & Genome ID: **OQV24628, BV898_01687**
Genome annotation: **Hypothetical protein (unknown function)**
Closest pBLAST annotation: **hypothetical protein BV898_14510 [*Hypsibius exemplaris*] (e-value = 1e-06)**
GO annotations**: nucleosome, nucleosome assembly, nucleus, nucleosomal DNA binding**
Length: **154 aa** Molecular weight: **16.59 kDa**
Avg. IAP Abundance: **430,633** Log2 fold change in IAP vs WB**: 1.69**
Reason for selection: **iAPF = 1, high score in ranking system**

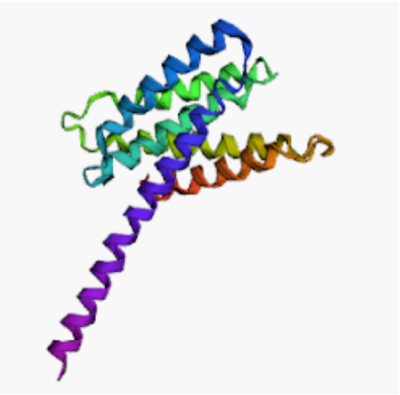

Tardigrade Candidate IBP #4
NCBI Accession number: **OQV14909.1, BV898_10940**
Genome annotation: **Hypothetical protein (unknown function)**
Closest pBLAST annotation: **unnamed protein product [Vitrella brassicaformis CCMP3155] (e-value 0.006)**
GO annotations**: extracellular space, mucilage biosynthesis**
Length: **97 aa** Molecular weight: **10.67 kDa**
Avg. IAP Abundance : **24903** Log2 fold change in IAP vs WB**: 1.033**
Reason for selection: **iAFP = 1, high score in ranking system**

SF3.2 Additional description of 4 selected candidate tardigrade IBPs, with predicted structures modeled by trRosetta with default parameters iAFP score represents detection of ice-binding function, according to the prediction model of Yu and Lu 2011. All four candidate tardigrade IBPs listed here were heterologously expressed and purified for downstream assays i*n vitro*, measuring ice-binding activity (thermal hysteresis).

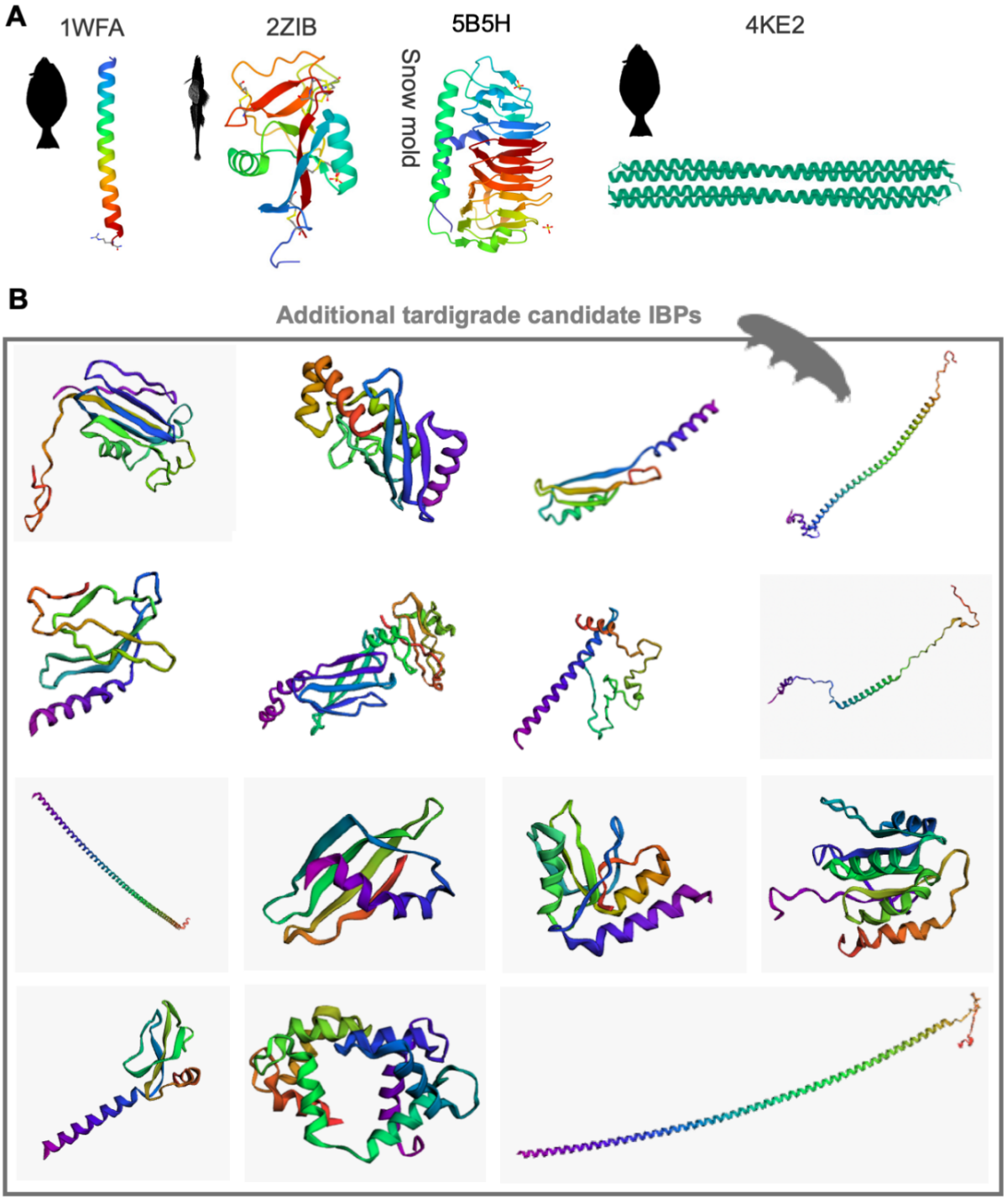

SF3.3 Predicted structures of additional 15 top-ranked candidate tardigrade IBPs
A) Four example protein structures from PDB, of confirmed IBPs in other organisms.
B) Fifteen additional candidate tardigrade IBPs are shown here, all of which scored highly according the the ranking system described in Figure 3.5. Protein structures with grey backgrounds were modeled by trRosetta with default parameters and structures with white background were modeled by Robetta (default parameters *ab initio*).

Accession	Description (Proteins more abundant in cold)	log2 FC	-log10 (q-value)	Mean Abund. Cold WB
OQV12573.1	Cytochrome P450 2U1	2.09	2.88	802961.67
OWA50972.1	Transmembrane and coiled-coil domains protein 1	1.82	1.24	52442.33
OQV18904.1	hypothetical protein BV898_06966	1.5	1.05	428913
OQV12536.1	Pantothenate kinase 1	1.41	1.13	14988
OQV19911.1	hypothetical protein BV898_06179	1.32	1.26	27766.33
OQV24856.1	Acidic mammalian chitinase	1.28	1.97	330580.67
OQV23682.1	hypothetical protein BV898_02420	1.22	1.59	308107
OQV14030.1	Histidine ammonia-lyase	1.2	1	19716.33
OQV22851.1	putative Plasma kallikrein	1.17	1.13	32336.33
OQV20245.1	Ras-related C3 botulinum toxin substrate 1	1.07	1.26	84090
OQV16857.1	hypothetical protein BV898_09029	1.03	1.18	138800
OQV23765.1	hypothetical protein BV898_02496	1.01	1.04	62404.67
OQV17453.1	hypothetical protein BV898_08387	0.95	1.13	686425.67
OQV16628.1	putative 60S ribosomal protein L36	0.91	1.26	300170
OWA54155.1	hypothetical protein BV898_18571	0.86	1.13	66434.67
OWA50272.1	hypothetical protein BV898_14794	0.81	1.43	162968.67
OWA53886.1	hypothetical protein BV898_18305	0.8	1.13	199693
OQV22648.1	hypothetical protein BV898_03473	0.79	1.26	352015.67
OQV20964.1	putative Transient recep. cation chan. subfam. M 6	0.78	1.13	1328816
OQV15711.1	Leucine carboxyl methyltransferase 1	0.76	1.13	768535.67
OQV13140.1	ERC protein 2	0.71	1.13	1243912.33
OQV23488.1	hypothetical protein BV898_02605	0.63	1.12	120159
OQV24861.1	hypothetical protein BV898_01447	0.63	1.04	260297.33
OQV20248.1	Fumarylacetoacetase	0.61	1.13	398559
OQV16396.1	hypothetical protein BV898_09539	0.59	1.13	1826189.67
OQV16302.1	hypothetical protein BV898_09610	0.59	1.04	201232
OWA54356.1	Myosin heavy chain, muscle	0.56	1	900691.33
OQV22714.1	Macrophage colony-stimulating factor 1 receptor 2	0.53	1.03	233342.33

ST3.1 Additional description of proteins more abundant in tardigrades after cold treatment log2 FC represents change in protein abundance between cold-treated tardigrades and room temperature tardigrades (whole-body). Cells highlighted in grey illustrate proteins that were previously undescribed in the tardigrade reference genome from Yoshida et al. 2017.

Accession	Description (Proteins less abundant in cold)	log2 FC	-log10 (q-value)	Mean Abund. Cold WB
OQV25865.1	Fatty acid synthase	-0.58	1.04	235289.67
OQV23840.1	Cathepsin L	-0.59	1.04	129161.67
OQV22175.1	Catalase HPII	-0.6	1.13	185354.33
OQV14621.1	putative Proteasome subunit beta type-2	-0.64	1.12	469417.33
OQV16319.1	Zinc-type alcohol dehydrogenase-like protein	-0.65	1.03	57137.33
OQV19097.1	Coiled-coil domain-containing protein 6	-0.66	1.04	177918
OWA52325.1	putative Leucine-rich repeat-containing protein 15	-0.66	1.04	360959.67
OQV20428.1	putative aminopeptidase NPEPL1	-0.67	1.04	36670
OQV22369.1	putative Cellular retinoic acid-binding protein 1	-0.68	1.03	228022.33
OWA49978.1	hypothetical protein BV898_14510	-0.68	1.13	522450.33
OQV17908.1	hypothetical protein BV898_08037	-0.68	1.21	78280.67
OQV24734.1	hypothetical protein BV898_01327	-0.72	1.21	66804.33
OQV22838.1	3-hydroxyacyl-CoA dehydrogenase type-2	-0.73	1.12	35510.67
OQV21465.1	Cytosolic Fe-S cluster assembly factor nubp2	-0.75	1.04	66661
OQV24854.1	hypothetical protein BV898_01442	-0.79	1.25	59589.33
OQV19206.1	hypothetical protein BV898_06842	-0.79	1.15	373708.67
OQV20754.1	hypothetical protein BV898_05332	-0.8	1.15	34473.33
OQV25067.1	putative Pancreatic triacylglycerol lipase	-0.82	1.03	591298.67
OQV18722.1	hypothetical protein BV898_07161	-0.83	1.26	47096
P0CU40.1	Secretory-abundant heat soluble protein 53582	-0.83	1.15	8095136.67
OQV24592.1	hypothetical protein BV898_01652	-0.84	1.39	49293.33
OQV13291.1	putative Prosaposin	-0.86	1.18	34159.33
OQV24733.1	hypothetical protein BV898_01326	-0.87	1.24	233640.33
OQV21922.1	hypothetical protein BV898_04135	-0.9	1.21	36560
OQV23788.1	hypothetical protein BV898_02514	-0.9	1.24	49278
OQV23159.1	putative Pancreatic triacylglycerol lipase	-0.92	1.04	107705.67
OQV13852.1	Procollagen-lysine,2-oxoglutarate 5-dioxygenase 3	-0.94	1.13	14745.67
OQV17559.1	Vitellogenin-6	-0.96	1.03	2122830.33
OWA49851.1	put. Elongation of very long chain fatty acids protein 5	-0.96	1.21	28084.67
OQV13843.1	Eukaryotic	-1.01	1.59	373698.67
OQV14848.1	hypothetical protein BV898_10995	-1.01	1.18	51589.67
OQV22418.1	putative La-related protein	-1.04	1.13	14055.33
OQV17764.1	hypothetical protein BV898_08221	-1.04	1.13	37165.67
OQV25732.1	Allene oxide synthase-lipoxygenase protein	-1.05	1.26	625287.33
OQV21481.1	Xaa-Pro dipeptidase	-1.06	1.05	20543.67
OQV11417.1	Hydroxymethylglutaryl-CoA synthase, cytoplasmic	-1.07	1.56	28539.67
OQV14251.1	hypothetical protein BV898_11488	-1.07	1.26	34910.33
OQV16777.1	hypothetical protein BV898_09133	-1.08	1.16	42951.33
OQV25731.1	Allene oxide synthase-lipoxygenase protein	-1.11	1.5	321941.67
OQV20556.1	Chorion peroxidase	-1.11	1.04	16522.67
OQV21904.1	Vitellogenin-6	-1.16	1.47	6976458.33
OQV16319.1	Zinc-type alcohol dehydrogenase-like protein	-1.19	1.77	43519
OQV20744.1	Nose resistant to fluoxetine protein 6	-1.21	1.15	125052.33
OQV19039.1	hypothetical protein BV898_06895	-1.28	1.13	6869.33
OQV16226.1	hypothetical protein BV898_09709	-1.28	1.13	6240.67
OQV24865.1	Chorion peroxidase	-1.35	1.13	5896.67
OWA54228.1	hypothetical protein BV898_18639	-1.46	1.03	5554.67
OQV26136.1	hypothetical protein BV898_00258	-1.47	1.88	39977
OQV24876.1	Pancreatic lipase-related protein 2	-1.56	2.16	33819
OWA52228.1	hypothetical protein BV898_16686	-1.58	1.26	9989.67
OQV17094.1	hypothetical protein BV898_08810	-1.67	2.88	27677.33
OQV13017.1	putative Very low-density lipoprotein receptor	-1.75	1.28	10412.33
OQV22246.1	Pyrroline-5-carboxylate reductase 1, mitochondrial	-1.83	2.88	18481.33
OQV24625.1	hypothetical protein BV898_01684	-2.26	1.65	5469.33
OQV14977.1	hypothetical protein BV898_10878	-2.52	1.65	1905
OQV21547.1	hypothetical protein BV898_04449	-2.62	2.88	3003
OQV23464.1	Oxidative stress-induced growth inhibitor 2	-3.17	1.04	3565335.33
OQV23553.1	hypothetical protein BV898_02672	-3.26	1.59	567.35
OQV19204.1	hypothetical protein BV898_06840	-3.83	1.88	2036.53
OQV23800.1	putative Glutaredoxin-related protein 5, mitochondrial	-3.83	1.88	2036.53
OWA55468.1	hypothetical protein BV898_19855	-3.83	1.88	2036.53

ST3.2 Description of proteins less abundant in tardigrades after cold treatment

Table 1 of 2

Accession	Description	GO ID	Cat.	GO description
OQV12573.1	Cytochrome P450 2U1	GO:0004497	MF	monooxygenase activity
		GO:0005506	MF	iron ion binding
		GO:0016021	CC	integral component of membrane
		GO:0016705	MF	oxidoreductase activity acting on paired donors with incorporation or reduction of molecular oxygen
		GO:0020037	MF	heme binding
OWA50972.1	Transmembrane and coiled-coil domains protein 1	GO:0000137	CC	Golgi cis cisterna
		GO:0005262	MF	calcium channel activity
		GO:0030176	CC	integral component of endoplasmic reticulum membrane
		GO:0032469	BP	endoplasmic reticulum calcium ion homeostasis
		GO:0070588	BP	calcium ion transmembrane transport
OQV18904.1	hypothetical protein BV898_06966*	GO:0030431	BP	sleep
		GO:0032222	BP	regulation of synaptic transmission, cholinergic
		GO:1903818	BP	positive regulation of voltage-gated potassium channel activity
OQV12536.1	Pantothenate kinase 1	GO:0004594	MF	pantothenate kinase activity
		GO:0005524	MF	ATP binding
		GO:0015937	BP	coenzyme A biosynthetic process
		GO:0016310	BP	phosphorylation
OQV19911.1	hypothetical protein BV898_06179			
OQV24856.1	Acidic mammalian chitinase	GO:0000981	MF	DNA-binding transcription factor activity, RNA polymerase II-specific
		GO:0003677	MF	DNA binding
		GO:0005576	CC	extracellular region
		GO:0005634	CC	nucleus
		GO:0005975	BP	carbohydrate metabolic process
		GO:0006357	BP	regulation of transcription by RNA polymerase II
		GO:0008061	MF	chitin binding
		GO:2000112	BP	regulation of cellular macromolecule biosynthetic process
OQV23682.1	hypothetical protein BV898_02420			
OQV14030.1	Histidine ammonia-lyase	GO:0016829	MF	lyase activity
OQV22851.1	putative Plasma kallikrein	GO:0004252	MF	serine-type endopeptidase activity
		GO:0005615	CC	extracellular space
		GO:0006508	BP	proteolysis
OQV20245.1	Ras-related C3 botulinum toxin substrate 1	GO:0001764	BP	neuron migration
		GO:0003924	MF	GTPase activity
		GO:0005525	MF	GTP binding
		GO:0005856	CC	cytoskeleton
		GO:0005886	CC	plasma membrane
		GO:0005938	CC	cell cortex
		GO:0006996	BP	organelle organization
		GO:0007163	BP	establishment or maintenance of cell polarity
		GO:0007264	BP	small GTPase mediated signal transduction
		GO:0008045	BP	motor neuron axon guidance
		GO:0008360	BP	regulation of cell shape
		GO:0019901	MF	protein kinase binding
		GO:0030029	BP	actin filament-based process
		GO:0031410	CC	cytoplasmic vesicle
		GO:0032956	BP	regulation of actin cytoskeleton organization
		GO:0033563	BP	dorsal/ventral axon guidance
		GO:0042995	BP	cell projection
		GO:0043652	BP	engulfment of apoptotic cell
		GO:0048675	BP	axon extension
		GO:0097435	BP	supramolecular fiber organization
		GO:1902284	BP	neuron projection extension involved in neuron projection guidance
OQV16857.1	hypothetical protein BV898_09029			
OQV23765.1	hypothetical protein BV898_02496	GO:0016021	CC	integral component of membrane
OQV17453.1	hypothetical protein BV898_08387			
OQV16628.1	putative 60S ribosomal protein L36	GO:0000228	CC	nuclear chromosome
		GO:0003735	MF	structural constituent of ribosome
		GO:0005730	CC	nucleolus
		GO:0005829	CC	cytosol
		GO:0005840	CC	ribosome
		GO:0006412	BP	translation
		GO:1990904	CC	ribonucleoprotein complex

ST3.3a Full list of GO annotations of proteins more abundant in cold (Part 1 of 2) Cells highlighted in grey illustrate proteins that were previously undescribed in Yoshida et al. 2017. Proteins highlighted in pale yellow illustrate those with one or more significantly enriched GO annotation (shades of blue according to GO-category). Bright yellow signifies previously undescribed proteins with significantly enriched GO term(s).

Table 2 of 2

Accession	Description	GO ID	Cat.	GO description
OWA54155.1	hypothetical protein BV898_18571			
OWA50272.1	hypothetical protein BV898_14794			
OWA53886.1	hypothetical protein BV898_18305	GO:0005576	CC	extracellular region
		GO:0008061	MF	chitin binding
		GO:0016021	CC	integral component of membrane
OQV22648.1	hypothetical protein BV898_03473	GO:0016021	CC	integral component of membrane
OQV20964.1	putative Transient recep. cation chan. subfam. M 6	GO:0006811	CC	GINS complex
		GO:0016021	CC	integral component of membrane
OQV15711.1	Leucine carboxyl methyltransferase 1	GO:0005829	CC	cytosol
		GO:0007088	BP	regulation of mitotic nuclear division
		GO:0008168	MF	methyltransferase activity
		GO:0008213	BP	protein alkylation
		GO:0010906	BP	regulation of glucose metabolic process
		GO:0018410	BP	C-terminal protein amino acid modification
		GO:0030071	BP	regulation of mitotic metaphase/anaphase transition
		GO:0031333	BP	negative regulation of protein-containing complex assembly
		GO:0032259	BP	methylation
		GO:0033047	BP	regulation of mitotic sister chromatid segregation
		GO:0042981	BP	regulation of apoptotic process
		GO:0090231	BP	regulation of spindle checkpoint
		GO:0140096	MF	catalytic activity, acting on a protein
OQV13140.1	ERC protein 2	GO:0003700	MF	DNA-binding transcription factor activity
		GO:0005737	CC	cytoplasm
		GO:0006355	BP	regulation of DNA-templated transcription
		GO:2000112	BP	regulation of cellular macromolecule biosynthetic process
OQV23488.1	hypothetical protein BV898_02605*	GO:0016021	CC	integral component of membrane
		GO:0030431	BP	sleep
		GO:0032222	BP	regulation of synaptic transmission, cholinergic
		GO:1903818	BP	positive regulation of voltage-gated potassium channel activity
OQV24861.1	hypothetical protein BV898_01447	GO:0006508	BP	proteolysis
		GO:0008237	MF	metallopeptidase activity
OQV20248.1	Fumarylacetoacetase	GO:0004334	MF	fumarylacetoacetase activity
		GO:0006525	BP	arginine metabolic process
		GO:0006558	BP	L-phenylalanine metabolic process
		GO:0006572	BP	tyrosine catabolic process
		GO:0009063	BP	cellular amino acid catabolic process
		GO:0009065	BP	glutamine family amino acid catabolic process
		GO:0046872	MF	metal ion binding
		GO:1902000	BP	homogentisate catabolic process
		GO:1902222	BP	erythrose 4-phosphate/phosphoenolpyruvate fam.aa catabolic process
OQV16396.1	hypothetical protein BV898_09539	GO:0000786	CC	nucleosome
		GO:0003677	MF	DNA binding
		GO:0006323	BP	chromosome organization
		GO:0006333	BP	chromatin organization
		GO:0034622	BP	protein-containing complex assembly
		GO:0034728	BP	nucleosome organization
		GO:0065004	BP	protein-DNA complex assembly
OQV16302.1	hypothetical protein BV898_09610	GO:0016021	CC	integral component of membrane
OWA54356.1	Myosin heavy chain muscle	GO:0003774	MF	cytoskeletal motor activity
		GO:0005524	MF	ATP binding
		GO:0016459	CC	myosin complex
		GO:0030017	CC	sarcomere
		GO:0051015	MF	actin filament binding
OQV22714.1	Macrophage colony-stimulating factor 1 receptor 2	GO:0004713	MF	protein tyrosine kinase activity
		GO:0005524	MF	ATP binding
		GO:0016021	CC	integral component of membrane
		GO:0018108	BP	peptidyl-tyrosine phosphorylation

ST3.3b Full list of GO annotations of proteins more abundant in tardigrades after cold treatment (Part 2 of 2)

Table 1 of 3

Accession	Description	GO ID	Cat.	GO description
OQV25865.1	Fatty acid synthase	GO:0004315	MF	3-oxoacyl-[acyl-carrier-protein] synthase activity
		GO:0004320	MF	oleoyl-[acyl-carrier-protein] hydrolase activity
		GO:0006633	BP	fatty acid biosynthetic process
		GO:0016295	MF	myristoyl-[acyl-carrier-protein] hydrolase activity
		GO:0016296	MF	palmitoyl-[acyl-carrier-protein] hydrolase activity
		GO:0031177	MF	phosphopantetheine binding
OQV23840.1	Cathepsin L	GO:0004175	MF	endopeptidase activity
		GO:0004869	MF	cysteine-type endopeptidase inhibitor activity
		GO:0005615	CC	extracellular space
		GO:0005764	CC	lysosome
		GO:0006508	BP	proteolysis
		GO:0008234	MF	cysteine-type peptidase activity
		GO:0010951	BP	negative regulation of endopeptidase activity
		GO:0016021	CC	integral component of membrane
		GO:0044257	BP	protein catabolic process
OQV22175.1	Catalase HPII	GO:0004096	MF	catalase activity
		GO:0006979	BP	response to oxidative stress
		GO:0020037	MF	heme binding
		GO:0042744	BP	hydrogen peroxide catabolic process
		GO:0046872	MF	metal ion binding
		GO:0098869	BP	cellular oxidant detoxification
OQV14621.1	putative Proteasome subunit beta type-2	GO:0004298	MF	threonine-type endopeptidase activity
		GO:0005634	CC	nucleus
		GO:0005737	CC	cytoplasm
		GO:0005839	CC	proteasome core complex
		GO:0051603	BP	proteolysis involved in protein catabolic process
OQV16319.1	Zinc-type alcohol dehydrogenase-like protein	GO:0008152	BP	metabolic process
		GO:0008270	MF	zinc ion binding
		GO:0016491	MF	oxidoreductase activity
OQV19097.1	Coiled-coil domain-cont. protein 6			
OWA52325.1	putative Leucine-rich repeat-cont. 15			
OQV20428.1	putative aminopeptidase NPEPL1	GO:0005737	CC	cytoplasm
		GO:0006508	BP	proteolysis
		GO:0030145	MF	manganese ion binding
		GO:0070006	MF	metalloaminopeptidase activity
OQV22369.1	putative Cellular retinoic acid-binding protein 1	GO:0001947	BP	heart looping
		GO:0005634	CC	nucleus
		GO:0005829	CC	cytosol
		GO:0008289	MF	lipid binding
		GO:0015908	BP	fatty acid transport
		GO:0016021	CC	integral component of membrane
		GO:0033293	MF	monocarboxylic acid binding
		GO:0043009	BP	chordate embryonic development
OWA49978.1	hypothetical protein BV898_14510			
OQV17908.1	hypothetical protein BV898_08037			
OQV24734.1	hypothetical protein BV898_01327			
OQV22838.1	3-hydroxyacyl-CoA dehydrogenase type-2	GO:0004312	MF	fatty acid synthase activity
		GO:0016491	MF	oxidoreductase activity
OQV21465.1	Cytosolic Fe-S cluster assembly factor nubp2	GO:0000922	CC	spindle pole
		GO:0005515	MF	protein binding
		GO:0005524	MF	ATP binding
		GO:0005634	CC	nucleus
		GO:0005737	CC	cytoplasm
		GO:0005815	CC	microtubule organizing center
		GO:0005929	CC	cilium
		GO:0016226	BP	iron-sulfur cluster assembly
		GO:0016887	MF	ATP hydrolysis activity
		GO:0030030	BP	cell projection organization
		GO:0046872	MF	metal ion binding
		GO:0051539	MF	4 iron, 4 sulfur cluster binding
OQV24854.1	hypothetical protein BV898_01442			
OQV19206.1	hypothetical protein BV898_06842			
OQV20754.1	hypothetical protein BV898_05332	GO:0004930	MF	G protein-coupled receptor activity
		GO:0007186	BP	G protein-coupled receptor signaling pathway
		GO:0016021	CC	integral component of membrane
OQV25067.1	putative Pancreatic triacylglycerol lipase	GO:0004806	MF	triglyceride lipase activity
		GO:0005576	CC	extracellular region
OQV18722.1	hypothetical protein BV898_07161			
P0CU40.1	Secretory-abundant heat soluble protein 53582	GO:0005576	CC	extracellular region
		GO:0008289	MF	lipid binding
OQV24592.1	hypothetical protein BV898_01652	GO:0016021	CC	integral component of membrane
OQV13291.1	putative Prosaposin	GO:0005576	CC	extracellular region
		GO:0005764	CC	lysosome
		GO:0006665	BP	sphingolipid metabolic process

ST3.4a Full list of GO terms of proteins less abundant in cold (Part 1 of 3) Shades of pink according to GO-category, otherwise following the color scheme of figure ST3.3.

Table 2 of 3

Accession	Description	GO ID	Cat.	GO description
OQV24733.1	hypothetical protein BV898_01326			
OQV21922.1	hypothetical protein BV898_04135			
OQV23788.1	hypothetical protein BV898_02514			
OQV23159.1	putative Pancreatic triacylglycerol lipase	GO:0004806	MF	triglyceride lipase activity
		GO:0005576	CC	extracellular region
		GO:0006629	BP	lipid metabolic process
		GO:0046872	MF	metal ion binding
OQV13852.1	Procollagen-lysine 2-oxoglutarate 5-dioxygenase 3	GO:0001755	BP	neural crest cell migration
		GO:0005506	MF	iron ion binding
		GO:0005581	CC	collagen trimer
		GO:0005783	CC	endoplasmic reticulum
		GO:0008045	BP	motor neuron axon guidance
		GO:0008475	MF	procollagen-lysine 5-dioxygenase activity
		GO:0016021	CC	integral component of membrane
		GO:0016740	MF	transferase activity
		GO:0017185	BP	peptidyl-lysine hydroxylation
		GO:0031090	CC	organelle membrane
		GO:0031418	MF	L-ascorbic acid binding
		GO:0031984	CC	organelle subcompartment
		GO:0042175	CC	nuclear outer membrane-endoplasmic reticulum membrane network
OQV17559.1	Vitellogenin-6	GO:0005319	MF	lipid transporter activity
		GO:0006869	BP	lipid transport
OWA49851.1	put. Elongation of very long chain fatty acids protein 5	GO:0005783	CC	endoplasmic reticulum
		GO:0006636	BP	unsaturated fatty acid biosynthetic process
		GO:0009922	MF	fatty acid elongase activity
		GO:0016021	CC	integral component of membrane
		GO:0019367	BP	fatty acid elongation, saturated fatty acid
		GO:0019368	BP	fatty acid elongation, unsaturated fatty acid
		GO:0030148	MF	L-ascorbic acid binding
		GO:0030425	CC	dendrite
		GO:0031090	CC	organelle membrane
		GO:0031984	CC	organelle subcompartment
		GO:0035338	BP	long-chain fatty-acyl-CoA biosynthetic process
		GO:0042175	CC	nuclear outer membrane-endoplasmic reticulum membrane network
		GO:0042759	BP	long-chain fatty acid biosynthetic process
		GO:0042761	BP	very long-chain fatty acid biosynthetic process
		GO:0043025	CC	neuronal cell body
		GO:0045723	BP	positive regulation of fatty acid biosynthetic process
		GO:0102756	MF	very-long-chain 3-ketoacyl-CoA synthase activity
OQV13843.1	"Eukaryotic" [?]	GO:0000049	MF	tRNA binding
		GO:0002181	BP	cytoplasmic translation
		GO:0003743	MF	translation initiation factor activity
		GO:0003746	MF	translation elongation factor activity
		GO:0003924	MF	GTPase activity
		GO:0005525	MF	GTP binding
		GO:0005850	CC	eukaryotic translation initiation factor 2 complex
		GO:0006413	BP	translational initiation
		GO:0006414	BP	translational elongation
		GO:0022618	BP	ribonucleoprotein complex assembly
		GO:0034622	BP	protein-containing complex assembly
		GO:0045903	BP	positive regulation of translational fidelity
OQV14848.1	hypothetical protein BV898_10995	GO:0004061	MF	arylformamidase activity
		GO:0016021	CC	integral component of membrane
		GO:0019441	BP	tryptophan catabolic process to kynurenine
OQV22418.1	putative La-related protein	GO:0003723	MF	RNA binding
OQV17764.1	hypothetical protein BV898_08221			
OQV25732.1	Allene oxide synthase-lipoxygenase protein	GO:0005737	CC	cytoplasm
		GO:0016021	CC	Integral component of membrane
		GO:0016702	MF	oxidoreductase activity, acting on single donors with incorporation of molecular oxygen incorporation of two atoms of oxygen
		GO:0046872	MF	metal ion binding
OQV21481.1	Xaa-Pro dipeptidase	GO:0006508	BP	proteolysis
		GO:0030145	MF	manganese ion binding
		GO:0030574	BP	collagen catabolic process
		GO:0070006	MF	metalloaminopeptidase activity
		GO:0102009	MF	proline dipeptidase activity
OQV11417.1	Hydroxymethylglutaryl-CoA synthase cytoplasmic	GO:0004421	MF	hydroxymethylglutaryl-CoA synthase activity
		GO:0005829	CC	cytosol
		GO:0006084	BP	acetyl-CoA metabolic process
		GO:0006695	BP	cholesterol biosynthetic process
		GO:0010142	BP	farnesyl diphosphate biosynthetic process, mevalonate pathway
		GO:0014003	BP	oligodendrocyte development
		GO:0014033	BP	neural crest cell differentiation
		GO:0042803	MF	protein homodimerization activity
		GO:0048703	BP	embryonic viscerocranium morphogenesis
		GO:0048821	BP	erythrocyte development
OQV14251.1	hypothetical protein BV898_11488			

ST3.4b Full list of GO terms of proteins less abundant in cold (Part 2 of 3)

Table 3 of 3

Accession	Description	GO ID	Cat.	GO description
OQV16777.1	hypothetical protein BV898_09133	GO:0003723	MF	RNA binding
OQV25731.1	Allene oxide synthase-lipoxygenase protein	GO:0005737	CC	cytoplasm
		GO:0016702	MF	oxidoreductase activity, acting on single donors with incorporation of molecular oxygen incorporation of two atoms of oxygen
		GO:0034440	BP	lipid oxidation
		GO:0046872	MF	metal ion binding
OQV20556.1	Chorion peroxidase	GO:0004601	MF	peroxidase activity
		GO:0006979	BP	response to oxidative stress
		GO:0016021	CC	integral component of membrane
		GO:0020037	MF	heme binding
		GO:0098869	BP	cellular oxidant detoxification
OQV21904.1	Vitellogenin-6	GO:0005319	MF	lipid transporter activity
		GO:0006869	BP	lipid transport
OQV16319.1	Zinc-type alcohol dehydrogenase-like protein	GO:0004601	MF	peroxidase activity
		GO:0006979	BP	response to oxidative stress
		GO:0020037	MF	heme binding
		GO:0098869	BP	cellular oxidant detoxification
OQV20744.1	Nose resistant to fluoxetine protein 6	GO:0016021	CC	integral component of membrane
		GO:0016747	MF	acyltransferase activity, transferring groups other than amino-acyl groups
OQV19039.1	hypothetical protein BV898_06895			
OQV16226.1	hypothetical protein BV898_09709	GO:0005576	CC	extracellular region
		GO:0005975	BP	carbohydrate metabolic process
		GO:0008061	MF	chitin binding
		GO:0016810	MF	hydrolase activity, acting on carbon-nitrogen (but not peptide) bonds
		GO:0019213	MF	deacetylase activity
OQV24865.1	Chorion peroxidase	GO:0004601	MF	peroxidase activity
		GO:0006979	BP	response to oxidative stress
		GO:0020037	MF	heme binding
		GO:0098869	BP	cellular oxidant detoxification
OWA54228.1	hypothetical protein BV898_18639	GO:0030246	MF	carbohydrate binding
OQV26136.1	hypothetical protein BV898_00258			
OQV24876.1	Pancreatic lipase-related protein 2	GO:0004806	MF	triglyceride lipase activity
		GO:0005576	CC	extracellular region
		GO:0006629	BP	lipid metabolic process
		GO:0046872	MF	metal ion binding
OWA52228.1	hypothetical protein BV898_16686			
OQV17094.1	hypothetical protein BV898_08810	GO:0004869	MF	cysteine-type endopeptidase inhibitor activity
		GO:0005737	CC	cytoplasm
		GO:0010951	BP	negative regulation of endopeptidase activity
OQV13017.1	put. Very low-density lipoprotein rec.			
OQV22246.1	Pyrroline-5-carboxylate red. 1 mito.	GO:0004735	MF	pyrroline-5-carboxylate reductase activity
		GO:0005737	CC	cytoplasm
		GO:0055129	BP	L-proline biosynthetic process
OQV24625.1	hypothetical protein BV898_01684			
OQV14977.1	hypothetical protein BV898_10878			
OQV21547.1	hypothetical protein BV898_04449	GO:0005634	CC	nucleus
		GO:0005737	CC	cytoplasm
OQV23464.1	Oxidative stress-induced growth inhibitor 2	GO:0005737	CC	cytoplasm
		GO:0006516	BP	glycoprotein catabolic process
		GO:0016787	MF	hydrolase activity
OQV23553.1	hypothetical protein BV898_02672			
OQV19204.1	hypothetical protein BV898_06840			
OQV23800.1	put. Glutaredoxin-rel. 5 mito.			
OWA55468.1	hypothetical protein BV898_19855			

ST3.4c Full list of GO terms of proteins less abundant in cold (Part 3 of 3)

```
#IBP Type I Motifs
IBPtypeI_1 <- str_detect(df[,"AminoAcid"], "AAAA[TSNQ]", negate = FALSE)
IBPtypeI_2 <- str_detect(df[,"AminoAcid"], "AAAA[KL]", negate = FALSE)
IBPtypeI_3 <- str_detect(df[,"AminoAcid"], "T..N.......", negate = FALSE)
#IBP Type II Motifs
IBPtypeII_1 <- str_detect(df[,"AminoAcid"], "CP.G", negate = FALSE)
IBPtypeII_2 <- str_detect(df[,"AminoAcid"], "NLASVHS..E..F", negate = FALSE)
IBPtypeII_3 <- str_detect(df[,"AminoAcid"], ".LASVH", negate = FALSE)
IBPtypeII_4 <- str_detect(df[,"AminoAcid"], ".LAS", negate = FALSE)
IBPtypeII_5 <- str_detect(df[,"AminoAcid"], "WLWSDGS", negate = FALSE)
#Type "Other" Motifs
#OTHER_1 <- str_detect(df[,"seq"], "L.L.", negate = FALSE)
IBPother_1 <- str_detect(df[,"AminoAcid"], ".TCT.S..C..A", negate = FALSE)
IBPother_2 <- str_detect(df[,"AminoAcid"], ".TCT.S", negate = FALSE)
IBPother_3 <- str_detect(df[,"AminoAcid"], "T.T.T.T", negate = FALSE)
IBPother_4 <- str_detect(df[,"AminoAcid"], "BHPQYMZQTOCNFJ", negate = FALSE)
IBPother_5 <- str_detect(df[,"AminoAcid"], "WQZGKKKJIJFFOK", negate = FALSE)
IBPother_6 <- str_detect(df[,"AminoAcid"], "AAALA", negate = FALSE)
IBPother_7 <- str_detect(df[,"AminoAcid"], "AGAAA", negate = FALSE)
IBPother_8 <- str_detect(df[,"AminoAcid"], "L..L..", negate = FALSE)
IBPother_9 <- str_detect(df[,"AminoAcid"], "L...L.L", negate = FALSE)
IBPintermediate <- str_detect(df[,"AminoAcid"], "C.G.YC.G..", negate = FALSE)
IBPtypePPII_AFP <- str_detect(df[,"AminoAcid"], "G..G..G..{3,6}", negate = FALSE)

#AFGP (Antifreeze glycoproteins) Motifs
AFGP_1 <- str_detect(df[,"AminoAcid"], "AAT", negate = FALSE)
AFGP_2 <- str_detect(df[,"AminoAcid"], "TAA", negate = FALSE)

#INP (Ice-nucleating protein) Motifs
INP_1 <- str_detect(df[,"AminoAcid"], "AGYGST.TAG..SSLI", negate = FALSE)
INP_2 <- str_detect(df[,"AminoAcid"], "AGYGST.TAG..S.LT", negate = FALSE)
INP_3 <- str_detect(df[,"AminoAcid"], "AGYGST.T", negate = FALSE)
INP_4 <- str_detect(df[,"AminoAcid"], "AGTGSTKT", negate = FALSE)
INP_5 <- str_detect(df[,"AminoAcid"], "TG.T", negate = FALSE)
INP_6 <- str_detect(df[,"AminoAcid"], "AG.T", negate = FALSE)
INP_7 <- str_detect(df[,"AminoAcid"], "TG.N", negate = FALSE)
INP_8 <- str_detect(df[,"AminoAcid"], "AG.N", negate = FALSE)
INP_9 <- str_detect(df[,"AminoAcid"], "..N.V.G", negate = FALSE)
```

ST3.5 List of known IBP amino acid motifs used in custom regex script according to Bar Dolev et al. 2016

ST3.6 Output of iAFP analysis of the top 4 candidate tardigrade IBPs according to prediction model of Yu and Lu 2011

Tardigrade Candidate IBP #1

NCBI Accession number & Genome ID: **OQV18962.1, BV898_07018**

SeqID.544 : BV898_07018.p01

iAFP Prediction :

1 classifier recognized on afp : Dj3,

fold of preference as ANTIFREEZE PROTEIN : -3.024

SVMGA key residues reports :

No.	Res.	SVMGA Votes	Rp Value	Coding Features
1	M	3	-1.00	C+X6-O3X5-
2	Q	3	-1.58	Dj1-C-O3X5-
3	F-	5	-2.32	Dj3-C-X7-O3X5-S2X5-
4	A+	5	0.58	Dj1-X6+X7+N7C+S2X5-
5	I	2	-1.00	D-X7-
6	L	3	-1.58	D-Dj3-N7C-
7	A=	4	0.00	Dj3-X6+X7+N7C-
8	L	2	0.00	Dj6-N7C+
9	F-	6	-2.58	D-C-X7-N7C-N11C-S2X5-
10	V-	5	-2.00	D-Dj1-Dj3-N7C+S2X5-
11	A	3	1.00	X6+X7+N7C-
12	F-	6	-2.32	Dj1-C-X7-N7C-N11C+S2X5-
13	G	1	0.00	S2X5-
14	C	1	0.00	N7C+
15	V	2	-1.00	Dj1-Dj6-
16	M	3	1.00	C+X6-N7C+
17	A	3	1.00	Dj1-X6+X7+
18	D	1	0.00	D-
19	E-	9	-3.17	D-Dj3-C-X5-X6-X7-O3X5-P3X5-S2X5-
20	P-	4	-1.58	N11C+O3X5-P3X5-S2X5-
21	A=	4	0.00	X6+X7+O3X5-P3X5-
22	A	2	1.00	X6+X7+
23	D	3	-1.58	Dj3-Dj6-S2X5-
24	P	2	-1.00	N11C-S2X5-
25	V	1	0.00	Dj1-
26	S	1	0.00	N7C+
27	A	3	1.00	Dj1-Dj6+X6+
28	A	1	0.00	X6+
29	R	0	----	
30	A	3	-1.00	Dj6-Dj6-X6+
31	M=	4	0.00	Dj3+C+X6-X7-
32	M	3	-1.00	Dj6-C+X7-
33	A	2	1.00	D+N7C+
34	N	3	1.58	D+Dj6+X5+
35	R	2	0.00	Dj1-Dj3+
36	I	3	1.00	D-Dj1+N7C+
37	L-	5	-2.32	D-D-Dj1-Dj6-N7C-
38	T-	8	-1.58	D-Dj1+Dj1-Dj3-C+N7C-P3X5-S2X5-
39	A-	4	-1.58	Dj6-N7C+P3X5-S2X5-
40	D-	4	-2.00	Dj1-X7-P3X5-P3X5-
41	P-	4	-2.00	Dj3-N7C-N11C-P3X5-
42	S-	6	-2.32	Dj3-X6-N7C+N11C-P3X5-P3X5-
43	T	2	0.00	C+P3X5-
44	F-	5	-2.32	D-C-X5-X6-P3X5-
45	V	3	-1.58	D-Dj3-X7-
46	D	2	-1.00	X7-O3X5-
47	C-	4	-1.58	X5-X6+N7C-O3X5-
48	R	2	-1.00	Dj1-O3X5-

49	N	0	----	
50	D-	5	-2.32	D-Dj1-Dj6-X7-P3X5-
51	E-	5	-2.32	D-Dj6-C-N11C-P3X5-
52	A	2	0.00	D+P3X5-
53	N	3	-1.00	D+X7-S2X5-
54	G	3	-1.58	Dj3-N7C-S2X5-
55	C-	4	-1.58	X5-X6+X7-O3X5-
56	A	2	-1.00	O3X5-P3X5-
57	A-	4	-2.00	Dj6-O3X5-P3X5-S2X5-
58	K-	8	-3.00	Dj3-Dj6-X5-N11C-P3X5-P3X5-S2X5-S2X5-
59	P-	4	-2.00	X7-P3X5-P3X5-S2X5-
60	G-	4	-2.00	Dj3-P3X5-P3X5-P3X5-
61	W	3	-1.58	Dj6-P3X5-P3X5-
62	K-	4	-1.58	X5-N11C+O3X5-P3X5-
63	C-	4	-2.00	Dj3-X5-X7-O3X5-
64	Q-	4	-2.00	Dj3-C-O3X5-S2X5-
65	P-	4	-2.00	D-X7-N11C-S2X5-
66	L-	4	-1.58	D-Dj3-X6-N7C+
67	M=	4	0.00	Dj3-C+X5+N7C-
68	K-	4	-1.58	Dj6-X5-N11C+P3X5-
69	M-	5	-0.58	C+X5+N7C-N11C-P3X5-
70	C-	6	-2.32	Dj3-Dj3+X5-X7-O3X5-P3X5-
71	S-	4	-1.58	Dj1-N11C+O3X5-S2X5-
72	P-	5	-2.32	X7-N11C-O3X5-P3X5-S2X5-
73	G-	5	-2.32	Dj1-Dj3-N7C-P3X5-P3X5-
74	N-	6	-2.32	Dj1-Dj3+X7-P3X5-P3X5-P3X5-
75	S	3	-1.00	N11C+P3X5-P3X5-
76	P-	4	-2.00	Dj1-X7-N11C-P3X5-
77	K	3	-1.58	Dj3-X5-N7C-
78	M	3	1.00	C+N7C+P3X5-
79	E-	5	-2.00	Dj1-C-X7+N11C-P3X5-
80	A-	6	-1.00	Dj6+X5+O3X5-P3X5-P3X5-S2X5-
81	V-	5	-2.32	Dj1-O3X5-P3X5-P3X5-S2X5-
82	E-	7	-2.58	Dj3-C-X7+N11C-O3X5-P3X5-P3X5-
83	G	2	-1.00	Dj3-P3X5-
84	S	3	-1.58	N11C-O3X5-P3X5-
85	C	2	-1.00	O3X5-P3X5-
86	E-	8	-2.81	Dj3-Dj3-C-X7+N7C-N11C-O3X5-P3X5-
87	N	2	0.00	Dj3-Dj6+
88	T	3	1.00	Dj1-C+X5+
89	G	2	-1.00	D-N7C-
90	D-	5	-2.32	D-Dj1-Dj3-X7-N7C-
91	C	1	0.00	P3X5-
92	R-	5	-2.32	Dj1-X5-X7-N11C-P3X5-
93	P-	5	-2.00	D-N11C+P3X5-P3X5-S2X5-
94	L-	5	-2.32	D-Dj1-X7-P3X5-S2X5-
95	F	2	-1.00	C-P3X5-
96	R	2	-1.00	X5-X7-
97	C	2	0.00	Dj3-N7C+
98	N	2	-1.00	O3X5-S2X5-
99	K-	5	-2.32	X5-N11C-O3X5-O3X5-S2X5-
100	D-	5	-2.32	D-X7-O3X5-O3X5-O3X5-
101	K-	6	-2.58	D-Dj3-X5-N11C-O3X5-O3X5-
102	K	3	-1.58	X5-N11C-O3X5-
103	C	1	0.00	N7C+
104	A	3	1.00	X5+N7C+P3X5-
105	F-	5	-0.58	D-C-N7C+N11C+P3X5-
106	V-	6	-2.32	D-Dj3+O3X5-P3X5-P3X5-S2X5-
107	G-	5	-2.00	N7C+O3X5-P3X5-S2X5-S2X5-
108	P-	4	-1.58	X6+O3X5-P3X5-S2X5-
109	R	2	0.00	X5-X7+
110	A	2	1.00	Dj3+X5+
111	C	0	----	

112	E-	4	-2.00	Dj3-C-O3X5-P3X5-
113	S-	4	-2.00	N7C-N11C-O3X5-P3X5-
114	E-	6	-2.58	C-N11C-O3X5-O3X5-P3X5-P3X5-
115	A	2	-1.00	O3X5-P3X5-
116	D-	4	-1.58	Dj3-N7C+O3X5-P3X5-
117	C	1	0.00	Dj3+
118	N-	4	-1.58	Dj1+Dj3-N7C-O3X5-
119	G	2	0.00	N7C+O3X5-
120	A=	4	0.00	D+Dj1+Dj6-O3X5-
121	N=	4	0.00	D+Dj3+Dj3-N7C-
122	V	1	0.00	Dj3-
123	D	1	0.00	N7C+
124	G	3	-1.58	D-N7C-N11C-
125	V-	4	-2.00	D-Dj1-Dj3-S2X5-
126	S	3	-1.00	Dj3-N11C+S2X5-
127	F-	5	-2.00	Dj1-Dj6-C-N7C-N11C+
128	D	2	-1.00	X6-N7C-
129	C	1	0.00	N7C+
130	K-	6	-2.32	Dj1-Dj3-N7C+N11C-O3X5-P3X5-
131	E-	5	-2.00	C-X7-N11C+O3X5-P3X5-
132	L-	5	-2.32	Dj1-N7C-O3X5-P3X5-S2X5-
133	S-	4	-2.00	N7C-N11C-O3X5-S2X5-
134	K-	4	-2.00	N7C-N11C-O3X5-O3X5-
135	N-	4	-2.00	Dj1-O3X5-O3X5-O3X5-
136	A-	4	-2.00	Dj6-N11C-O3X5-O3X5-
137	P	3	-1.58	Dj1-N11C-O3X5-
138	G	2	-1.00	N7C-O3X5-
139	K-	4	-2.00	N11C-O3X5-O3X5-P3X5-
140	R-	4	-1.58	X7+O3X5-O3X5-P3X5-
141	C	3	-1.58	O3X5-P3X5-P3X5-
142	W	3	-1.58	X6-N7C-P3X5-
143	L	3	-1.00	Dj6-N7C+P3X5-
144	K	1	0.00	N11C+
145	C	2	0.00	Dj3+S2X5-
146	S	2	-1.00	N11C-S2X5-
147	S	1	0.00	N11C-
148	D	2	-1.00	Dj1-X6-
149	N	2	0.00	Dj3+N11C-
150	E-	6	-2.58	Dj1-Dj6-C-X7-N11C-P3X5-
151	C	2	-1.00	Dj3-P3X5-
152	H	1	0.00	P3X5-
153	G	1	0.00	N7C+
154	C	0	----	
155	K	3	-1.58	Dj3-N11C-P3X5-
156	A	1	0.00	P3X5-
157	D-	4	-1.58	Dj6-N7C+P3X5-S2X5-
158	G	3	-1.58	N7C-O3X5-S2X5-
159	S-	4	-1.58	Dj1+N7C-N11C-O3X5-
160	E-	4	-2.00	C-X7-O3X5-P3X5-
161	C	3	1.00	Dj1+X6+P3X5-
162	R-	5	-2.32	X5-X6-X7-P3X5-P3X5-
163	V	1	0.00	P3X5-
164	P	2	0.00	N11C+P3X5-
165	E	3	-1.58	C-X7-N11C-
166	N	1	0.00	P3X5-
167	F-	8	-2.81	C-X5-X6-X7-N7C-N11C+O3X5-P3X5-
168	R-	6	-2.58	X5-X6-X7-O3X5-P3X5-P3X5-
169	K-	5	-2.32	Dj6-N7C-N11C-O3X5-P3X5-
170	H	3	-1.58	N7C-P3X5-P3X5-
171	I	3	-1.58	X6-X7-P3X5-
172	G	2	-1.00	Dj6-P3X5-
173	C	2	1.00	Dj3+X6+
174	C	1	0.00	X6+

```
        175    Q      2            -1.00  C-S2X5-
        176    G      2            -1.00  Dj6-S2X5-
        177    T      3             1.00  Dj3+C+S2X5-
        178    C=     4             0.00  Dj3+X6+O3X5-S2X5-
        179    Q-     5            -2.32  Dj6-C-O3X5-O3X5-P3X5-
        180    R-     8            -3.00  X5-X6-X7-O3X5-O3X5-O3X5-P3X5-P3X5-
        181    K-     4            -2.00  N11CO3X5-O3X5-P3X5-P3X5-
        182    N-     4            -1.58  Dj3+O3X5-P3X5-S2X5-
        183    A      1            0.00   S2X5-
        184    C      1             0.00  X6+
        185    S      0             0.00  N7CN11C
        186    A      0             ----
*******************************************************************************
```

Tardigrade Candidate IBP #2

NCBI Accession number & Genome ID: **none, BV898_09539**

```
SeqID.823 : BV898_09539.p01
        iAFP Prediction :
              2 classifier recognized on afp : X6, X7,
              fold of preference as ANTIFREEZE PROTEIN : -2.524
        SVMGA key residues reports :
        No.    Res.   SVMGA Votes   Rp Value     Coding Features
-------------------------------------------------------------------------------
        1      M      3            -1.00  Dj6-C+X6-
        2      A      2             1.00  X6+X7+
        3      D      2            -1.00  O3X5-P3X5-
        4      T=     4             0.00  C+N7C+O3X5-P3X5-
        5      A=     4             0.00  X6+X7+O3X5-P3X5-
        6      A      2             1.00  X6+X7+
        7      A      2             1.00  X6+X7+
        8      A+     4             1.58  Dj1+Dj6-X6+X7+
        9      G      0             ----
        10     Q-     4            -1.58  Dj1+Dj1-C-S2X5-
        11     V      3            -1.00  Dj1-Dj3+S2X5-
        12     A+     4             1.58  Dj1-X6+X7+N7C+
        13     A      3             1.00  Dj1-X6+X7+
        14     A      2             1.00  X6+X7+
        15     A      3             1.58  D+Dj3+X6+
        16     N=     6             0.00  D+X5+X6+O3X5-P3X5-S2X5-
        17     A      3            -1.58  O3X5-P3X5-S2X5-
        18     T=     4             0.00  C+N7C+O3X5-P3X5-
        19     P      1            0.00   N11C-
        20     A      1            0.00   S2X5-
        21     K-     5            -2.32  Dj6-X5-P3X5-S2X5-S2X5-
        22     R-     4            -2.00  P3X5-P3X5-S2X5-S2X5-
        23     G-     4            -2.00  Dj1-P3X5-P3X5-S2X5-
        24     A      2            -1.00  P3X5-P3X5-
        25     G-     5            -2.32  Dj1-Dj3-Dj6-P3X5-S2X5-
        26     R      3            -1.58  P3X5-S2X5-S2X5-
        27     P      3            -1.00  N7C+S2X5-S2X5-
        28     K-     6            -2.58  Dj6-Dj6-X5-P3X5-S2X5-S2X5-
        29     K-     7            -2.81  Dj3-Dj6-X5-P3X5-P3X5-S2X5-S2X5-
        30     A      3            -1.58  P3X5-P3X5-S2X5-
        31     A      1            0.00   P3X5-
        32     G      2            -1.00  Dj3-Dj6-
        33     S      3            -1.00  N7C+P3X5-S2X5-
        34     A      3            -1.58  P3X5-S2X5-S2X5-
        35     K-     6            -2.58  Dj6-X5-P3X5-P3X5-S2X5-S2X5-
        36     K-     7            -2.81  Dj3-Dj6-X5-P3X5-P3X5-S2X5-S2X5-
        37     A-     4            -2.00  P3X5-P3X5-P3X5-S2X5-
        38     G      3            -1.58  P3X5-P3X5-P3X5-
        39     A      3            -1.00  X5+P3X5-P3X5-
        40     K      2            -1.00  X5-P3X5-
```

41	K	1	0.00	X5-
42	V	3	-1.00	Dj3-X7+S2X5-
43	A	2	0.00	X5+S2X5-
44	K	2	-1.00	Dj1-X5-
45	K	1	0.00	X5-
46	P	3	-1.58	Dj1-Dj3-S2X5-
47	A	3	-1.00	X5+S2X5-S2X5-
48	A	2	0.00	X5+S2X5-
49	K	2	-1.00	Dj6-X5-
50	K	1	0.00	X5-
51	A	1	0.00	X5+
52	S	2	0.00	Dj3-N7C+
53	P	2	0.00	X6+S2X5-
54	A	2	0.00	X5+S2X5-
55	K	3	-1.00	Dj6-X5-N7C+
56	K-	4	-2.00	Dj3-Dj6-Dj6-X5-
57	A	1	0.00	X5+
58	A	0	----	
59	G	2	-1.00	D-Dj3-
60	V	2	-1.00	D-S2X5-
61	T-	6	-1.00	Dj1-C+X6-N7C+O3X5-S2X5-
62	K	3	-1.58	Dj6-Dj6-O3X5-
63	K-	6	-2.58	Dj1-Dj3-Dj6-O3X5-O3X5-P3X5-
64	K	2	-1.00	O3X5-P3X5-
65	V	3	-1.58	Dj1-O3X5-P3X5-
66	A	0	----	
67	A	2	-1.00	Dj1-O3X5-
68	K	3	-1.58	Dj1-O3X5-O3X5-
69	K-	4	-2.00	Dj6-O3X5-O3X5-O3X5-
70	P	3	-1.58	Dj1-O3X5-O3X5-
71	A	1	0.00	O3X5-
72	A	1	0.00	O3X5-
73	K	2	-1.00	O3X5-O3X5-
74	K	2	-1.00	O3X5-O3X5-
75	A	1	0.00	O3X5-
76	V	1	0.00	Dj3-
77	A	0	----	
78	K	1	0.00	Dj1-
79	K	0	----	
80	P	2	-1.00	Dj1-Dj3-
81	A	1	0.00	O3X5-
82	A	1	0.00	O3X5-
83	K	1	0.00	O3X5-
84	K	0	----	
85	A	0	----	
86	A	1	0.00	O3X5-
87	A	1	0.00	O3X5-
88	K	2	-1.00	Dj1-O3X5-
89	K	0	----	
90	P	1	0.00	Dj1-
91	A	1	0.00	O3X5-
92	A	1	0.00	O3X5-
93	K	1	0.00	O3X5-
94	K	0	----	
95	A	0	----	
96	A	1	0.00	O3X5-
97	A	1	0.00	O3X5-
98	K	1	0.00	O3X5-
99	K	0	----	

****

Tardigrade Candidate IBP #3

NCBI Accession number & Genome ID: **OQV24628, BV898_01687**

SeqID.87 : BV898_01687.p01

iAFP Prediction :
1 classifier recognized on afp : Dj6,
fold of preference as ANTIFREEZE PROTEIN : -4.044

SVMGA key residues reports :

No.	Res.	SVMGA Votes	Rp Value	Coding Features
1	M	2	0.00	C+X6-
2	M	2	0.00	C+X6-
3	S	0	----	
4	L	1	0.00	D-
5	T-	4	-1.58	D-C+N7C-O3X5-
6	T	3	-1.00	C+N7C-O3X5-
7	F-	5	-2.32	C-X7-N11C-O3X5-S2X5-
8	L	3	-1.58	D-Dj3-S2X5-
9	L	3	-1.00	D-D+Dj1-
10	V	2	0.00	D+N7C-
11	G	1	0.00	Dj1-
12	C	3	-1.58	Dj3-Dj3-N7C-
13	L	2	0.00	D+Dj6-
14	V	3	1.00	D+D-N7C+
15	F-	5	-2.00	D-C-X7-N11C+S2X5-
16	L-	4	-1.58	Dj3-Dj6-N7C+S2X5-
17	A+	4	1.58	Dj1+X6+X7+N7C-
18	V	2	0.00	Dj3+N7C-
19	Q	2	0.00	Dj1+C-
20	Q-	6	-2.58	Dj1-Dj6-C-O3X5-P3X5-S2X5-
21	G	3	-1.58	O3X5-P3X5-S2X5-
22	A=	6	0.00	Dj1-Dj3+X6+X7+O3X5-P3X5-
23	Q-	5	-2.32	Dj1-Dj6-C-O3X5-P3X5-
24	S-	4	-2.00	Dj3-N7C-O3X5-P3X5-
25	A-	5	-2.00	Dj1-Dj6-X6+O3X5-P3X5-
26	D	2	-1.00	X7-P3X5-
27	D-	4	-2.00	D-Dj6-X7-P3X5-
28	K-	4	-2.00	D-Dj3-N7C-P3X5-
29	I	1	0.00	N7C+
30	Y	2	-1.00	C-X5-
31	H	2	0.00	N7C+S2X5-
32	L	3	-1.00	Dj6-N7C+S2X5-
33	E	3	-1.58	C-N7C-P3X5-
34	A	3	-1.58	Dj6-P3X5-P3X5-
35	T-	5	-0.58	Dj1-C+N7C+P3X5-P3X5-
36	D	2	-1.00	X7-P3X5-
37	S-	5	-2.00	Dj1-Dj6-X6-N7C+S2X5-
38	V-	4	-1.58	D-X7-N7C+S2X5-
39	L-	4	-2.00	D-D-Dj3-Dj6-
40	L-	5	-2.32	D-D-Dj3-Dj6-O3X5-
41	T-	4	-1.58	D-C+N7C-O3X5-
42	Y	3	-1.58	C-N11C-O3X5-
43	T	3	-1.00	Dj3-C+N7C-
44	T-	4	-1.58	Dj3-Dj6-C+P3X5-
45	T	2	0.00	C+P3X5-
46	Q-	4	-2.00	Dj6-C-X6-P3X5-
47	Q	3	-1.58	Dj6-C-X6-
48	R	2	0.00	Dj1-N7C+
49	D	3	-1.58	Dj1-Dj6-P3X5-
50	D-	4	-2.00	Dj1-Dj1-P3X5-P3X5-
51	L-	7	-2.81	D-Dj1-Dj1-Dj3-X6-P3X5-P3X5-
52	L-	4	-2.00	D-Dj1-X6-P3X5-
53	Q-	4	-2.00	Dj1-Dj3-C-N7C-
54	T-	4	-1.58	Dj3-C+N7C-S2X5-

55	I-	4	-2.00	D-Dj3-O3X5-S2X5-
56	A-	5	-2.32	D-Dj6-Dj6-N7C-O3X5-
57	G-	4	-2.00	Dj3-N7C-O3X5-P3X5-
58	S-	4	-1.58	Dj3-N7C+P3X5-P3X5-
59	W-	4	-1.58	N7C+P3X5-P3X5-P3X5-
60	N-	4	-2.00	X7-P3X5-P3X5-P3X5-
61	A-	5	-2.00	X5+P3X5-P3X5-P3X5-S2X5-
62	V-	7	-2.58	D-X7+N7C-P3X5-P3X5-S2X5-S2X5-
63	L-	6	-2.58	D-Dj6-X6-N7C-P3X5-S2X5-
64	S	1	0.00	N7C+
65	R	1	0.00	X5-
66	H	1	0.00	N7C-
67	K	3	-1.00	Dj1-X5-N7C+
68	I	0	----	
69	T=	4	0.00	Dj1-C+X5+N7C-
70	D	1	0.00	X7-
71	I	0	----	
72	H	2	-1.00	N7C-O3X5-
73	V	2	-1.00	Dj1-O3X5-
74	S	2	-1.00	O3X5-P3X5-
75	F-	5	-2.00	D-Dj1-C-N7C+P3X5-
76	V	3	-1.58	D-Dj3-P3X5-
77	S	0	----	
78	E-	4	-1.58	Dj6-C-X7+O3X5-
79	K	3	-1.58	X5-N7C-O3X5-
80	D-	5	-2.32	Dj1-Dj3-X7-N7C-O3X5-
81	A	2	0.00	X5+S2X5-
82	G-	4	-1.58	Dj1-Dj3-N7C+S2X5-
83	T-	5	-0.58	Dj1-C+X5+X6-N7C-
84	A	2	1.00	Dj1+X5+
85	K	3	-1.58	Dj1-Dj6-X5-
86	Q	3	-1.00	Dj1+Dj3-C-
87	V	1	0.00	S2X5-
88	V	1	0.00	S2X5-
89	Y	3	-1.00	C-X6-N11C+
90	K	1	0.00	X5-
91	V	1	0.00	S2X5-
92	S	1	0.00	S2X5-
93	G	2	0.00	Dj1-N7C+
94	N	2	-1.00	Dj1-O3X5-
95	G	3	-1.58	Dj1-N7C-O3X5-
96	P=	4	0.00	Dj1-X6+N11C+O3X5-
97	P	2	1.00	X6+N11C+
98	G	2	-1.00	Dj6-N7C-
99	A	2	1.00	D+N11C+
100	N	3	-1.00	D+O3X5-P3X5-
101	G-	4	-2.00	N7C-O3X5-O3X5-P3X5-
102	E-	5	-2.32	C-N11C-O3X5-O3X5-P3X5-
103	K	3	-1.00	N7C+O3X5-O3X5-
104	N-	4	-1.58	Dj1+Dj3-O3X5-O3X5-
105	G-	4	-2.00	Dj6-N7C-O3X5-O3X5-
106	A	2	0.00	Dj1+O3X5-
107	R	1	0.00	X7+
108	V	2	0.00	Dj3-N7C+
109	P	2	0.00	Dj1-N11C+
110	Q	1	0.00	C-
111	I	2	-1.00	Dj1-Dj6-
112	K	2	0.00	N7C+O3X5-
113	A	2	-1.00	N7C-O3X5-
114	A	2	-1.00	N7C-O3X5-
115	I	0	----	
116	R	1	0.00	X7+
117	K	3	-1.00	N7C+O3X5-P3X5-

118	N-	4	-2.00	Dj3-Dj6-O3X5-P3X5-
119	I-	4	-2.00	Dj1-Dj6-O3X5-P3X5-
120	Q	1	0.00	C-
121	S	1	0.00	Dj1-
122	V	2	-1.00	Dj3-O3X5-
123	N	3	-1.58	D-Dj1-O3X5-
124	N-	4	-2.00	D-O3X5-P3X5-S2X5-
125	P-	6	-2.32	Dj1-Dj1-N7C+N11C-P3X5-S2X5-
126	N-	5	-2.00	Dj1+Dj6-P3X5-P3X5-S2X5-
127	I-	5	-2.32	D-Dj1-X6-P3X5-S2X5-
128	A=	4	0.00	D-Dj1+N7C+P3X5-
129	L	3	-1.00	D-X5-N7C+
130	L	3	-1.00	D-X5-N7C+
131	S	2	0.00	N7C+O3X5-
132	A	2	0.00	Dj1+O3X5-
133	D-	4	-2.00	Dj6-O3X5-O3X5-P3X5-
134	Q-	5	-2.00	Dj1+Dj1-C-O3X5-P3X5-
135	Q-	5	-2.32	Dj1-C-O3X5-P3X5-S2X5-
136	A	3	-1.58	Dj1-N7C-S2X5-
137	A	3	-1.00	Dj1-Dj6+N7C-
138	F-	4	-2.00	C-X5-X6-X7-
139	D	1	0.00	S2X5-
140	A-	4	-1.58	Dj6-Dj6+N7C-S2X5-
141	S	2	-1.00	N7C-O3X5-
142	S	2	0.00	N7C+O3X5-
143	D	2	-1.00	Dj1-O3X5-
144	N-	5	-0.58	D-Dj6+Dj6+P3X5-S2X5-
145	L-	8	-3.00	D-Dj1-Dj1-X5-X7-O3X5-P3X5-S2X5-
146	D	3	-1.58	Dj6-O3X5-P3X5-
147	N-	4	-1.58	Dj1-Dj6+O3X5-P3X5-
148	M	2	0.00	C+P3X5-
149	R-	4	-2.00	X5-X6-X7-P3X5-
150	T	3	-1.00	Dj1-C+N7CO3X5-
151	T	3	1.00	Dj6+C+N7CO3X5-
152	K	3	-1.58	Dj1-O3X5-P3X5-
153	A	3	-1.58	Dj6-P3X5-P3X5-
154	H	3	-1.58	P3X5-P3X5-P3X5-

****

Tardigrade Candidate IBP #4

NCBI Accession number: **OQV14909.1, BV898_10940**

SeqID.969 : BV898_10940.p01

iAFP Prediction :

1 classifier recognized on afp : D,

fold of preference as ANTIFREEZE PROTEIN : -4.044

SVMGA key residues reports :

No.	Res.	SVMGA Votes	Rp Value	Coding Features
1	M-	4	-1.58	D-C+X6-O3X5-
2	N-	7	-0.42	D-Dj3-X5+X6+X7+O3X5-S2X5-
3	V	3	-1.00	Dj3+O3X5-S2X5-
4	S	1	0.00	Dj6-
5	I	3	1.00	Dj1+X7-N7C+
6	V	2	-1.00	Dj3-N7C-
7	T+	4	1.58	Dj1+Dj3+C+N7C-
8	L	1	0.00	D-
9	L	3	-1.00	D-D+N7C-
10	V	3	-1.00	D+Dj1-N7C-
11	T=	4	0.00	Dj1-Dj6-C+N7C+
12	F-	6	-2.32	Dj1-C-X7-N7C-N11C+S2X5-
13	G	3	-1.58	D-Dj1-S2X5-
14	V	2	-1.00	D-X7-
15	C	1	0.00	N7C+
16	S	1	0.00	N11C-
17	V-	4	-1.58	D-Dj3+X7-N7C-
18	L	3	1.00	D-D+N7C+
19	V=	4	0.00	D+Dj1-X7-N7C+
20	D	2	-1.00	X7-P3X5-
21	A	3	-1.00	Dj1-Dj3+P3X5-
22	S-	4	-1.58	X6-N7C+P3X5-P3X5-
23	S-	5	-2.32	X6-N7C-P3X5-P3X5-S2X5-
24	L-	7	-2.58	D-Dj3-N7C+P3X5-P3X5-S2X5-S2X5-
25	R-	5	-2.32	D-Dj1-P3X5-S2X5-S2X5-
26	Y	3	-1.58	C-S2X5-S2X5-
27	D	3	-1.58	Dj1-O3X5-S2X5-
28	V-	5	-0.58	Dj3-Dj3+X7+O3X5-S2X5-
29	R-	4	-2.00	O3X5-P3X5-S2X5-S2X5-
30	R-	6	-2.58	Dj3-N7C-P3X5-P3X5-S2X5-S2X5-
31	G-	5	-2.32	N7C-P3X5-P3X5-P3X5-S2X5-
32	T-	5	-0.58	Dj1-Dj3+C+P3X5-P3X5-
33	D	2	-1.00	N7C-P3X5-
34	Y	3	-1.58	Dj1-Dj3-C-
35	P	3	-1.00	X7-N11C+P3X5-
36	G	3	-1.00	Dj3-N7C+P3X5-
37	N	2	-1.00	X7-P3X5-
38	D	1	0.00	N7C-
39	I	2	-1.00	Dj6-S2X5-
40	Q-	4	-2.00	Dj3-Dj3-C-S2X5-
41	I	1	0.00	S2X5-
42	N	2	-1.00	S2X5-S2X5-
43	R	3	-1.58	X5-X7-S2X5-
44	G-	5	-2.00	D-Dj3-N7C+O3X5-S2X5-
45	V-	7	-2.58	D-Dj3+O3X5-O3X5-P3X5-S2X5-S2X5-
46	A-	8	-2.81	Dj6-X5+N7C-N11C-O3X5-O3X5-P3X5-S2X5-
47	T-	5	-0.58	C+X5+N7C-O3X5-P3X5-
48	E	3	-1.00	C-X7+N7C-
49	A	3	1.00	Dj3+X5+S2X5-
50	A=	4	0.00	Dj6+X5+P3X5-S2X5-
51	C	1	0.00	P3X5-
52	W	3	-1.58	N7C-P3X5-P3X5-
53	K	3	-1.58	X5-N11C-P3X5-
54	S-	4	-1.58	N11C+O3X5-P3X5-P3X5-

```
      55     C      2            -1.00  O3X5-P3X5-
      56     K-     4            -2.00  X5-N11C-O3X5-P3X5-
      57     N      2             0.00  Dj1-Dj6+
      58     H      3            -1.58  X5-X6-X7-
      59     P-     5            -2.00  Dj1-Dj3-X6+N11C-S2X5-
      60     T      3            -1.00  C+X6-S2X5-
      61     C      1             0.00  N7C+
      62     H      3            -1.58  X5-X6-X7-
      63     V      1            0.00   Dj3-
      64     A      0             ----
      65     V      1            0.00   P3X5-
      66     Y-     4            -2.00  C-X6-N11C-P3X5-
      67     S      3            -1.58  Dj3-N7C-P3X5-
      68     A      3            -1.00  Dj1+Dj6-S2X5-
      69     S-     4            -2.00  N7C-N11C-O3X5-S2X5-
      70     Q      3            -1.00  Dj1+C-O3X5-
      71     K-     5            -2.32  Dj3-N11C-O3X5-O3X5-P3X5-
      72     D      3            -1.58  X6-O3X5-P3X5-
      73     C-     4            -1.58  Dj3+O3X5-P3X5-P3X5-
      74     W      3            -1.58  X6-N11C-P3X5-
      75     L-     4            -1.58  Dj1-Dj6-N7C+P3X5-
      76     K      2             0.00  N7C-N11C+
      77     N-     4            -1.58  Dj1-Dj3+P3X5-S2X5-
      78     I      2            -1.00  P3X5-S2X5-
      79     K      3            -1.58  Dj1-N7C-P3X5-
      80     A      1             0.00  N7C+
      81     L-     5            -2.00  D-Dj1-X5-X7-N7C+
      82     T      3            -1.00  D-C+N7C-
      83     A      0             ----
      84     A      0             ----
      85     S      1            0.00   N7C-
      86     V      0             ----
      87     S      1             0.00  N7C+
      88     H      2            -1.00  O3X5-P3X5-
      89     P      2            -1.00  N11CO3X5-P3X5-
      90     E-     8            -3.00  C-X7-N7C-N11CO3X5-O3X5-P3X5-P3X5-S2X5-
      91     R-     6            -2.58  X5-X6-X7-O3X5-P3X5-S2X5-
      92     N      2            -1.00  O3X5-P3X5-
      93     T      1             0.00  C+
      94     F-     5            -2.32  C-X5-X6-X7-O3X5-
      95     R-     4            -2.00  X5-X6-X7-O3X5-
      96     D      2            -1.00  O3X5-S2X5-
      97     V      2            -1.00  S2X5-S2X5-
*****************************************************************************
```

Bibliography

Abdul Aziz, M., Sabeem, M., Mullath, S. K., Brini, F. and Masmoudi, K. (2021). Plant Group II LEA Proteins: Intrinsically Disordered Structure for Multiple Functions in Response to Environmental Stresses. Biomolecules 11,.

Adar, C., Sirotinskaya, V., Bar Dolev, M., Friehmann, T. and Braslavsky, I. (2018). Falling water ice affinity purification of ice-binding proteins. Sci. Rep. 8, 11046.

Alexa A, R. J. (2022). topGO: Enrichment Analysis for Gene Ontology.

Andersen, J. L., Manenti, T., Sørensen, J. G., MacMillan, H. A., Loeschcke, V. and Overgaard, J. (2015). How to assess *Drosophilacold* tolerance: chill coma temperature and lower lethal temperature are the best predictors of cold distribution limits. Funct. Ecol. 29, 55–65.

Andersen, M. K. and Overgaard, J. (2019). The central nervous system and muscular system play different roles for chill coma onset and recovery in insects. Comp. Biochem. Physiol. A Mol. Integr. Physiol. 233, 10–16.

Arai, T., Fukami, D., Hoshino, T., Kondo, H. and Tsuda, S. (2019). Ice-binding proteins from the fungus *Antarctomyces psychrotrophicus* possibly originate from two different bacteria through horizontal gene transfer. FEBS J. 286, 946–962.

Arny, D. C., Lindow, S. E. and Upper, C. D. (1976). Frost sensitivity of *Zea mays* increased by application of *Pseudomonas syringae*. Nature 262, 282–284.

Bar Dolev, M., Braslavsky, I. and Davies, P. L. (2016). Ice-Binding Proteins and Their Function. Annu. Rev. Biochem. 85, 515–542.

Bauerfeind, S. S., Kellermann, V., Moghadam, N. N., Loeschcke, V. and Fischer, K. (2014). Temperature and photoperiod affect stress resistance traits in *Drosophila melanogaster*. Physiol. Entomol. 39, 237–246.

Bayley, J. S., Winther, C. B., Andersen, M. K., Grønkjær, C., Nielsen, O. B., Pedersen, T. H. and Overgaard, J. (2018). Cold exposure causes cell death by depolarization-mediated Ca^{2+} overload in a chill-susceptible insect. Proc. Natl. Acad. Sci. U. S. A. 115, E9737–E9744.

Beck, S. D. (2012). Insect Photoperiodism. Elsevier.

Bemm, F., Burleigh, L., Förster, F., Schmucki, R., Ebeling, M., Janzen, C. J., Dandekar, T., Schill, R. O., Certa, U. and Schultz, J. (2017). Draft genome of the Eutardigrade *Milnesium tardigradum* sheds light on ecdysozoan evolution.

Bertolani, R. and Biserov, V. I. (1996). Leg and Claw Adaptations in Soil Tardigrades, with Erection of Two New Genera of Eutardigrada, *Macrobiotidae: Pseudohexapodibius* and *Xerobiotus*. Invertebr. Biol. 115, 299–304.

Bertolani, R., Guidetti, R., Altiero, T., Nelson, D. R. and Rebecchi, L. (2019). Dormancy in Freshwater Tardigrades. In Dormancy in Aquatic Organisms. Theory, Human Use and Modeling (ed. Alekseev, V. R.) and Pinel-Alloul, B.), pp. 43–51. Cham: Springer International Publishing.

Bertolani, R., Guidetti, R., Joensson, K. I., Altiero, T., Boschini, D. and Rebecchi, L. (2004). Experiences with dormancy in tardigrades. 63, 16–25.

Białkowska, A., Majewska, E., Olczak, A. and Twarda-Clapa, A. (2020). Ice Binding Proteins: Diverse Biological Roles and Applications in Different Types of Industry. Biomolecules 10,.

Bileschi, M. L., Belanger, D., Bryant, D. H., Sanderson, T., Carter, B., Sculley, D., Bateman, A., DePristo, M. A. and Colwell, L. J. (2022). Using deep learning to annotate the protein universe. Nat. Biotechnol.

Boothby, T. C., Tapia, H., Brozena, A. H., Piszkiewicz, S., Smith, A. E., Giovannini, I., Rebecchi, L., Pielak, G. J., Koshland, D. and Goldstein, B. (2017). Tardigrades Use Intrinsically Disordered Proteins to Survive Desiccation. Mol. Cell 65, 975–984.e5.

Boschini, D., Bertolani, R. and Rebecchi, L. (2006). Thermotolerance and thermal acclimation in active tardigrades. 10th International Symposium on Tardigrada 19.

Campbell, L. I., Rota-Stabelli, O., Edgecombe, G. D., Marchioro, T., Longhorn, S. J., Telford, M. J., Philippe, H., Rebecchi, L., Peterson, K. J. and Pisani, D. (2011). MicroRNAs and phylogenomics resolve the relationships of Tardigrada and suggest that velvet worms are the sister group of Arthropoda. Proc. Natl. Acad. Sci. U. S. A. 108, 15920–15924.

Castañeda, L. E., Lardies, M. A. and Bozinovic, F. (2005). Interpopulational variation in recovery time from chill coma along a geographic gradient: a study in the common woodlouse, Porcellio laevis. J. Insect Physiol. 51, 1346–1351.

Chen, X., Shi, X., Cai, X., Yang, F., Li, L., Wu, J. and Wang, S. (2021). Ice-binding proteins: a remarkable ice crystal regulator for frozen foods. Crit. Rev. Food Sci. Nutr. 61, 3436–3449.

Cid, F. P., Rilling, J. I., Graether, S. P., Bravo, L. A., Mora, M. de L. L. and Jorquera, M. A. (2016). Properties and biotechnological applications of ice-binding proteins in bacteria. FEMS Microbiol. Lett. 363,.

Cobb, T., Damschroder, D. and Wessells, R. (2021). Sestrin regulates acute chill coma recovery in *Drosophila melanogaster.* Insect Biochem. Mol. Biol. 133, 103548.

Cochet, N. and Widehem, P. (2000). Ice crystallization by *Pseudomonas syringae.* Appl. Microbiol. Biotechnol. 54, 153–161.

Colinet, H., Rinehart, J. P., Yocum, G. D. and Greenlee, K. J. (2018). Mechanisms underpinning the beneficial effects of fluctuating thermal regimes in insect cold tolerance. J. Exp. Biol. 221,.

Davies, P. L. (2014). Ice-binding proteins: a remarkable diversity of structures for stopping and starting ice growth. Trends Biochem. Sci. 39, 548–555.

Davies, P. L. (2022). Reflections on antifreeze proteins and their evolution. Biochem. Cell Biol.

Davis, H. E., Cheslock, A. and MacMillan, H. A. (2021). Chill coma onset and recovery fail to reveal true variation in thermal performance among populations of *Drosophila melanogaster.* Sci. Rep. 11, 10876.

de Sousa Abreu, R., Penalva, L. O., Marcotte, E. M. and Vogel, C. (2009). Global signatures of protein and mRNA expression levels. Mol. Biosyst. 5, 1512–1526.

Deng, C., Cheng, C.-H. C., Ye, H., He, X. and Chen, L. (2010). Evolution of an antifreeze protein by neofunctionalization under escape from adaptive conflict. Proc. Natl. Acad. Sci. U. S. A. 107, 21593–21598.

Denlinger, D. L. and Lee, R. E., Jr (2010). Low Temperature Biology of Insects. Cambridge University Press.

Duman, J. G. (2015). Animal ice-binding (antifreeze) proteins and glycolipids: an overview with emphasis on physiological function. J. Exp. Biol. 218, 1846–1855.

Durak, R. and Durak, T. (2021). Metabolic Response of Aphid *Cinara tujafilina* to Cold Stress. Biology 10,.

Ernst, R., Ejsing, C. S. and Antonny, B. (2016). Homeoviscous Adaptation and the Regulation of Membrane Lipids. J. Mol. Biol. 428, 4776–4791.

Findsen, A., Pedersen, T. H., Petersen, A. G., Nielsen, O. B. and Overgaard, J. (2014). Why do insects enter and recover from chill coma? Low temperature and high extracellular potassium compromise muscle function in *Locusta migratoria.* J. Exp. Biol. 217, 1297–1306.

Fischer, K., Liniek, S., Bauer, M., Baumann, B., Richter, S. and Dierks, A. (2012). Phenotypic plasticity in temperature stress resistance is triggered by photoperiod in a fly. Evol. Ecol. 26, 1067–1083.

Fleming, J. F., Pisani, D. and Arakawa, K. (2021). New Tardigrade Opsins and Differential Expression Analyses Show Ontogenic Variation in Light Perception. Genome Biol. Evol. 13,.

Förster, F., Beisser, D., Grohme, M. A., Liang, C., Mali, B., Siegl, A. M., Engelmann, J. C., Shkumatov, A. V., Schokraie, E., Müller, T., et al. (2012). Transcriptome analysis in tardigrade species reveals specific molecular pathways for stress adaptations. Bioinform. Biol. Insights 6, 69–96.

GĄ Asiorek, P., Stec, D., Morek, W. and Michalczyk, Ł. (2018). An integrative redescription of *Hypsibius dujardini* (Doyère, 1840), the nominal taxon for *Hypsibioidea* (*Tardigrada: Eutardigrada*). Zootaxa 4415, 45–75.

Gade, V. R., Traikov, S., Oertel, J., Fahmy, K. and Kurzchalia, T. V. (2020). *C. elegans* possess a general program to enter cryptobiosis that allows dauer larvae to survive different kinds of abiotic stress. Sci. Rep. 10, 13466.

Gibert, P. and Huey, R. B. (2001). Chill-Coma Temperature in *Drosophila*: Effects of Developmental Temperature, Latitude, and Phylogeny. Physiol. Biochem. Zool. 74, 429–434.

Gibert, P., Moreteau, B., Pétavy, G., Karan, D. and David, J. R. (2001). Chill-coma tolerance, a major climatic adaptation among *Drosophila species*. Evolution 55, 1063–1068.

Giovannini, I., Altiero, T., Guidetti, R. and Rebecchi, L. (2018). Will the Antarctic tardigrade A*cutuncus antarcticus* be able to withstand environmental stresses related to global climate change? J. Exp. Biol. 221,.

Goldstein, B. (2018). The Emergence of the Tardigrade *Hypsibius exemplaris* as a Model System. Cold Spring Harb. Protoc. 2018,.

Gross, V. and Mayer, G. (2019). Cellular morphology of leg musculature in the water bear *Hypsibius exemplaris (Tardigrada)* unravels serial homologies. R Soc Open Sci 6, 191159.

Gross, V., Treffkorn, S., Reichelt, J., Epple, L., Lüter, C. and Mayer, G. (2019). Miniaturization of tardigrades (water bears): Morphological and genomic perspectives. Arthropod Struct. Dev. 48, 12–19.

Guidetti, R. and Møbjerg, N. (2018). Environmental Adaptations: Encystment and Cyclomorphosis. In Water Bears: The Biology of Tardigrades (ed. Schill, R. O.), pp. 249–271. Cham: Springer International Publishing.

Guidetti, R., Altiero, T. and Rebecchi, L. (2011b). On dormancy strategies in tardigrades. J. Insect Physiol. 57, 567–576.

Guidetti, R., Altiero, T., Bertolani, R., Grazioso, P. and Rebecchi, L. (2011). Survival of freezing by hydrated tardigrades inhabiting terrestrial and freshwater habitats. Zoology 114, 123–128.

Guidetti, R., Altiero, T., Bertolani, R., Grazioso, P. and Rebecchi, L. (2011a). Survival of freezing by hydrated tardigrades inhabiting terrestrial and freshwater habitats. Zoology 114, 123–128.

Guidetti, R., Boschini, D., Altiero, T., Bertolani, R. and Rebecchi, L. (2008). Diapause in tardigrades: a study of factors involved in encystment. J. Exp. Biol. 211, 2296–2302.

Guil, N. and Giribet, G. (2012). A comprehensive molecular phylogeny of tardigrades-adding genes and taxa to a poorly resolved phylum-level phylogeny. Cladistics 28, 21–49.

Halberg, K. A., Larsen, K. W., Jørgensen, A., Ramløv, H. and Møbjerg, N. (2013). Inorganic ion composition in *Tardigrada*: cryptobionts contain a large fraction of unidentified organic solutes. J. Exp. Biol. 216, 1235–1243.

Hatanaka, R., Hagiwara-Komoda, Y., Furuki, T., Kanamori, Y., Fujita, M., Cornette, R., Sakurai, M., Okuda, T. and Kikawada, T. (2013). An abundant LEA protein in the anhydrobiotic midge, PvLEA4, acts as a molecular shield by limiting growth of aggregating protein particles. Insect Biochem. Mol. Biol. 43, 1055–1067.

Hazell, S. P. and Bale, J. S. (2011). Low temperature thresholds: are chill coma and CT(min) synonymous? J. Insect Physiol. 57, 1085–1089.

Heidemann, N. W. T., Smith, D. K. and Hygum, T. L. (2016). Osmotic stress tolerance in semi-terrestrial tardigrades. Zool. J. Linn. Soc.

Heikes, K. L. and Goldstein, B. (2018). Live Imaging of Tardigrade Embryonic Development by Differential Interference Contrast Microscopy. Cold Spring Harb. Protoc. 2018,.

Hengherr, S. and Schill, R. O. (2018). Environmental Adaptations: Cryobiosis. In Water Bears: The Biology of Tardigrades (ed. Schill, R. O.), pp. 295–310. Cham: Springer International Publishing.

Hengherr, S., Reuner, A., Brümmer, F. and Schill, R. O. (2010). Ice crystallization and freeze tolerance in embryonic stages of the tardigrade Milnesium tardigradum. Comp. Biochem. Physiol. A Mol. Integr. Physiol. 156, 151–155.

Hengherr, S., Worland, M. R., Reuner, A., Brümmer, F. and Schill, R. O. (2009). Freeze tolerance, supercooling points and ice formation: comparative studies on the subzero temperature survival of limno-terrestrial tardigrades. J. Exp. Biol. 212, 802–807.

Hering, L., Bouameur, J.-E., Reichelt, J., Magin, T. M. and Mayer, G. (2016). Novel origin of lamin-derived cytoplasmic intermediate filaments in tardigrades. Elife 5, e11117.

Jönsson, K. I. (2020). Tardigrades -- evolutionary explorers in extreme environments. Extremophiles as Astrobiological Models 255–274.

Jørgensen, A., Kristensen, R. M. and Møbjerg, N. (2018). Phylogeny and Integrative Taxonomy of Tardigrada. In Water Bears: The Biology of Tardigrades (ed. Schill, R. O.), pp. 95–114. Cham: Springer International Publishing.

Kamilari, M., Jørgensen, A., Schiøtt, M. and Møbjerg, N. (2019). Comparative transcriptomics suggest unique molecular adaptations within tardigrade lineages. BMC Genomics 20, 607.

Kayukawa, T., Chen, B., Hoshizaki, S. and Ishikawa, Y. (2007). Upregulation of a desaturase is associated with the enhancement of cold hardiness in the onion maggot, *Delia antiqua*. Insect Biochem. Mol. Biol. 37, 1160–1167.

Kosová, K., Klíma, M., Prášil, I. T. and Vítámvás, P. (2021). COR/LEA Proteins as Indicators of Frost Tolerance in *Triticeae*: A Comparison of Controlled versus Field Conditions. Plants 10,.

Koziol, U. (2018). Precursors of neuropeptides and peptide hormones in the genomes of tardigrades. Gen. Comp. Endocrinol. 267, 116–127.

Kristensen, T. N., Hoffmann, A. A., Overgaard, J., Sørensen, J. G., Hallas, R. and Loeschcke, V. (2008). Costs and benefits of cold acclimation in field-released \textitDrosophila. Proc. Natl. Acad. Sci. U. S. A. 105, 216–221.

Kuiper, M. J., Lankin, C., Gauthier, S. Y., Walker, V. K. and Davies, P. L. (2003). Purification of antifreeze proteins by adsorption to ice. Biochem. Biophys. Res. Commun. 300, 645–648.

Kuramochi, M., Takanashi, C., Yamauchi, A., Doi, M., Mio, K., Tsuda, S. and Sasaki, Y. C. (2019). Expression of Ice-Binding Proteins in Caenorhabditis elegans Improves the Survival Rate upon Cold Shock and during Freezing. Sci. Rep. 9, 6246.

Lebaron, P., Catala, P. and Parthuisot, N. (1998). Effectiveness of SYTOX Green stain for bacterial viability assessment. Appl. Environ. Microbiol. 64, 2697–2700.

Leroi, A. M., Bennett, A. F. and Lenski, R. E. (1994). Temperature acclimation and competitive fitness: an experimental test of the beneficial acclimation assumption. Proceedings of the National Academy of Sciences 91, 1917–1921.

Li, X. and Wang, L. (2005). Effect of temperature and thermal acclimation on locomotor performance of *Macrobiotus harmsworthi* Murray (Tardigrada, *Macrobiotidae*). J. Therm. Biol. 30, 588–594.

Lubawy, J., Chowański, S., Adamski, Z. and Słocińska, M. (2022). Mitochondria as a target and central hub of energy division during cold stress in insects. Front. Zool. 19, 1.

Macdonald, S. S., Rako, L., Batterham, P. and Hoffmann, A. A. (2004). Dissecting chill coma recovery as a measure of cold resistance: evidence for a biphasic response in *Drosophila melanogaster*. J. Insect Physiol. 50, 695–700.

MacMillan, H. A. (2013). Ionic and Osmotic Mechanisms Of Insect Chill-Coma And Chilling Injury.

MacMillan, H. A. and Sinclair, B. J. (2011). Mechanisms underlying insect chill-coma. J. Insect Physiol. 57, 12–20.

MacMillan, H. A., Knee, J. M., Dennis, A. B., Udaka, H., Marshall, K. E., Merritt, T. J. S. and Sinclair, B. J. (2016). Cold acclimation wholly reorganizes the *Drosophila melanogaster* transcriptome and metabolome. Sci. Rep. 6, 28999.

MacMillan, H. A., Williams, C. M., Staples, J. F. and Sinclair, B. J. (2012). Reestablishment of ion homeostasis during chill-coma recovery in the cricket *Gryllus pennsylvanicus*. Proc. Natl. Acad. Sci. U. S. A. 109, 20750–20755.

Mahatabuddin, S. and Tsuda, S. (2018). Applications of Antifreeze Proteins: Practical Use of the Quality Products from Japanese Fishes. In Survival Strategies in Extreme Cold and Desiccation: Adaptation Mechanisms and Their Applications (ed. Iwaya-Inoue, M.), Sakurai, M.), and Uemura, M.), pp. 321–337. Singapore: Springer Singapore.

Maki, L. R., Galyan, E. L., Chang-Chien, M. M. and Caldwell, D. R. (1974). Ice nucleation induced by *Pseudomonas syringae*. Appl. Microbiol. 28, 456–459.

Mali, B., Grohme, M. A., Förster, F., Dandekar, T., Schnölzer, M., Reuter, D., Wełnicz, W., Schill, R. O. and Frohme, M. (2010). Transcriptome survey of the anhydrobiotic tardigrade *Milnesium tardigradum* in comparison with *Hypsibius dujardini* and *Richtersius coronifer*. BMC Genomics 11, 168.

Mangiagalli, M., Brocca, S., Orlando, M. and Lotti, M. (2020). The “cold revolution''. Present and future applications of cold-active enzymes and ice-binding proteins. N. Biotechnol. 55, 5–11.

Mapalo, M. A., Robin, N., Boudinot, B. E., Ortega-Hernández, J. and Barden, P. (2021). A tardigrade in Dominican amber. Proc. Biol. Sci. 288, 20211760.

Marshall, C. J., Basu, K. and Davies, P. L. (2016). Ice-shell purification of ice-binding proteins. Cryobiology 72, 258–263.

Martin, C., Gross, V., Hering, L., Tepper, B., Jahn, H., de Sena Oliveira, I., Stevenson, P. A. and Mayer, G. (2017). The nervous and visual systems of onychophorans and tardigrades: learning about arthropod evolution from their closest relatives. J. Comp. Physiol. A Neuroethol. Sens. Neural Behav. Physiol. 203, 565–590.

Mathis, A., Mamidanna, P., Cury, K. M., Abe, T., Murthy, V. N., Mathis, M. W. and Bethge, M. (2018). DeepLabCut: markerless pose estimation of user-defined body parts with deep learning. Nat. Neurosci. 21, 1281–1289.

McInnes, S. J. and Pugh, P. J. A. (2018). Tardigrade Biogeography. In Water Bears: The Biology of Tardigrades (ed. Schill, R. O.), pp. 115–129. Cham: Springer International Publishing.

McMullen and Storey (2008). Suppression of Na^+ K^+-ATPase activity by reversible phosphorylation over the winter in a freeze-tolerant insect. J. Insect Physiol.

McNuff, R. (2018). Laboratory Culture of *Hypsibius exemplaris*. Cold Spring Harb. Protoc. 2018,.

Megumu, T., Yoshida, Y., Imura, S. and Arakawa, K. (2017). Comparative transcriptome analysis of the Antarctic tardigrade, *Acutuncus antarcticus*, in response to changes in temperature. Book of Abstracts 333.

Møbjerg, A., Kodama, M., Ramos-Madrigal, J., Neves, R. C., Jørgensen, A., Schiøtt, M., Gilbert, M. T. P. and Møbjerg, N. (2022). Extreme freeze-tolerance in cryophilic tardigrades relies on controlled ice formation but does not involve significant change in transcription. Comp. Biochem. Physiol. A Mol. Integr. Physiol. 271, 111245.

Møbjerg, N. and Neves, R. C. (2021). New insights into survival strategies of tardigrades. Comp. Biochem. Physiol. A Mol. Integr. Physiol. 254, 110890.

Neves, R. C., Hvidepil, L. K. B., Sørensen-Hygum, T. L., Stuart, R. M. and Møbjerg, N. (2020). Thermotolerance experiments on active and desiccated states of Ramazzottius varieornatus emphasize that tardigrades are sensitive to high temperatures. Sci. Rep. 10, 94.

Neves, R. C., Hvidepil, L. K. B., Sørensen-Hygum, T. L., Stuart, R. M. and Møbjerg, N. (2020a). Thermotolerance experiments on active and desiccated states of *Ramazzottius varieornatus* emphasize that tardigrades are sensitive to high temperatures. Sci. Rep. 10, 94.

Neves, R. C., Møbjerg, A., Kodama, M., Ramos-Madrigal, J., Gilbert, M. T. P. and Møbjerg, N. (2022). Differential expression profiling of heat stressed tardigrades reveals major shift in the transcriptome. Comp. Biochem. Physiol. A Mol. Integr. Physiol. 267, 111169.

Neves, R. C., Stuart, R. M. and Møbjerg, N. (2020b). New insights into the limited thermotolerance of anhydrobiotic tardigrades. Commun. Integr. Biol. 13, 140–146.

Nirody, J. A., Duran, L. A., Johnston, D. and Cohen, D. J. (2021). Tardigrades exhibit robust interlimb coordination across walking speeds and terrains. Proc. Natl. Acad. Sci. U. S. A. 118,.

Ono, M., Takeuchi, N. and Zawierucha, K. (2021). Snow algae blooms are beneficial for microinvertebrates assemblages (*Tardigrada* and *Rotifera*) on seasonal snow patches in Japan. Sci. Rep. 11, 5973.

Overgaard, J. and MacMillan, H. A. (2017). The Integrative Physiology of Insect Chill Tolerance. Annu. Rev. Physiol. 79, 187–208.

Overgaard, J., Gerber, L. and Andersen, M. K. (2021). Osmoregulatory capacity at low temperature is critical for insect cold tolerance. Curr Opin Insect Sci 47, 38–45.

Overgaard, J., Tomcala, A., Sørensen, J. G., Holmstrup, M., Krogh, P. H., Simek, P. and Kostál, V. (2008). Effects of acclimation temperature on thermal tolerance and membrane phospholipid composition in the fruit fly *Drosophila melanogaster*. J. Insect Physiol. 54, 619–629.

Papadopoulos, N. T., Moraiti, C. A. and Verykouki, E. (2022). Chill coma recovery of *Ceratitis capitata* adults across the Northern Hemisphere.

Perry, R. N. and Wharton, D. A. (2011). Molecular and Physiological Basis of Nematode Survival. CABI.

Philogene, B. J. R. (1982). Development Rate Changes in Insects: The Importance of Photoperiod. Am. Nat. 120, 269–272.

Ramløv, H. and Westh, P. (1992). Survival of the cryptobiotic eutardigrade *Adorybiotus coronifer* during cooling to- 196 C: effect of cooling rate, trehalose level, and short-term acclimation. Cryobiology 29, 125–130.

Raymond, J. A. (2014). The ice-binding proteins of a snow alga, *Chloromonas brevispina*: probable acquisition by horizontal gene transfer. Extremophiles 18, 987–994.

Raymond, J. A. and Remias, D. (2019). Ice-Binding Proteins in a *Chrysophycean Snow Alga*: Acquisition of an Essential Gene by Horizontal Gene Transfer. Front. Microbiol. 10, 2697.

Richaud, M. and Galas, S. (2018). Defining the viability of tardigrades with a molecular sensor related to death. PLoS One 13, e0206444.

Rinehart, J. P., Hayward, S. A. L., Elnitsky, M. A., Sandro, L. H., Lee, R. E., Jr and Denlinger, D. L. (2006). Continuous up-regulation of heat shock proteins in larvae, but not adults, of a polar insect. Proc. Natl. Acad. Sci. U. S. A. 103, 14223–14227.

Rinehart, J. P., Li, A., Yocum, G. D., Robich, R. M., Hayward, S. A. L. and Denlinger, D. L. (2007). Up-regulation of heat shock proteins is essential for cold survival during insect diapause. Proc. Natl. Acad. Sci. U. S. A. 104, 11130–11137.

Robertson, R. M., Spong, K. E. and Srithiphaphirom, P. (2017). Chill coma in the locust, *Locusta migratoria*, is initiated by spreading depolarization in the central nervous system. Sci. Rep. 7, 10297.

Roth, B. L., Poot, M., Yue, S. T. and Millard, P. J. (1997). Bacterial viability and antibiotic susceptibility testing with SYTOX Green nucleic acid stain. Appl. Environ. Microbiol. 63, 2421–2431.

Schill, R. O. (2018). Water Bears: The Biology of Tardigrades. Springer, Cham.

Schill, R. O., Mali, B., Dandekar, T., Schnölzer, M., Reuter, D. and Frohme, M. (2009). Molecular mechanisms of tolerance in tardigrades: new perspectives for preservation and stabilization of biological material. Biotechnol. Adv. 27, 348–352.

Schokraie, E., Hotz-Wagenblatt, A., Warnken, U., Mali, B., Frohme, M., Förster, F., Dandekar, T., Hengherr, S., Schill, R. O. and Schnölzer, M. (2010). Proteomic analysis of tardigrades: towards a better understanding of molecular mechanisms by anhydrobiotic organisms. PLoS One 5, e9502.

Shcherbakov, D., Schill, R. O., Brümmer, F. and Blum, M. (2010). Movement behaviour and video tracking of *Milnesium tardigradum* Doyère, 1840 (Eutardigrada, Apochela). Contrib. Zool. 79, 33–38.

Sinclair, B. J., Vernon, P., Jaco Klok, C. and Chown, S. L. (2003). Insects at low temperatures: an ecological perspective. Trends Ecol. Evol. 18, 257–262.

Sinensky, M. (1974). Homeoviscous adaptation—a homeostatic process that regulates the viscosity of membrane lipids in *Escherichia coli.* Proc. Natl. Acad. Sci. U. S. A. 71, 522–525.

Smith, F. W., Boothby, T. C., Giovannini, I., Rebecchi, L., Jockusch, E. L. and Goldstein, B. (2016). The Compact Body Plan of Tardigrades Evolved by the Loss of a Large Body Region. Curr. Biol. 26, 224–229.

Steele, J. E. (1981). The Role of Carbohydrate Metabolism in Physiological Function. In Energy Metabolism in Insects (ed. Downer, R. G. H.), pp. 101–133. Boston, MA: Springer US.

Somme, L. and Meier, T. (1995). Cold tolerance in *Tardigrada* from Dronning Maud land, Antarctica. Polar Biol. 15,.

Teets, N. M. and Denlinger, D. L. (2013). Physiological mechanisms of seasonal and rapid cold-hardening in insects. Physiol. Entomol. 38, 105–116.

Thakur, S., Cattoni, D. I. and Nöllmann, M. (2015). The fluorescence properties and binding mechanism of SYTOX Green, a bright, low photo-damage DNA intercalating agent. Eur. Biophys. J. 44, 337–348.

Thorp, J., A. Covich (1991) Ecology and Classification of North American Freshwater Invertebrates - 1st Edition. ISBN 978-0126906455, 0126906459.

Törönen, P., Medlar, A. and Holm, L. (2018). PANNZER2: a rapid functional annotation web server. Nucleic Acids Res. 46, W84–W88.

Toxopeus, J., Warner, A. H. and MacRae, T. H. (2014). Group 1 LEA proteins contribute to the desiccation and freeze tolerance of *Artemia franciscana* embryos during diapause. Cell Stress Chaperones 19, 939–948.

Tsujimoto, M., Imura, S. and Kanda, H. (2016). Recovery and reproduction of an Antarctic tardigrade retrieved from a moss sample frozen for over 30 years. Cryobiology 72, 78–81.

Voets, I. K. (2017). From ice-binding proteins to bio-inspired antifreeze materials. Soft Matter 13, 4808–4823.

Vogel, C. and Marcotte, E. M. (2012). Insights into the regulation of protein abundance from proteomic and transcriptomic analyses. Nat. Rev. Genet. 13, 227–232.

Wallingford, A. K., Lee, J. C. and Loeb, G. M. (2016). The influence of temperature and photoperiod on the reproductive diapause and cold tolerance of spotted-wing drosophila,*Drosophila suzukii*. Entomol. Exp. Appl. 159, 327–337.

Walther, D. M., Kasturi, P., Zheng, M., Pinkert, S., Vecchi, G., Ciryam, P., Morimoto, R. I., Dobson, C. M., Vendruscolo, M., Mann, M., et al. (2015). Widespread Proteome Remodeling and Aggregation in Aging *C. elegans*. Cell 161, 919–932.

Wang, W., Flury, A. G., Garrison, J. L. and Brem, R. B. (2021). Cold Survival and Its Molecular Mechanisms in a Locally Adapted Nematode Population. Genome Biol. Evol. 13,.

Westh, P. and Kristensen, R. (1992). Ice formation in the freeze-tolerant eutardigrades *Adorybiotus coronifer* and *Amphibolus nebulosus* studied by differential scanning calorimetry. Polar Biol. 12,.

Westh, P., Kristiansen, J. and Hvidt, A. (1991). ICE-nucleating activity in the freeze-tolerant tardigrade *Adorybiotus coronifer*. Comp. Biochem. Physiol. A Physiol. 99, 401–404.

Wharton, D. A., Downes, M. F., Goodall, G. and Marshall, C. J. (2005). Freezing and cryoprotective dehydration in an Antarctic nematode (*Panagrolaimus davidi*) visualized using a freeze substitution technique. Cryobiology 50, 21–28.

Williams, C. M., Henry, H. A. L. and Sinclair, B. J. (2015). Cold truths: how winter drives responses of terrestrial organisms to climate change. Biol. Rev. Camb. Philos. Soc. 90, 214–235.

Williams, C. M., Watanabe, M., Guarracino, M. R., Ferraro, M. B., Edison, A. S., Morgan, T. J., Boroujerdi, A. F. B. and Hahn, D. A. (2014). Cold adaptation shapes the robustness of metabolic networks in *Drosophila melanogaster*. Evolution 68, 3505–3523.

Woods, H. A. and Harrison, J. F. (2002). Interpreting rejections of the beneficial acclimation hypothesis: when is physiological plasticity adaptive? Evolution 56, 1863–1866.

Wright, J. C. (2001). Cryptobiosis 300 Years on from van Leuwenhoek: What Have We Learned about Tardigrades? Zoologischer Anzeiger - A Journal of Comparative Zoology 240, 563–582.

Yakimovich, K. M., Engstrom, C. B. and Quarmby, L. M. (2020). Alpine Snow Algae Microbiome Diversity in the Coast Range of British Columbia. Front. Microbiol. 11, 1721.

Yamaguchi, A., Tanaka, S., Yamaguchi, S., Kuwahara, H., Takamura, C., Imajoh-Ohmi, S., Horikawa, D. D., Toyoda, A., Katayama, T., Arakawa, K., et al. (2012). Two novel heat-soluble protein families abundantly expressed in an anhydrobiotic tardigrade. PLoS One 7, e44209.

Yi, S.-X., Moore, C. W. and Lee, R. E., Jr (2007). Rapid cold-hardening protects *Drosophila melanogaster* from cold-induced apoptosis. Apoptosis 12, 1183–1193.

Yoshida, Y., Horikawa, D. D., Sakashita, T., Yokota, Y., Kobayashi, Y., Tomita, M. and Arakawa, K. (2021). RNA sequencing data for gamma radiation response in the extremotolerant tardigrade *Ramazzottius varieornatus*. Data Brief 36, 107111.

Yoshida, Y., Koutsovoulos, G., Laetsch, D. R., Stevens, L., Kumar, S., Horikawa, D. D., Ishino, K., Komine, S., Kunieda, T., Tomita, M., et al. (2017). Comparative genomics of the tardigrades *Hypsibius dujardini* and *Ramazzottius varieornatus*. PLoS Biol. 15, e2002266.

Yu, C.-S. and Lu, C.-H. (2011). Identification of antifreeze proteins and their functional residues by support vector machine and genetic algorithms based on n-peptide compositions. PLoS One 6, e2044

Zachariassen, K. E. (1985). Physiology of cold tolerance in insects. Physiol. Rev. 65, 799–832.